Application of MagLev-based isolation technology for the rapid and sensitive concentration of influenza viruses

by

Muhammad Faizan Khalid

B.Sc., The University of British Columbia Okanagan, 2018

A THESIS SUBMITTED IN PARTIAL FULFILLMENT OF

THE REQUIREMENTS FOR THE DEGREE OF

MASTER OF APPLIED SCIENCE

in

THE COLLEGE OF GRADUATE STUDIES

(Mechanical Engineering)

THE UNIVERSITY OF BRITISH COLUMBIA

(Okanagan)

February 2021

The undersigned certify that they have read, and recommend to the College of Graduate Studies for acceptance, a thesis entitled:

Application of a MagLev-based isolation technology for rapid and sensitive detection of influenza viruses

---

Submitted by Muhammad Faizan Khalid in partial fulfilment of the requirements of

The degree of: Master of Applied Science in Engineering

Dr. Sepideh Pakpour, School of Engineering, Faculty of Applied Science: Mechanical

Supervisor, Assistant Professor

Dr. Isaac Li, IKBSAS: Chemistry

Supervisory Committee Member, Assistant Professor

Dr. Mohammad Hossein Zarifi, School of Engineering, Faculty of Applied Science: Electrical

Supervisory Committee Member, Assistant Professor

Dr. Andrew Jirasek, IKBSAS: Physics

University Examiner, Professor

Abstract

Viruses are a fundamental branch of the tree of life. They are responsible for several biological processes and a major source of human and plant diseases. Despite their relevance to life however, most techniques to study them are dependent on indirect and invasive methods like PCR or immunological and cytological assays which require large numbers of whole viruses to function reliably. This is also true for the influenza virus which has caused several pandemics in human history. Many established techniques in virology additionally require extensive storage and intermediary steps to preserve and increase viral titters for analysis. These steps impose constraints on the process of detection and isolation while also destroying virus particles. To reduce the constraints imposed by things like primer bias, storage conditions and virus host interactions during enumeration steps, in this thesis I present a Magnetic Levitation (MagLev) based technique for the isolation and detection of influenza viruses. My main objective was to assess the performance of Magnetic Levitation (MagLev) based techniques for the sensitive and rapid isolation of intact influenza viruses in biological samples.

The results show that influenza virions are levitated within a MagLev systems column consistently and distinctly using either Gadobutrol or Super Paramagnetic Iron Oxide Nanoparticle (SPION) solutions (in the MagLev) but do not produce a reliable visible marker for identification. However, the pure influenza A viral stock used in the experiment did produce a visualization in two trials which was used to determine a first ever direct MagLev based estimate of influenza A viral density ($\sim 0.978 \pm 0.02$ g/cm^3). Which is notably lower than previous estimates of viral density (1.014-1.265 g/cm^3) obtained through sucrose gradient based ultracentrifugation. Additionally, the results of viral quantification via Q-RTPCR and Tissue Culture Infectious Dose 50 (TCID50) assays corroborated the evidence of viral levitation. Both validation methods produced relatively consistent results, wherein fractions of the MagLev systems column produced a lower C_t value or higher TCID50/ml indicating a higher presence of intact influenza A virus in regions of the MagLev column as a consequence of levitation. This work shows that influenza virions can be levitated reliably and non-invasively using a MagLev based apparatus, thus opening up room for future work using the technology. With MagLev based techniques, we can develop novel ways of collecting, studying and concentrating viral samples that reduce the constraints imposed by traditional virology techniques.

Preface

This thesis presents an experimental design and proof of functionality for a MagLev based viral particle isolation system. This research was conducted at the University of British Columbia, Okanagan campus, under supervision of Dr. Sepideh Pakpour. Part of the experiments were carried out as part of a MITAC's globalink research award, at TUFTS university, Grafton, Massachusetts, USA, Cummings School of veterinary medicine; Department of Infectious Disease and Global Health (IDGH). During the award period, the project was mentored by Dr. Jonathan Runstadler at TUFTS University and Dr. Morteza Mahmoudi at Harvard University.

Table of contents

List of figures

List of tables

List of equations

Acknowledgements

This dissertation represents the contributions of a community of scientists, living and dead, whom I have grown to respect and value immeasurably during the process of my thesis writing. With that being said, the work presented herein would not be possible without the ongoing support and guidance from my supervisor Dr. Sepideh Pakpour and contributing co-supervisors Dr. Morteza Mahmoudi and Dr. Jonathan Runstadler. The expertise and resources provided by the principal investigators, helped develop and complete the work presented and will pave the way for future research. Following the pandemic of 2020, the support and guidance offered by my principal investigators was key in the completion of this dissertation.

The bulk of this research was conducted in 2019 and the results presented here are from that period with various aspects of the dissertation having to accommodate the ongoing effects of the 2020 Sars-COV-2 Pandemic. Consequently, I am eternally grateful to Dr. Wendy Blay Puryear and Alexa Foss at the Jonathan Runstadler lab for teaching me the necessary techniques and bearing with my lack of experience to help conduct the research for this dissertation. Without the contributions of the strong women in my life I would neither be equipped nor able to complete this novel interdisciplinary research on my own, much less during a global pandemic.

Speaking of strong women, I would also like to thank a few very special individuals in my life. I had the privilege of working with Dr. Sepideh Pakpour and Ms. Negin Kazemian during my bachelors studies at UBC. Witnessing their passion and commitment for research allowed me to push myself and pursue a master's degree in engineering which was a significant shift for me as microbiologist. Their guidance and support throughout the years along with other lab members has meant a lot to me and I am a better person for having met these people. Briefly, I would also like to thank the community at UBCO, my friends in the anime club and other students for helping me during my studies and being the support that kept me afloat throughout my time at UBCO. The friendship and knowledge I received will never be forgotten. Thank you, everyone, for always inspiring me by doing what you do.

Lastly, I would like to thank my amazing family for all their support. Thank you to my amazing brother, Umar Faruq, for always being there for me. Thank you to my parents whose sacrifices I cannot even begin to comprehend. Your efforts have paved the way towards the future my siblings and I strive for.

Muhammad Faizan Khalid

University of British Columbia

10/01/2021

Dedication

I dedicate this work to my parents Naheed and Khalid Faruq, the people who raised me and taught me the value of hard work. Two people who I may never fully understand but love unconditionally and owe my entire life and accomplishments to. I would also like to thank my grandfathers' Ch. Muhammad Aslam and Ch. Murid Ahmad, each of whom inspired a thirst for knowledge in me that may never be quenched.

A quote that has guided me throughout my life:

"(Anyone) One who has taught me a single word, has made me his slave (I owe them everything)"

- Ali ibn Abi Talib

Chapter 1. Background and Thesis Organization

1.1 Introduction

Previous work in the field of magnetic levitation (MagLev) has demonstrated a variety of applications of the technology within biology[1–4]. It has been demonstrated that individual cells can be levitated on the basis of their density[4–6]. Additionally, proteins and complex drugs can also be isolated directly from samples[2,7–9] using only MagLev, indicating a growing role for the technology in various industries. Furthermore, given our groups previous success and experience in developing MagLev based systems for the detection of rare proteins found in opioid use disorders and isolating them from human plasma directly[1]. There is potential within the field of MagLev to present a non-invasive and low-cost method for isolating viruses from environmental and biological samples directly. Thus, providing access to whole intact virions to virologists[2–5,9–12] as well as a simple and direct way for estimating viral density. This is because MagLev based separation techniques are based on density (not mass or volume) and accomplish separation by taking advantage of gravitational and magnetic forces acting on diamagnetic particles suspended in a paramagnetic fluid medium[1].

While viruses have existed and been identified since 1899[13], there is no direct method for measuring the density of any virus known or unknown despite the use for such information in diagnostics and understanding the dynamics of viruses in the environment. Most methods for virus isolation and density estimation require access to ultracentrifuges[14–20] or specialized equipment, expertise, materials or environments[15,20–23]. Even in previous studies involving MagLev based techniques, conventional paramagnetic liquid media have been incapable of separating sub-micrometre biological entities, but the use of superparamagnetic iron oxide nanoparticles (SPIONS) can substantially enhance the susceptibility of magnetic media and therefore enable a MagLev to generate strong continuous gradients in effective density to separate and levitate smaller particles like viruses[1,10,24]. Given that the density of viruses relative to other complex molecules found in samples may be distinct, MagLev devices and techniques can reduce the time taken to isolate viruses from complex samples while providing much higher and robust yields. Leading to potentially faster identification and subsequent vaccine production for deadly pathogens like influenza[25].

Influenza is a notorious viral pathogen responsible for annually claiming thousands of lives (~650 000 per year)[25] and posing a significant threat to all human life. In Canada, Influenza pandemics lead to direct economic losses including medical costs estimated at an average cost

per ICU treatment of a laboratory confirmed case costing $14,612.00 and $133 prior to hospital admission[26]. This is in addition to indirect economic losses resulting from substantial workplace absence (Avg 10.8 days)[26]. Additionally, the mutative nature of the virus results in annual shifts in circulating strains, making it difficult to study and synthesize preventative vaccines for the circulating virus and all of its forms[27,28]. Consequently, an elusive goal of infectious disease research and prevention is the development of a rapid and sensitive test capable of isolating and detecting novel influenza strains quickly to ultimately decrease the spread of illness. Although several strategies have been developed for isolation and detection of influenza in a timely manner[29–31], these approaches have limitations. Some of which arise from the hours or days required for processing[14,20,22,32], enumeration[32,33] and storage[34] of samples which contribute to contamination and significant loss in viral load of whole infectious particles[15,34–36]. Furthermore, without the presence of intact virion particles, it is difficult to maintain laboratory stocks as well as identify newer infectious strains. Hence, scientists are continuously looking for faster and more efficient ways to isolate prevalent strains of the virus from environmental and biological samples[27].

These stated issues extend to viruses beyond influenza and include the novel corona virus classified by the WHO as SARS-CoV-2. The global SARS-CoV-2 pandemic significantly affected the lives of humans and the welfare of entire nations[37] despite the long history of corona viruses affecting human civilizations (SARS in the 2000s, MERS in the 2010s, and now SARS-CoV-2)[38]. Even now, at the time of writing this thesis, there are no commercially available vaccines to combat any iteration of the corona virus. This scenario is indicative of difficulties faced by industry and medical systems to combat viruses as agents of systemic global change. Looking at the broader spectrum of viruses, beyond one species of virus it is important to note that in the 2020 pandemic, the pneumonia caused by the pandemic strain of the corona virus is accompanied by reported pathogens like seasonal influenza, adenovirus, coronavirus 229E/NL63/OC43, human bocavirus, human metapneumovirus, parainfluenza virus 1/2/3, rhinovirus and respiratory syncytial virus. These viruses can cause co-infection in the setting of community-acquired bacterial pneumonia[38]. Each agent listed has the potential to take life and must be treated with caution. Additionally, as in the case of Entrovirus 71 (EV71) many viruses can pose ongoing threats on a global scale but persist indefinitely on local ones[39]. Developing identification methods for unknown and unique viral agents and subsequently streamline a procedure for the development of vaccines against said agent are

worthwhile goals in virology. Hence, any advancement of said techniques and procedures is an acknowledgment of the sheer scale of the process and difficulties surrounding it[40].

Recent advancement in vaccine research and development show that it is intimately tied to our understanding of the structural proteins of viruses[38–41]. Furthermore, some vaccines derived from intact viruses can offer higher immunity and better results such as in the case of influenza [42]. Additionally, many regions in the world do not have the facilities to purify vaccines based on viruses and virus targets for human use[15,20,21,43,44]. Ultimately, the production and development of all vaccines and study of viral targets is aided by the availability and differential access to whole viral particles. Hence the necessity for new innovative ways to both detect and isolate individual viruses is necessary. This is imperative if better local or sub-regional vaccine networks are the key to preventing future pandemics[39]. In our previous work we have seen remarkable detection of rare proteins as a part of an entire protein cloud using Maglev based techniques[1]. Discovery of rare proteins is thus facilitated by MagLev and can lead to similar findings in other scenarios. In summary, these techniques are less invasive and more robust compared to current photometric and centrifugation based methods that often remove or cannot detect rare proteins like the ones on the surfaces of viruses which are responsible for conferring infectivity[30,42,45,46]. Magnetic levitation thus can serve as a robust basis for developing streamlined isolation and identification strategies that can be a cost-effective standard for viral specimen preparation, research and vaccine development.

1.2 Motivation behind this research

Viruses represent a fundamental aspect of nature but more importantly a significant threat to human life[25,38]. Given the quantity of viruses present in the world and their ability to mutate and evolve, resulting in independent (for each virus) and disproportionate impacts across the world[39,45,46]. It is necessary then to identify areas of potential constraint to virologists and develop novel methods and devices to improve access to intact viruses from samples. In this thesis we identify a number of issues relating to the storage[34,35],quantification[47–49], identification[29,30,50] and enumaration[51,52] of viruses which are active constraints to virologic research. These issues are present within the influenza screening and response pipeline as well, making it an ideal candidate for study and use in an experiment like the one presented here. Influenza is a significant disease source[25], routinely studied[19,27] and often sampled from environmental and clinical settings[53,54]. Furthermore, there is often a necessity in influenza research to store the virus and enumerate it before analysis. There is literature which shows

that enumeration and storage can add potentially confounding variables such as mutations[32,33,35,52] to viral research and current identification methods are susceptible to biases and errors[29,32,34,35,55]. Given this information, there is potential for the introduction of novel techniques to limit or circumvent the errors in processing of viruses and improve detection such that it favours the identification and isolation of intact viruses in a cost effective and reliable fashion.

Given the success of MagLev based system for the detection and isolation of rare proteins directly from human plasma[1]. There is potential within the field of magnetic levitation to present a low-cost method to potentially isolate viruses from complex samples by levitating samples within a MagLev system. A levitated sample within a MagLev is separated based on density (not mass or volume) and hence a distinctly dense virus may be visualized and isolated as a unique levitating precipitate relative to other molecules in a sample. Notably, no such previous methods have been utilized for obtaining measurements for viral density and can be a significant discovery from this work. Mainly however, levitation of viruses would limit the steps required to identify an unknown virus within a sample while also providing a portable system for isolating all or most of the viruses within a given sample based on density. Furthermore, MagLev systems have been shown to be useful in cell culture and other biological applications due to the non-invasive nature of magnetic forces[2,4,5,11]. Hence, they may provide reliable and cost-efficient access to whole intact virions to researchers across the world[14-22].

1.3 Objectives

Previous work with MagLev systems has demonstrated the effectiveness of MagLev in levitating proteins[1], living cells[4,5] and many chemical substrates[2,7]. However, no literature exists on the effectiveness of MagLev systems in levitating viruses or the effects of paramagnetic media (used in the MagLev system) on viruses. Furthermore, the density of viruses has thus far been an ignored property in virology with measurements heavily relying on assumptions and use of extensive processing to obtain measurements[16,19,36,56]. My main objective thus is to validate and test an innovative MagLev based technique for the sensitive and rapid isolation, detection and concentration of influenza A in a given sample. An additional aim is to test the performance of popular and SPION based paramagnetic media on the levitation of viruses. Furthermore, I will test the viability or infectivity of influenza A following exposure to the MagLev. Lastly, MagLev separation techniques are based on density (not mass or volume)[1,2,2,10–12] and so can offer a first ever direct MagLev based estimate for the density

of influenza A. Given the utility offered by MagLev based techniques to other fields such as mining, chemistry and biology[7] it can offer similar solutions to issues prevalent in virology. Such as issues resulting from a need to enumerate viruses from samples and use invasive techniques to identify, isolate and study each virus individually[32,35,49,51,52].

To capture this overall objective, the specific aims are as follows:

Aim 1: Investigate if viruses can be levitated within the MagLev. The virus chosen to meet this objective is influenza A/Puerto Rico/8/1934 (lab grown strain of an enveloped virus)

Aim 2: Investigate the performance of different paramagnetic media (GdCl3, Gadobutrol and SPIONs) in levitation of viruses

Aim 3: Investigate if viruses are infective (MDCK host) or even intact after separation via MagLev

Aim 4: Determine a first ever MagLev based density estimate for the influenza A virus

1.4 Thesis outline

Chapter 1 describes the objectives and motivation of the study. Chapter 2 includes a literature review of MagLev, MagLev systems and viruses with emphasis on influenza, its properties and identification techniques. Chapter 3 provides the methodology and materials used in this study to fulfil the objectives defined in section **1.3**. Chapter 4 presents the results and a discussion on the results obtained for RT-QPCR tests, TCID 50 assays and determination of viral density. Chapter 5 includes the main conclusions and shortcomings of the study as well as outlines potential future work. This work also includes some appended results and figures showing results mentioned in this thesis but not presented in detail.

Chapter 2. Literature Review

2.1 Viruses

Viruses are a fundamental branch of the tree of life. They are responsible for many biological processes and a major source of human disease. First shown to be biological agents in the 19th century [13,57] viruses are crystalline particles which display properties of living organisms once within their host. Structurally viruses are relatively simple with single stranded (ss) or double stranded (ds) DNA or RNA based genetic material enclosed within protein structures. Viruses can be broadly categorised as RNA viruses and DNA viruses[46] or alternatively as enveloped and non-enveloped viruses[58]. A completely intact virus, with its contents and the parcel containing it is referred to as a virion.

Beyond their general features there is vast versatility in viral structures, metabolism and function. Furthermore, many viruses are prone to random mutation and evolution resulting in numerous subtypes and strains existing simultaneously across the world. RNA viruses are especially difficult to categorize based on species due to more errors in transcription and replication which are a consequence of having RNA as the basis for their genetic material[46]. Additionally, many viruses are encapsulated by their hosts plasma membrane or rely on host proteins, resulting in many distinct host dependent virion structures[32,59]. In addition to host dependent changes, genomic mutations and recombination also result in structural changes to the virion. These factors, in tandem, make studying the morphologies of viruses difficult[59].

To elaborate on the structural features of viruses, they are composed of genetic material which can exist in the form of DNA or RNA that either directly encodes for viral proteins or requires their host organisms' proteins to first produce viral mRNA. The genetic material can be complexed with proteins, divided into several segments or be present as a single linear or circular segment. Furthermore, the genome can be composed of single stranded or double stranded polynucleotide chains[58,60]. The genetic material of viruses and any accompanying proteins are enclosed within a protein capsule called the capsid. The capsid may be additionally coated by an envelope composed of lipids and glycoproteins. All of these defining features of viruses are associated with their function as the entire lifecycle of a virus is contingent on its ability to infect its host and gain access to the cellular machinery necessary for the virus to transcribe and replicate its genome[46,58,60]. A complete and infective viral package is called a virion, the size of which can range from 17nm (Porcine circovirus) in diameter to 750nm (mimivirus)[61].

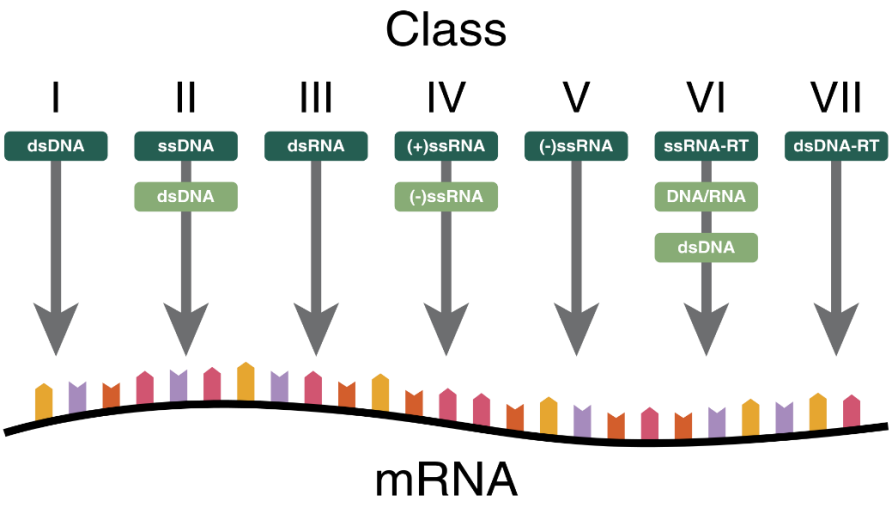

Fig 1. The Baltimore classification of viruses[62]. There are 7 major classes based on the steps leading to viral mRNA production. Viral mRNA production is integral to the metabolism of viruses[63].

There are several ways dedicated to the classification of viruses. The simplest is based on their genome and its ability to produce viral mRNA which can encode viral proteins, leading to the production of new infectious viral particles. This is referred to as the Baltimore classification system for viruses[63] (**Fig 1**). In this system there are 7 major classes of viruses differentiated based on whether they have DNA vs RNA, single stranded (ss) vs double stranded (ds), (+) sense vs (-) anti-sense and whether reverse transcription (RT) is required to produce viral messenger RNA[62,63]. This however is only an example of one classification system for viruses. There are more comprehensive systems that consider protein structures, capsid shape, genetic similarity and other characteristics of viruses to determine their classification such as the database of the International Committee on Taxonomy of Viruses (ICTV) [60].

2.2 Non-Human viruses

While human viruses are an important agent of global change and consequence, the wide diversity of viruses is most readily represented in non-human viruses. The initial discovery of viruses was spurred by experiments conducted on agricultural disease like tobacco mosaic virus[13,57]. Furthermore, viruses go beyond just eukaryotic organisms and have host ranges that span every major class of living organism. This is a testament to their success as obligate parasitic life forms. The major class of consequence beyond human viruses is bacteriophages which utilize the breadth of bacterial species present on earth as their obligate hosts. The most

astonishing feature of bacteriophages is their abundance and diversity, with estimates indicating that they may be the most prevalent entities in the biosphere. Although only a fraction of the phage population has been examined closely, these display a seemingly limitless variety of morphologies[64]. Furthermore, these phages manifest a corresponding heterogeneity in genome size, gene content and gene organization[64]. Hence, viral research is far more varied and consequential with regards to its global impact. A novel change and improvement to virologic research thus can have broad impacts on our understanding of biological processes in a range of contexts.

2.3 Human viruses

There are many examples of viruses serving as human pathogens and being the source of major global pandemics and socio-economic change. Some key examples are the Spanish flu (influenza) of 1918, AIDS (HIV) 2005-2012 and the SARS-CoV-2 pandemic of 2020. From these, the influenza virus alone has been a source of pandemics four times in the past 100 years (1918, 1956, 1968 and 2009)[65], thus acting as a continuous threat to the human population. The most recent influenza pandemic was the 2009 H1N1 strain of the flu (Swine flu) which resulted in between 151,700 and 575,400 deaths worldwide between 2009-2011 and also still persists today as a circulating strain of seasonal flu[65,66]. Similarly, it is important to note that in the 2020 pandemic, the pneumonia caused by the pandemic strain of the corona virus (SARS-CoV-2) is accompanied by reported pathogens like seasonal influenza, adenovirus, coronavirus 229E/NL63/OC43, human bocavirus, human metapneumovirus, parainfluenza virus 1/2/3, rhinovirus and respiratory syncytial virus. The breadth of viruses are an ever present fixture of our world[53] and each virus can cause co-infection in the setting of community-acquired bacterial pneumonia[38]. Co-infections and mutation play a major role in the seasonal shifts observed in viruses, as well as explain the emergence of more virulent or lethal strains of viruses like influenza and corona[45].

Notably, flu resulting from highly virulent strains of influenza viruses is associated with a significant number of deaths annually (~650,000 worldwide)[25] despite there being international screening programs for seasonal flu strains[25–27]. This is evidence of a need for better methods to study and identify viruses at local and global scales[27,39–41]. More importantly, broader enumeration and primer independent methods are necessary to accurately identify previously unknown viruses and newly emerging viruses[29,32,33,59]. Notably, there are examples of human viruses, which were sufficiently well studied such that vaccines were developed to immunize

a majority of the human population against them. These viruses are polio and measles which are almost entirely eradicated from the list of harmful human viruses[67]. Given the very real economic costs referred to as disease burden for viruses like influenza[26] and the potential to eradicate viral diseases, it is worthwhile both economically and from a humanitarian perspective to develop techniques to evolve the field of virology to reduce the expanding list of viral threats to human life.

2.3.1 Influenza typology

Influenza is a contagious respiratory illness caused by members of the viral family Orthomyxoviridae (Segmented RNA viruses) which infect the nose, throat, and sometimes the lungs of vertebrates. The infection causes mild to severe illness but can lead to death, especially if the sufferers are immunocompromised, old (>65) or very young (<2)[27]. The influenza virus is broadly broken down into 4 types of viruses based on host range, membrane proteins and the number of genome segments[68,69]. The subtypes are Alpha-influenza virus (type A), Beta-influenza virus (type B), Gamma-influenza virus (type C) and Delta-influenza virus (type D)[45]. Influenza A viruses (IAV) are further classified into subtypes based on the combinations of 18 different hemagglutinin (HA1-18) and 11 different neuraminidase proteins (NA 1-11) on the surface envelope of the Alpha-influenza virus. Influenza B Viruses (IBV) are not classified into subtypes but can be broken down into two lineages B/Yamagata and B/Victoria[69]. Types A, B and C are of clinical importance because of their ability to infect humans, whereas type D is usually found in cattle and does not cause disease in humans[70]. Of the types which infect humans, IAV strains have been given greater clinical significance because they were responsible for several infectious pandemics like the Spanish (1918) and swine (2009) flu[25,65]. While science has evolved to understand the nature of influenza as a disease, it is not able to study it directly due to the ever-shifting physical characteristics of the virus[28].

Changes to influenza morphologies can result from host dependent factors, genetic shift, genetic drift and processing protocols[34,46,52,59]. Influenza viruses are enveloped viruses and their lipid-glycoprotein envelop is derived from their hosts plasma membranes and is representative of host proteins (**Fig 4**), resulting in many distinct host dependent virion structures[32,59]. In addition to host dependent changes, gene mutations (genetic drift) and recombination during co-infection with other RNA viruses and influenza strains (genetic shift) also result in structural changes to the virion (**Fig 3**)[45,46]. Further changes in shape and function can be introduced to the virus through enumeration protocols[32,51,59] and lab storage[34,52]. In summary, influenza

virions are pleiomorphic (ranging in shape from spheres to extremely long filaments) with a helical capsid (protein shell)[59,70]. Lab grown virions typically are spherical in shape with a mean outer diameter of 120 nm, but clinical isolates are pleiomorphic with a variant taking on a highly elongated filamentous shape (> 250 nm in length)[52]. While the purpose behind the filamentous form remains unclear, it is generally accepted that for influenza viruses, filament formation is a heritable trait which is selected for in natural transmission[52].

Beyond different morphologies, generally Haemagglutinin (HA) and neuraminidase (NA) are the two major viral glycoproteins necessary for host infection in the lipid envelope of influenza A and B[69,70]. Influenza C and D only have one such major glycoprotein necessary for infection called hemagglutinin-esterase fusion (HEF) protein[71,72]. In influenza A and B which are major human pathogens, these glycoproteins have a characteristic spike-like appearance in electron micrographs of virions and typically HA is in higher concentration than NA on the surface of virions. Underneath the envelop and protein capsid of the viruses resides a highly ordered matrix layer which is made of the M1 protein. The M1 polymerises with copies of itself to form a helical matrix, the organisation of which influences the final virion morphology[73,74]. The M1 and nucleoprotein (NP) of the influenza viruses are necessary for viral replication and distinct from the non-specific amounts of host proteins which account for a significant degree of variation between virions[59]. Hence, these proteins and their associated genes are often ideal markers for the genetic identification of viruses which is the standard used by the ICTV[53,59,60,69,72,73].

At any given moment, several factors are simultaneously causing influenza viruses in labs and the environment to evolve and add to the awesome diversity of viruses in the world. The consequences of such variability are challenges to disease researchers and virologists[27,28].

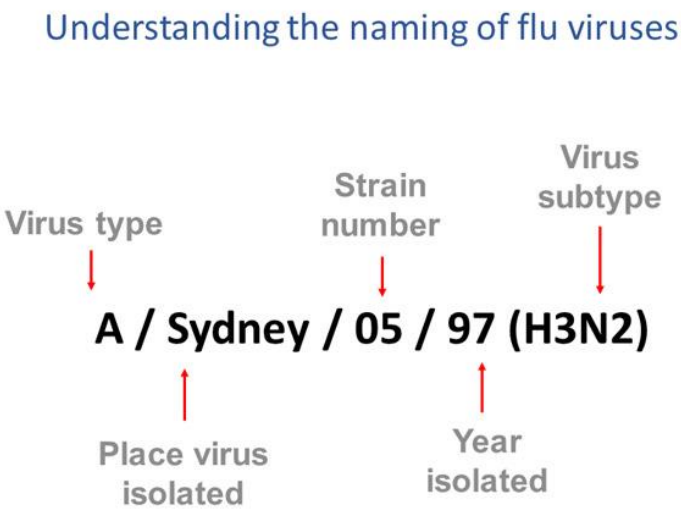

Fig 2. The naming convention for flu causing viruses[75]. Flu viruses are the colloquial term for influenza which has several circulating strains across the world that rapidly change over time. The example provided is for influenza A which is a major contributor to human disease[66,75].

2.3.2 Influenza genome

The genome of influenza viruses within their capsid consists of 6-8 segments (type dependent) of viral RNA bound[45] to the viral polymerase proteins (PB2, PB1 and PA/P3) and nucleoprotein (NP)[52]. The genome fragments are held in a double helical shape by NP with a central loop on one side[59,68,73]. The RNA in influenza viruses is single-stranded anti-sense (-) RNA, placing them under type 5 of the Baltimore classification of viruses[62,63]. Functionally, this means the RNA must first be transcribed into messenger RNA which can be translated to produce viral proteins. The viral RNA (vRNA) is also segmented and each virion contains 6-8 segments of vRNA[27,75], depending on the type of influenza virus (8 in IAV/IBV and 7 in ICV/IDV). The viral ribonucleoprotein (vRNP) travels to the host nuclease where it undergoes transcription and replication. The vRNA dependent polymerases use host RNA as primers to initiate transcription and replication of vRNA. RNA polymerases lack the proofreading capabilities of DNA polymerase, resulting in cumulative errors or mutations in the viral genome (antigenic drift)[28]. Moreover, the segmented genomes promote reassortment (antigenic shift), whereby genome segments from multiple strains are exchanged inside a co-infected cell[68]. Hence, the viral genome rapidly shifts and selects for more effective strains which can overcome a host's immune system or allow for the infection of a new host[28,45] (**Fig 2**).

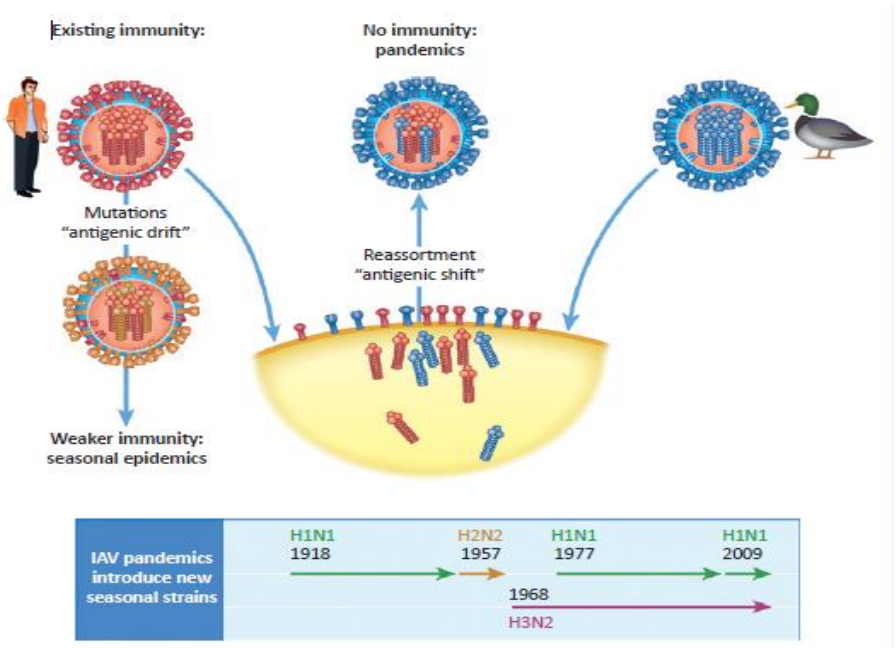

Fig 3. The antigenic drift and antigenic shift of influenza A virus[45]. Antigenic shift is the dramatic change in virus structure due to horizontal genome segment transfer in influenza during coinfection of a host by multiple mutants. While, antigenic drift is the gradual change in a virus due to point mutations over an extended period of time[45].

Influenza vRNA segments typically encode more than one protein and because of the mutation/recombination rates in influenza, the proteins may undergo changes in both structure and function. This makes talking about their genome and the related proteins difficult[28]. However, the protein and genomic profiles of clinically significant types of influenza (IAV/IBV) are relatively well understood, making them good examples of influenza viral metabolism within a host. The influenza A (IAV) strains contain eight, negative-sense, single-stranded RNA segments that are named according to their primarily encoded proteins: Polymerase Basic 2(PB2), Polymerase Basic 1(PB1), Polymerase Acidic (PA), Hemagglutinin (HA), nucleoprotein (NP), Neuraminidase (NA), Matrix protein(M) and Non-Structural protein (NS) (listed from longest to shortest segment)[68]. Similar to IAV, influenza B (IBV) strains have 8 genomic segments which code for the same family if not the identical protein, with the exception of one protein unique to IBV (NB membrane protein)[76]. However, unlike IAV, the two lineages of IBV (Yamagata and Victoria) have distinct genomes which are incompatible with one another resulting in slower antigenic shift or evolution[69]. Influenza C (ICV), the least harmful disease causing type of influenza only has 7 segments with the segment coding for HA and NA being absent in its genome in favor of (HEF) protein[71,75].

For all types of influenza viruses however, vRNA dependent polymerases bind to conserved complimentary regions on the 5' and 3' ends of each vRNA segment, starting transcription. The viral polymerases interact with the C-terminal domain (CTD) of (host) cellular RNA polymerase II which allows them to snatch 5' capped host RNA-transcripts[77]. Host RNA-transcripts are required as primers to start transcription and translation of the viral genome but are not required for viral replication. Viral replication is carried out using complimentary RNA (cRNA) transcribed from the vRNA. The process utilizes a different complex than the one for vRNA transcription[77]. After transcription and replication, the viral components are packaged into exosome like structures that form new virions (**Fig 4**). Only vRNA, not the protein coding or replication intermediate cRNA, is packaged into new virions due to vRNA preferentially interacting with the M1 viral-matrix protein[74]. The replicant viral genome is picked up from the cytoplasm of the host cell by M1 and sequestered into budding virions. Remarkably, the ratios of the 8 segments are roughly equimolar in each virion of (IAV/IBV)[73]. Neuraminidase cleaves the sialic acid-HA linkage releasing the newly formed virions from the cell surface[78].

2.3.3 Method of action

Influenza viruses primarily infect mammals and birds. IAV, IBV and ICV can infect the respiratory epithelium of humans[75]. The haemagglutinin (HA) proteins of IAV, IBV and the haemagglutinin-esterase-fusion (HEF) proteins of ICV bind sialic acid residues on the plasma membranes of cells leading to endocytosis[45] (**Fig 4**). The process of host invasion is started when host proteases cleave the HA precursor HA_0 on the viral envelop into two subunits (HA_1, HA_2)[45,70]. The subunits work in tandem to bind sialic acid residues on host membranes and facilitate endocytoses. However, it isn't until the HA residues interact with the low PH of an endosome that membrane fusion occurs allowing the viral components entry into the host cytoplasm. Natively, the viral genome segments are complexed with nucleoproteins and held within the virion by the M1 viral-matrix protein. Exposure to the low PH in endosomes causes the virion envelope and endosome membranes to fuse and release the viral Ribonucleoproteins (vRNP). In IAV, there is an ion channel (M2) imbedded within the envelope which facilitates the release of vRNP's. The M2 channel allows protons to enter the virion and weaken the bonds between viral components and the M1 matrix, freeing the viral components[59]. Once the components enter the cell, they move to the nucleus of the host to undergo transcription and replication (**Fig 4**).

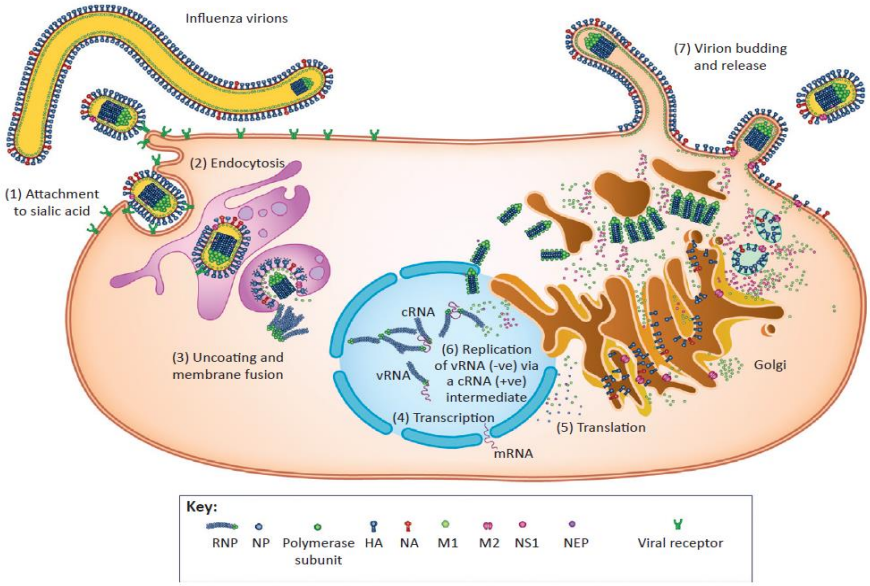

Fig 4. The metabolism of the influenza virus within a host[45]. HA binds to sialic acid residues on the surface of hosts cells. The virion enters the cell and once inside the host nucleus, utilizes host RNA to initiate its own replication. New virus particles are assembled in the cytoplasm and exit via exocytosis, facilitated by NA, lysing the host cell.

Translation of the viral genome results in the production of key viral proteins which play an important role in suppressing host immune responses and facilitating viral metabolism. These proteins are called non-structural proteins. Non-structural protein 1 (NS1) as an example, is a protein found in many viruses and works in several ways to support viral metabolism. In influenza A viruses, it prevents protein (Mov10) activity which removes vRNA's from the nucleus and degrades it[79]. Additionally, NS1 also inhibits interferon production, helps in moving viral mRNA's out of the nucleus and undermines the poly-adenylation of host mRNA, resulting in their premature degradation[79]. However, the activity of NS1 varies between viruses meaning it may display only half or none of the functionality it has in another virus[80]. Ultimately, there are many non-structural and partial-structural proteins in viruses, some are unique like PB1-F2 which is only found in IAV while others have varied activity like NS1. Co-infection with different strains of a virus can readily exchange such proteins between strains, resulting in drastic changes to functionality in viruses (genetic shift)[28]. These proteins are an important component of viral metabolism and can ultimately be what separates a global pandemic from a mild flu.

2.4 Collection, storage, handling and processing of viruses

Influenza viruses are routinely collected from clinal settings[27] and environmental samples[53]. In either case, often swabs are collected and stored in a special medium called viral transport medium (VTM) for safe storage until delivery to the lab for screening[53]. In some environmental samples, large volumes of soil, water or sewage are collected simulations from sites of interest. Samples are also frozen for storage which is necessary to preserve samples but damages virions in the process due to ice crystals being produced during freezing/thawing which rupture virions. Freezing and thawing samples in general is responsible for loss in intact influenza viruses[34] and damage to virus genomes[35]. Hence, many samples and large volumes need to be collected to account for the loss in transport and storage. Without ample intact virus particles or genomes, identification of a virus in a sample becomes challenging. Often times, Dimethyl Sulfoxide (DMSO) is used to prevent extensive damage from ice crystals in viruses but it requires access to liquid nitrogen for snap freezing to prevent any damage from the toxicity of DMSO[34,81]. Once samples arrive in the lab they can be stored and processed further.

Typical storage conditions for viruses are - 80°C for long term storage and 4°C for short term care. Viruses are frozen directly in the medium they are originally collected in. For environmental samples like water, large volumes are collected and frozen until tested. When samples are ready to be identified, they are thawed ideally once and used immediately. The processing required for each identification method varies but typically, in the case of influenza, RNA is extracted (by rupturing virions) from samples first and quantitative polymerase chain reaction (QPCR) is run to determine if any virus is present[53]. QPCR is the most sensitive of the detection methods for influenza and ideal because the presence and concentration of the virus within a sample is unknown[29]. Whether or not the results indicate any virus, frequently enumeration is necessary incase virus is present in minute or undetectable quantities. In the case of influenza, this often involves taking samples and infecting lab grown Madin Darby Canine Kidney (MDCK) cells with viruses to grow them to a sufficient concentration for further use or rescreening via QPCR[48,82]. If no intact virions and only viral RNA are present, this step is impossible as viral structure is highly specialized and necessary for successful infection[45,49,59,77,82]. Furthermore, repeated freeze thaws and storage periods that damage or mutate intact virions[34,35,52] can exacerbate low sample collection volumes and losses in transport. Ultimately, losses in transport, handling and processing steps can accumulate and result in researchers being dependent on enumeration of collected samples using lab grown (MDCK) cells which on its own can result in samples mutating, being contaminated or

changing such as to be a potential source of error[32,52]. Notably, there is a necessity for the development of technologies to aid in virus isolation, concentration and identification to limit losses and dependence on enumeration.

2.5 Identification of viruses

There are several methodologies when it comes to the identification of viruses. These include polymerase chain reaction (PCR) or genome based methods, antigen (viral protein) based methods and infection assays[29]. Each method has unique benefits and limitations which favor the identification of either a known or an unknown virus within a sample[29,83–85]. The most commonly used techniques in influenza identification rely on targeted polymerase chain reactions directed at specific targets in the influenza viral genome[47–49,54,55,86–90]. Similarly, immunological assays for influenza rely on the structure of known proteins (antigens) or antibodies against the proteins located on the surface of influenza viruses. Additionally, there are infection-based methods which depend on a virus's ability to infect and lyse host cells, relying on host cell lysis as an indicator of viral presence[29,30,48]. The sensitivity of these methods vary as well based on the targets and assumptions required for each method[29].

Influenza A is a known virus which is routinely tested for and identified. Clinical methodologies for the identification of the influenza virion are a model for other cases. Additionally, the molecular and genomic techniques for identification can be used in tandem to derive a range of information which would otherwise be ignored by any single method[49,82,91]. The main genomic approach used for the quantification and identification of influenza is called quantitative polymerase chain reaction(QPCR)[47,53,54,86–90]. This procedure is detailed below but in general, it uses probes and primers (RNA oligomers) designed to be analogous for specific conserved regions[59] in the influenza genome (typically M1, NP and HEF genes). The replication of the targeted region is started once a primer binds to its target and this replication of the viral genome is linked to the production of markers or florescence which can be measured in real time. Thus, allowing for the measurement and discovery of the influenza genome in an unknown sample during PCR. Notably, this technique is not sensitive for the discovery of intact or infectious virions, it only focuses on the presence of the targeted region of genome[87]. This dependence on genomes contributes to the sensitivity of this technique as even when no virions are present, you can accurately identify if they were at some point present based on the ruptured remains of a virus which will include its genome (6-8 segments per virion).

Protein and molecular identification methodologies expand upon this shortcoming of genomic methods. Two primary ways to molecularly identify the presence of influenza in an unknown sample are hemagglutination assays and enzyme linked immunosorbent assays (ELISA). In general, the hemagglutination assays utilize the structure of the hemagglutinin (HA) protein on the surface of influenza and its ability to prevent coagulation of blood cells. Alternatively, enzyme-based assays are focused on molecular fragments either present on the surface of influenza or generated as a consequence of influenza infection. These fragments in an ELISA procedure are tested for using antibodies targeting the antigen (Anything that binds to the antibody). Both methods are thus selective for virus structural elements and not just its genome[29,30]. Tissue culturing techniques are the gold standard for the detection of intact and viable virions as they rely on the ability of a virion to infect a range of host organisms[48]. To be infective, the virions must be intact, have their genome and surface antigens. The major downside however to these molecular, antigenic and culture-based identification and quantification strategies is that they are less sensitive or require more viruses to be sampled, stored and present for them to be as effective as PCR based techniques[29]. All of these methods, however, require prior knowledge of a virus or make assumptions regarding their targets. With the issues associated with storage, enumeration, mutation and processing however, there is room for simpler and streamlined strategies that are applicable to a broader range of viruses.

Notably, these detection methods require either primers or reactants designed for a known genome target or reactive elements for and on specific proteins on the viral surface. Additionally, some methods such as HA and infection assays require intact virions to function[29,48]. This necessity limits the ability of such assays to identify an unknown or new virus[29,30,84,90,91]. It is typically after the tests for a known virus are conducted that samples are sequenced in their entirety using whole genome sequencing or other Next Generation Sequencing (NGS) techniques to identify potentially new viruses or mutants. Once a new virus is identified via sequencing, it is then isolated, and its structure and functionality are categorized using various physical methods like electron microscopy. One recent example of this for influenza is the discovery of influenza type D[72]. In summary, many methods exist for the identification and classification of known viruses and new viruses. However, each method has its uses and limitations, but identification of new viruses is a notably different procedure from the identification of a known virus in a sample. In most clinical applications, the latter is a more typical goal.

2.5.1 Quantitative Polymerase Chain Reaction (QPCR)

The polymerase chain reaction (PCR) is a powerful tool used for biological research. All forms of life contain genetic material composed of a combination of 4 nucleotides which encode proteins and metabolic functions necessary for a life form. PCR utilizes enzymes and nucleotides to mimic the in vivo replicative capability of DNA and RNA to amplify (in vitro) sample genetic material from a living organism by several orders of magnitude. Additionally, PCR can be linked with fluorescent probes that bind to specific genome segments (**Fig 5**) and utilized to quantify the amount of target genetic material in a sample[87]. While some of the traditional methods function to quantify the end-products of PCR, modern techniques don't require the handling of PCR products and can quantify a sample in real time as PCR progresses[86,87]. This can be done for both DNA and RNA via a single coupled reaction (reverse transcriptase QPCR) or by turning viral RAN into translated complimentary DNA (cDNA) before the quantification step. In real-time reverse transcriptase quantitative PCR (RT-qPCR) which is typically used for influenza, PCR product is measured at each cycle of RNA replication and compared against a known standard to determine the relative or absolute quantity of genetic material in a sample.

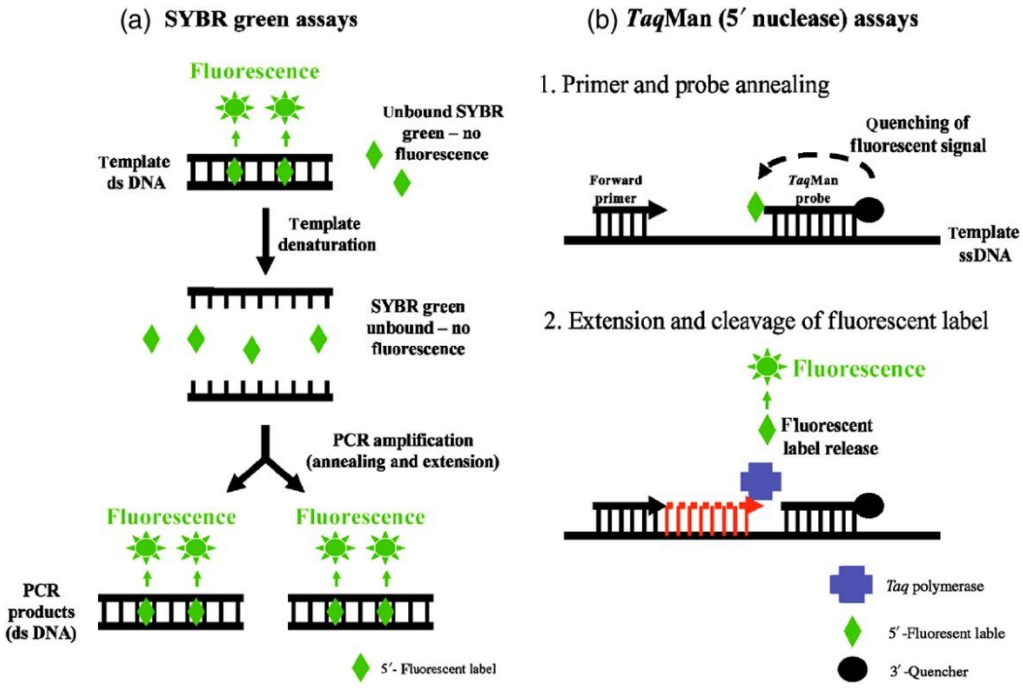

Fig 5. Fluorescence dyes and their method of action for QPCR[83]. (a) details the schematic for SYBR green dye which generally targets the products of the polymerase chain reaction and does not require probes. (b) details the schematic for TaqMan probe based QPCR which utilizes probes bound to dyes which target a specific genome target and are released during the PCR replication step. TaqMan based QPCR is generally more precise due to its use of probes[83,87,91].

QPCR utilizes a thermo cycler which cycles through a fixed range of temperatures to allow enzymes to bind strands of sample DNA/RNA for replication and release daughter strands of DNA or RNA at the end of one temperature cycle for the next cycle of replication. The principal utilized is that PCR doubles the quantity of genetic material at each cycle (of temperatures), which theoretically allows the determination of the initial quantity of genetic material in a sample[86]. In practice, this is done by measuring the amount of genetic material after each cycle via fluorescent dyes which either bind to PCR products (SYBR green) or come bound to PCR primers/probes (TaqMan) which are released during the replication process (**Fig 5**). The fluorescent dyes yield an increasing fluorescent signal proportional to the number of PCR product molecules generated in each cycle. The change in fluorescence over the course of the reaction is measured by an instrument with fluorescent dye scanning capability. By plotting fluorescence against the cycle number, the real-time PCR instrument generates an amplification plot that represents the accumulation of product over the duration of the PCR. This plot can be compared against standard plots of known quantities to determine the starting quantity of any target sample[86,87]. Quantification can thus be relative to a single known standard or absolute as determined by comparison with a range of standards with known starting quantities of genetic material. This process assumes that no non-specific binding occurs between primers themselves or contaminant genetic material present within a sample and that primers match their targets exactly. Samples are typically repeated on different wells and each well is treated as a unique assay to account for the variability in reactions[55,84,87].

For identification, sequence specific primers or probes need to be provided for each target organism to bind to a strand of DNA/RNA and start the replication procedure. In the case of influenza, which has RNA as its genetic material, there are type-specific conserved regions in the viral genome which can be used to quantify and amplify distinct types of influenza (A, B, C or D) present within a sample[59,90,91]. IAV and IBV can be reliably differentiated from one another based on their conserved matrix proteins (M1 gene), meaning a primer for one will not interfere with the other type of influenza[54,88,89]. For selectively quantifying ICV, primers for the hemagglutinin–esterase–fusion (HEF) gene can be utilized as it is unique to ICV. IAV subtyping at a strain level can be done using probes and primers for the different HA (1-18) proteins (HA-NA gene)[90,91]. Similarly, IBV lineages can be distinguished from one another based on their polymerase complex genes (PB2, PB1, PA) which are unique to each IBV lineage[69,90]. Despite such conserved and distinct regions however, it is recommended to separately carry out qPCR for subtyping influenza viruses as this reduces the chances of errors

in estimating counts from overlapping dyes and RNA polymers forming[84,89]. This variability adds to the costs associated with QPCR assays, as multiple sets of primers and probes need to be ordered for each identification/quantification assay depending on the specificity being sought. In summary, primers can be generated for a number of different known regions within the viral genome and if the region is specific to influenza, the primer (shorter primers allow more specificity) can be selectively used to amplify the target and in doing so allow detection and quantification.

While these quantification techniques allow for accurate quantification of virions in a sample, there are drawbacks to using specific primers beyond the initial requirement of needing prior knowledge of the genetic target for said primers. Many assays are burdened with false negativity due to primer dimer formation, mis-priming and or probe-binding failures[83,90]. This results from poor assay design and primers or samples degrading in transport, extraction, or storage[22,32,33,35,55,77,84]. Typically, it is considered good practice to validate PCR reagents and primers, especially in the case of shifting targets like influenza to maintain assay fidelity[55]. Ultimately, PCR based detection methods have accumulating sources of error starting from the samples themselves[32,33,59], the primers used[55,84] and from the assay itself [22,47,55,83,90] which can hinder viral identification and quantification. Initially, there is also a loss in intact virus samples as virions must be ruptured to obtain the virus genome. Following that, data cannot be obtained for viruses not being searched for or viruses which have mutated to an extensive degree. Furthermore, the sample, primers and standards being used in PCR can degrade such as to cause miss priming or errors due to a miss match between any of the reagents[22,35,55,84,90]. While newer PCR techniques can account for many of the issues within the assay itself, they are costly and necessitate a procedure for each virus independently[47,90]. In conclusion, despite the sensitivity offered by QPCR[29], there is room for the development of faster more direct detection methods which can identify a broader range of viruses while leaving them viable for enumeration and further study[46,83].

2.5.2 Infection assays for the detection of live viruses

For human viral pathogens like hepatitis and influenza, the most commonly used technique for the assessment of viral titers or infectious viral load is 50% tissue culture infectious dose or TCID50[49]. The procedure utilizes tissue culturing techniques and can allow for the quantification of viral titers due to the ability of viruses to infect their hosts and cause the lysis of cells. Samples are serially diluted before injection onto lawns of lab grown host cells. The

dilution factor is then compared against which lawns of cell show significant cell lysis in the form of plaques, allowing for the estimation of infective viruses in terms of viral titer/ml of sample used[48,92]. Ultimately, the technique is less sensitive than qPCR and dependent on infection of the host cells[29]. It does not work if no intact viruses are present as virus infection requires surface antigens and the viral genome in[45]. In the case of influenza A and B, the chosen host cells are either epithelial cells from a strain relevant organism or Madin-Darby canine kidney (MDCK) cells which can be adapted to serve as a model for strains of influenza[82]. The cells required for the assay must first be cultured carefully following tissue culturing protocols established by the commercial suppliers or lab protocols for culturing specific tissues. Depending on the plate or apparatus used for the assay, enough cells need to be present to form a lawn of tissue/cells which can require millions of cells to be grown and cared for. Ultimately, infection assays are one of the only ways to confirm the presence of intact virions which are required for the complete study of viruses.

As with other identification techniques, infections assays have their own set of limitations. First and foremost, tissue culturing techniques in general are susceptible to biological variation and are difficult to perform without proper techniques and specialized equipment[51,82]. Additionally, the host and virus must be matched for any infection to take place. In the case of influenza A and B, transformation of HA to its infectious subunit for sialic acid binding can be triggered using external enzymes allowing for the infection of MDCK cells[82]. This is however not possible if a virus is unknown or mutated such that no model host is available for it[33,51,92]. Furthermore, virus samples can be induced to change during storage and transport such that infection is affected[33,34,52]. In summary, while this method only works for viruses which induce lysis in their host, much variability within and between assays can result from environmental factors and factors affecting cell growth or viral infection. This leads to host cells dying due to biological variation, contamination or extraneous variables (false positives). Viruses can also be in too few numbers, mutated or poorly suited to host systems (false negatives). This lack of sensitivity in infection assays[29] causes losses in time and resources. Ultimately, while, infection assays in combination with PCR based techniques can improve viral quantification experiments[48,49], newer methods are necessary to identify unknown non-lytic and intact viruses to reduce dependence on tissue culturing.

2.6 Isolation and concentration of viruses

Often times, isolation and concentration are necessary in virology. This is especially true for vaccine research, purification and production for medical pourposes[21,43,44,93]. Isolation and concentration are also used prior to infection and QPCR analysis to improve the results of identification/quantification or following enumeration to remove cell debris from host lysis during infection[14,15,20]. Notably, the majority of viral isolation and concentration is dependent on ultracentrifugation which is a form of centrifugation which is conducted using a special apparatus with a high powered motor capable of very high revolutions per minute (RPM) for extended periods of time at low temperatures and often under pressure to reach high centrifugal forces (15,000 to >100,000 g). The centrifugal forces result in the deposition of heavier or denser particles in a solution as sediment. Ultracentrifugation can further be combined with density gradients in the form of solutions made with sucrose or caesium chloride (CsCl)[16,36]. When used with density gradients, the technique is referred to as density gradient centrifugation which can be further divided into rate zonal (sample is more dense than gradient solution) or isopycnic (sample is less dense than gradient solution) centrifugation[36]. In both cases however, the centrifugal forces result in the ions of the gradient solution separating within the tube to form a gradient of densities which can cushion or more precisely differentiate a sample. The density gradient present causes elements of a sample placed within or between the gradient solution(s) to differentiate based on their buoyant density relative to its surrounding gradient within a centrifuge tube. Sucrose gradient centrifugation has previously been used to determine estimates of the density of influenza A with varying results (1.014 - 1.257 g/cm^3)[16,19,56,93] based on the methodology, strain of virus, concentration of sucrose used to create the gradients and type of motor used in the centrifuge[18,93]. While density is a factor similar to the proposed methodology of using MagLev for the density based separation of viruses, ultracentrifugation is a long and arduous process requiring specialized equipment and reagents[21,43,44]. A MagLev based system may provide a portable method for isolating viruses with minimal processing[1,8], better virion retention[20,21] and more consistent estimates of viral density due to it being unaffected by particle size[1,7] and a lack of reliance on density gradients[16,19,36,93].

Ultracentrifugation requires the use of very specific density gradients made using precise concentrations of solutions[36]. This can have an have an impact on sample purity and in the case of viruses, their viability after the procedure[21,94]. Additionally, the technology is not widely available to researchers who may wish to pursue viral concentration and isolation or the purification of virus like particles as part of vaccine production[21,43]. Other less precise

techniques which can be used are ultra-filtration[20], filtration using specialized filters[43] and specialized chromatography based on size exclusion or ion exchange[15,21]. While ultracentrifugation is dependant on knowledge regarding the density of a target to be purified and the construction of appropriate density gradients, other methods are more robust. Newer methods are more readily accessable[21] and responsive to the fact that virions are complex pleiomorphic structures containing variable ratios of both viral and host proteins[44]. Ultimately, there is a growing focus on the accuracy of viral isolation and concentration to create more robust methods for finding novel viruses and mutants from samples. Ultracentrifugation has thus far been one of the most precise methods of virus isolation (~66% yield)[20] but industries are seeking more reliable techniques such as liquid chromatography and tandem mass spectrometry (LC-MS/MS) for working with large volume of known viral agents[44]. MagLev however, may offer a more direct and cost-effective method for viral isolation and concentration which can be used in non-industrial settings for high yields of minimally-processed intact virions. As highlighted, this can significantly improve detection and direct study of viruses such as influenza.

2.7 Magnetic levitation

Magnetic levitation (MagLev) or magnetic suspension is the phenomenon responsible for an object being suspended without the application of any external support other than magnetic fields. This suspension is mainly due to the Magnetic forces generated as a consequence of electrical current or the interaction of magnetic fields with each other or an electrical current[95–97]. In magnetic levitation, the magnetic force generated is being used to counteract the effects of gravitational acceleration and any other accelerations. To achieve stable levitation, there are two main issues which need to be addressed which include lift and stability. There is a need for lifting forces to provide an upward force sufficient to counteract gravity, and stabilizing forces to ensure that the system does not spontaneously slide or flip along the rotational axes into a configuration where the lift is neutralized or changed [95]. Its modern applications are numerous and show potential for its use in a system for the isolation of viruses[1,98].

2.7.1 Conventional magnetics

The study of magnetism dates back thousands of years to ancient Greece or even earlier[96,97]. However, what we consider to be modern magnetics and electromagnetism is the culmination of work conducted by Frenchman Andre Marie Ampere (1775-1836), Englishman Michael

Faraday (1791-1869), Scotsman, James Clerk Maxwell (1831-1879) and lastly Englishman Oliver Heaviside (1850-1925). These scientists provided the theoretical foundation for the physics of electromagnetism in the nineteenth century by showing that electricity and magnetism represent different aspects of the same fundamental force field[97].

In modern physics we study magnetic and electrical fields in parallel. This is because, under the unified theory of electromagnetism they are aspects of the main observable source of energy in the universe and together form the electromagnetic spectrum[96]. There are some significant overlaps and fundamental concepts which we need to consider when studying electric and magnetic fields. Similar to how electric charges exist in pairs of positive and negative, magnets exist as dipoles which we call north and south. However, unlike charges magnetic dipoles cannot exist on their own, they form a closed loop field where magnetic field lines extend from one pole and procced to the other in a circular fashion (**Fig 6**). Charges, however, can and do exist on their own and produce electric fields which can be open ended with the electric field extending from the positive charge and going to the negative[96,99]. The electric field at a particular point is in the direction of the force a positive charge would experience if it were placed at that point. Similarly, the magnetic field at a point is in the direction of the force a north pole of a magnet would experience if it were placed there. Hence, the north pole of a compass points in the direction of its magnetic field. Consequently, we can consider electric and magnetic fields as vector quantities having both a direction and a magnitude. The fields are unified however in that magnetic fields arise as a consequence of the movement of electric charges[99,100].

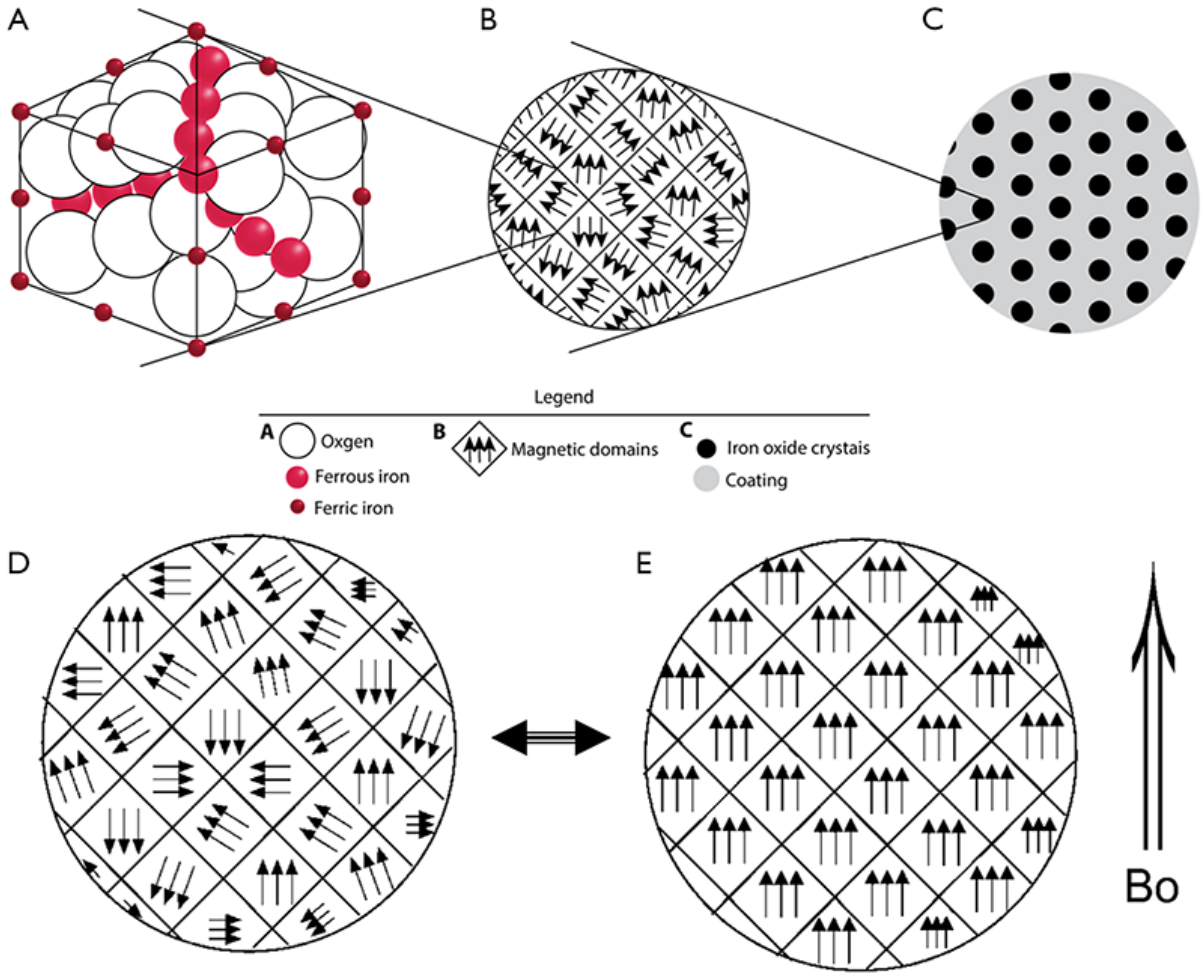

Fig 6. The alignment of magnetic domains in Iron Oxide. (A) the structure of iron oxide, (B) unaligned magnetic domains in iron oxide, (C) the structure of iron ions without oxygen. Magnetic domains in iron (D) and their alignment (E) as a consequence of the application of an external magnetic force B_o[101]

It was shown in the 19th century that magnetic fields arise as a consequence of molecular scale electron flow (electrospinning or current) within a material. In a permanent magnet, the magnetic field comes from the motion of the electrons inside the material, or more precisely, from something called the electron spin [99,100]. This rotation of free and unpaired electrons in the outer most shell of an atom around the nucleus resembles the rotation of the earth around the sun and its own axis. This movement of electrons under Faradays Law ($\vec{E} = - d\vec{B}/dt$) would result in the production of a weak magnetic field[99]. Individual molecular scale magnetic domains arise due to the atomic spin of free electrons present around most if not all known elements of the periodic table (**Fig 6**). The magnetic fields generated, cancel out if the electrons are paired in their orbitals with one moving opposite to the pair and cancelling out any resultant effects. What separates most weakly induced magnetic materials from strong or ferromagnetic

materials is the alignment and availability of free electrons which can spin independent of a pair[102,103]. Strong or ferromagnetic materials have more free electrons in their outermost shell which have the ability to enter into spin orientations which favour alignment in one direction thus producing strong and externally relevant magnetic fields. These molecular magnetic domains however are not always inclined to face in the same direction and produce external magnetic fields. The process of aligning or rather favouring the alignment of molecular magnetic domains so that they produce a strong magnetic field is called magnetization[96,103]. How easily a material is magnetized so that most of its internal molecular magnetic domains are in one direction is referred to as its magnetic susceptibility or coercivity[99,103,104].

Exposure to a modest magnetic field, heat or external current encourages the alignment of molecular scale microdomains such that most of the individual magnetic fields in a given material will align with the current generated magnetic field or applied magnetic field resulting in a non-magnetic material being magnetized[103]. Only permanent or ferromagnetic materials are able to retain this property and usually require strong stimulus to affix this property to themselves. In naturally occurring materials, while there may be an abundance of free electrons which in certain circumstances align themselves to a domain resulting in weak magnetic properties. Natural magnetic properties are weak due to bulk effects where several naturally occurring magnetic domains cancel each other out as they are not all aligned in one direction[99,102]. A number of factors are required to fix a material to retain its magnetic field. Some materials are consequently more inclined to magnetisation (magnetically susceptible) than others due to their ability to maintain electron movement within fixed domains. These properties of magnetic forces lend themselves to a variety of physical phenomenon and represent a diverse range of interactions and magnetic properties[7,103].

Knowing now that magnetism is linked to the electrons within atoms on a quantum scale[100] we can better understand and explain how a diverse array of electromagnetism exists. The major types are summarised in **Table 1**. The main differentiating features between these magnets is their ability to retain their magnetic properties and how they behave when placed within a magnetic field[7,99,103]. The three major forms that magnetism can take are Ferromagnetism, Para-magnetism and Diamagnetism. Ferromagnetism is the basic mechanism by which certain materials (such as iron) form permanent magnets (**Fig 6**) and para-magnetism is the form of magnetism whereby some materials are weakly attracted by an externally applied magnetic field. The main difference between ferro and para-magnetism is that ferromagnetic materials can be considered as permanent and strong magnets whereas paramagnetic materials do not

retain magnetic properties unless a current or external stimulus is applied. Both notably result in strong attractive force[103]. Diamagnetism is the most unique of the three forms of magnetism due to it generating the weakest force and the force being repulsive in nature. It is often defined as a quantum mechanical effect that occurs in all materials, due to non-permanent electro-spin alignment at an atomic level. It is typically suppressed by other stronger forms of magnetism in magnetic materials but when it is the only contribution to the magnetism, the material is called diamagnetic[99,102,105].

Table 1 Overview of major types magnetism and their properties[99,103]

Type of magnetism	Type of force experienced within a magnetic field	Strength of force	Type of material	Magnetic Coercivity/susceptibility
Ferromagnetism	Attractive	Strong	Permanent or induced magnets	High
Paramagnetic	Attractive	Strong	Induced magnets	High
Diamagnetism	Repulsive	Weak	All matter	Low

Diamagnetism is an innate property of all matter. This includes biological materials which can be coerced into displaying magnetic properties due to the presence of moving electrons in all matter[1,2,7,9]. Compared to other forms of magnetism, diamagnetic materials will only experience a weak repulsive force that goes against and resists the flow of very strong magnetic field lines when presented with a strong enough magnetic field. Only ferromagnetic materials however can hold their strong magnetic dipoles or permanent magnetic properties. Hence, diamagnetism is relevant to more materials, but the three forms of magnetism exist on a hierarchy with the stronger form of magnetism dominating the weaker and overtaking its effects.[99,103]

All types of magnets and magnetism have been used to generate lift for magnetic levitation. These include permanent magnets, electromagnets, diamagnetism, superconducting magnets and magnetism due to induced currents in conductors. The magnetic force or pressure exerted by a magnetic field on a superconductor can be calculated using Equation 1:

$$\boldsymbol{P_{mag} = B^2/2\mu_0} \quad \textbf{(Equation 1)}$$

Where P_{mag} is the force per unit area in Pascals, B is the magnetic flux density just above the superconductor in Teslas and $\mu_0 = 4\pi \times 10^{-7}\ N \cdot A^{-2}$ is the permeability of a vacuum[95,99].

2.7.2 Types of magnetic forces

There are some key considerations when we look at magnetic levitation and the forces responsible for the phenomenon. Samuel Earnshaw in 1842 proved that a collection of point charges cannot be maintained in a stable stationary equilibrium configuration solely by the electrostatic interaction of the charges[106]. This theorem when applied to electromagnetism and its special case of magnetic levitation means that no magnetically levitating system can stabilize itself on lift forces alone. Any levitating magnet levitating due to permanent or induced magnetism will eventually flip over to face opposing poles together to strengthen the overall magnetic field[106]. This theorem has been demonstrated experimentally and is consistent in its outcomes[107]. Magnetic suspension cannot be maintained without an external stabilizing force to keep a levitating object in a levitation equilibrium. Thus, there are two overarching sets of forces we must consider when it comes to traditional magnetic levitation systems, which are the levitation forces that are generating upwards lift and the forces responsible for stabilizing the levitation[95,96].

One of the clearest examples of magnetic levitation where sets of forces are required to successfully levitate a material is the case of MagLev trains. MagLev trains utilize electro-magnets with computer feedback or servomechanisms to constantly adjust and limit the strength of electrical currents, so the magnets used within the train maintain a constant stable levitation[95,108]. This example highlights dynamic equilibrium where magnetic levitation is achieved through a constant adjustment of the forces at play to maintain a constant levitation. There are typically multiple forces which need to be considered when talking about magnetic levitation, not just the effect of lift cancelling the acceleration due to gravity (**Fig 7**).

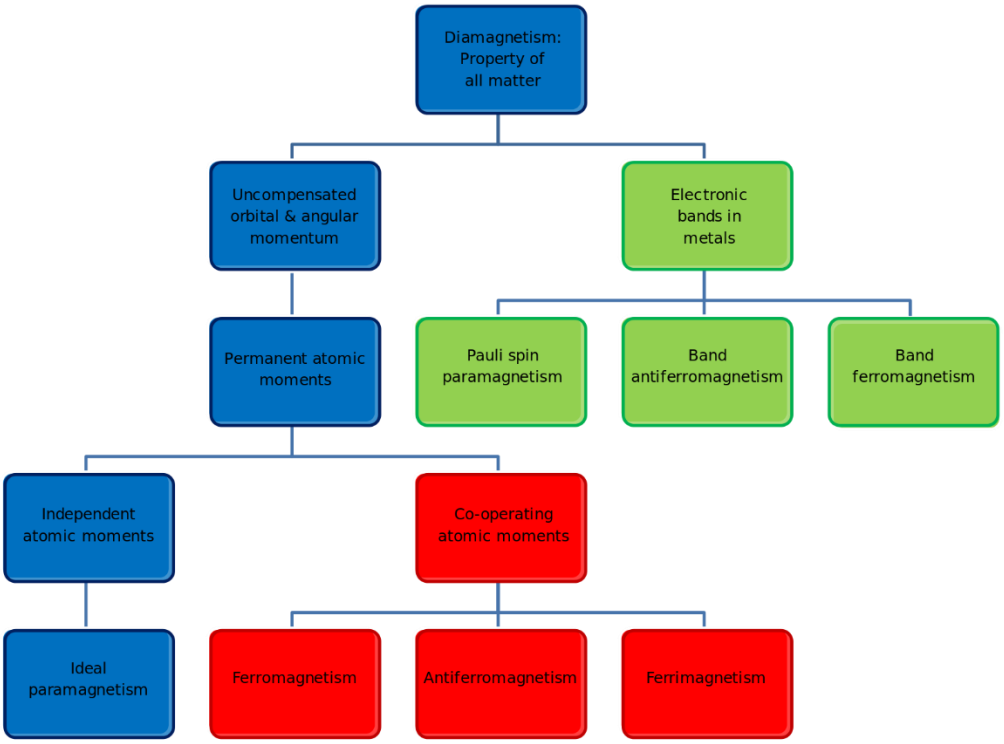

Fig 7. The hierarchical family tree of magnetic forces and magnetism[102]. The top of the tree is diamagnetism which is the weakest (blue) form of magnetism present in all matter. All subsequent magnetic properties stem from diamagnetism and cancel out weaker (green) magnetic effects in favour of the stronger (red) magnetic forces when they are present[96].

The fundamental equations for describing magnetic fields and forces are derivatives of the three Maxwell-Heaviside equations[97]. Here in we can start with the Lorentz force law which describes the relationship between charge, magnetic field and force (**Equation 2**).

$$\vec{F} = Q\vec{E} + Q\vec{V} * \vec{B} \quad \textbf{(Equation 2)}$$

Where $\vec{F}$ is the force experienced in Newtons (N), Q is the charge in Coulombs (C), $\vec{E}$ is the electric field or force exerted per unit column charge (NC^{-1}), $\vec{V}$ is the velocity of a charge in (ms^{-1}) and $\vec{B}$ is the magnetic flux density measured in Tesla (T)[96,99]. This equation describes the relationship between force and electromagnetism wherein a force is generated when a charged particle moves along the perpendicular of a magnetic field or an electric field. Both electric and magnetic field components can generate a force independent of one another. Additionally, this equation can help to explain that under any given circumstance a force can be experienced either due to an electric field or a magnetic one depending on the relative frame.

Hence, electromagnetic forces can be due to either electric or magnetic fields and this switch is dependent on the frame from which the force is being considered or observed[95–97,99,102].

For our case pertaining to MagLev of materials using a magnetic field, we can choose to only consider the magnetic side of the equation and derive a relationship between force, magnetic susceptibility and change in magnetic field strength over distance. This relationship can be described by Equation 3.

$$\vec{F} \sim \chi * H \frac{\partial H}{\partial X} \quad \textbf{(Equation 3)}$$

Where $\vec{F}$ is the force generated or experienced by the material in Newtons (N) and χ is the magnetic susceptibility of the material being levitated. Since, all materials are magnetic and either provide a $\chi > 0$ (para-, ferri- or ferromagnetic) or $\chi < 0$ (normal state diamagnetism, superconductivity)[2]. H here represents the magnetic field strength measured in amperes per meter (Am^{-1}) which is different from but related to magnetic flux density $\vec{B}$. The $\frac{\partial H}{\partial X}$ portion of equation 3 shows that the force generated is directly proportional to the change in magnetic field strength. This equation shows a simple relationship where in a magnetized object can experience a force proportional to the change in magnetic field strength and its own magnetic susceptibility [2,98].

Equation 3 can be further utilized in explaining the specifics of magnetic levitation. Since all materials can have diamagnetic properties under Lenz's Law[99], magnetic levitation can be performed upon any material[1,7,9,12,98]. The success then of magnetic levitation of a material is directly proportional to its magnetic susceptibility or permeability. The magnetic permeability $\mu_m$of a material is related to the magnetic permeability of space μ_0 and K_m the relative permeability of the material (Equation 4)[96,102].

$$\mu = \mu_m = \mu_0 * K_m \quad \textbf{(Equation 4)}$$

The magnetic susceptibility x of a material in equation 3 is just the relative permeability of the material minus one (Magnetic susceptibility: $\chi_m = K_m - 1$). Looking back at equation 3 we can further develop our understanding by considering the relationship between flux density $\vec{B}$ and the field strength H[96,99]. As previously mentioned, when considering two magnets acting upon each other, it is important to isolate the effects of the external magnetic forces and the magnetic

forces resulting from within a material. This is where the distinction between flux density $\vec{B}$ and the field strength H is important. This relationship is presented in equation 5.

$$\vec{B} = \mu_m * H \quad \textbf{(Equation 5)}$$

Magnetic flux density $\vec{B}$ (flux per unit area Wb/m^2) measured in Tesla (T) is the product of a magnetic field of strength H amperes per meter (Am^{-1}) experienced by a material with magnetic permeability μ_m (NA^{-2}).

Taking the formulas and concepts we have discussed thus far we can take equation 3 and equate it to the force of gravity such that it cancels or exceeds the force of gravity. This forms the basis of the lifting force $\overrightarrow{F_m}$ required for magnetic levitation[1,2,98]. This force is represented by Equation 6.

$$\overrightarrow{F_m} = \vec{\mu}(\nabla \cdot \vec{B})$$

$$\vec{\mu} = \frac{\chi}{\mu_0} V\vec{B} \text{ (magnetic moment)}$$

$$\Rightarrow \overrightarrow{F_m} = \frac{\chi}{\mu_0} V\vec{B}(\nabla \cdot \vec{B})$$

$$\overrightarrow{F_m} = \frac{\chi_s - \chi_m}{\mu_0} V\vec{B}(\nabla \cdot \vec{B}) \quad \textbf{(Equation 6)}$$

The calculation for $\overrightarrow{F_m}$ is as follows where $\vec{B}$ is the magnetic field and ∇ the vector component and χ is the magnetic susceptibility for either substrate being levitated (χ_s) or medium in which levitation is occurring(χ_m). μ_0 is the permeability of free space/vacuum. Equating $\overrightarrow{F_m}$ in the equation to 9.81ms^{-2} or the force of gravity completes equation 6 where in $\mu_0 = 4\pi\times10^{-7}$ N·A^{-2} is the magnetic permeability of a vacuum and χ_s is the magnetic susceptibility of the lifted object and χ_m is the magnetic susceptibility of the medium where in the levitation is occurring such as air or water. $\vec{B}$ is the magnetic field in Tesla (T)[24,98]. Lastly V is the volume of the magnet (m^3). We must also consider the fact that magnetic forces exist in three-dimensional space but all of the equations we have considered thus far are two dimensional[96,99]. Equation 6 can be rewritten so that $\nabla \cdot \vec{B}$ is a vector considering the magnetic flux density or total magnetic field change occurring along each of the three axes of $\vec{B}$ (x, y and z). Additionally, tensors can be utilized in calculations requiring the consideration of electric and magnetic fields

simultaneously in three dimensions. Those calculations however exceed the scope of this work[96,100,102].

As stated earlier, two types of forces are required to stably levitate materials using magnetic levitation. One is the lifting force which has previously been described. The secondary force is a stabilizing force required to maintain levitation. In our work we circumvent the need for a secondary stabilizing force by using diamagnetic levitation which is inherently stable[1,2,106]. Our scheme works due to biological material experiencing diamagnetic forces which are repulsive in nature and counteractive to an external magnetic field[1,2,4,6,8]. This is due to Lenz's law which states that; when a conductor is presented with a time-varying magnetic field, electrical currents in the conductor are set up which create an opposing magnetic field that causes a repulsive effect[96,99]. This phenomenon carries itself out on a molecular scale as well. The orbital motion of electrons creates tiny atomic current loops, which produce magnetic fields. When an external magnetic field is applied to a material, these current loops will tend to align in such a way as to oppose the applied field. This property of diamagnetism is present in biological agents like eukaryotic and bacterial cells[1,4–6,96,97]. Like the example of the magnetic train that uses computers to dynamically stabilize the magnetic lift using feedback loops, diamagnetic MagLev systems inherently utilize reverse feedback from Lenz's law to stabilize their levitation.

2.8 Applications of magnetic levitation

Magnetic levitation has been effectively used in various applications. The most commonly known applications are linear induction motors and in transport systems[97,99]. Other applications can be broken down into applications in industry, for separation of microscale materials and biology[2]. Industrial applications can be further broken down into mining and purification applications. Minerals are typically found as ores with varying degrees of contamination. One of the simplest industrial applications of magnetic levitation involves using strong magnets to levitate ore such that more metal rich fragments of ore can be separated from dirt, silt and clay which are by-products of the mining process[2]. A simple schematic of this process is shown in (**Fig 8**) wherein a magnetic field differentially interacts with fragments of ore containing more magnetic ore. The more magnetic or denser particles will be levitated differently in a solution and hence can be separated easily[2].

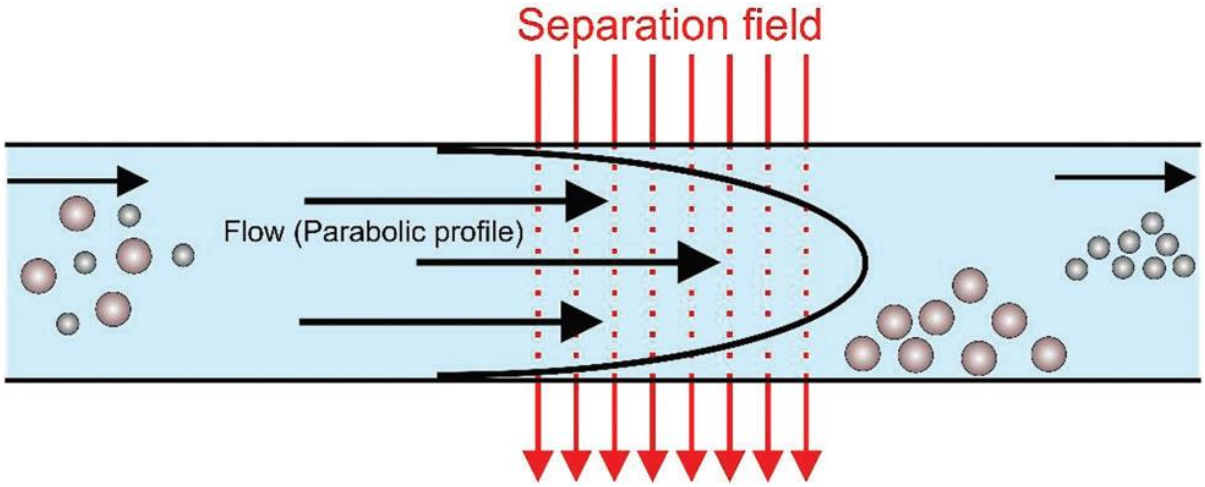

Fig 8. Schematic view of a field-flow fractionation channel. The figure showes the cross section of separation for magnetic particles where the laminar flow provides a parabolic velocity distribution[2].

Another unique application of magnetic levitation in industry is contactless heating[7,108]. In this process, materials are first levitated using electromagnetism so that they are not in contact with any direct surface. Following levitation, the material is heated using induction, where heat is generated within the material using strong and constantly changing magnetic fields. This can be achieved simply by utilizing a solenoid with a strong alternating current. As stated in Lenz's law, the levitated material will experience an opposing magnetic field and current as a result of the changing external magnetic field. The changing electromagnetic field results in the production of eddy currents which in a conductor can result in dissipated heat energy[96,99,102,108]. The energy here results from electrons colliding across a conductor's internal molecules which offer resistance to the electron flow. The higher the resistivity of a material the more Joule heating or energy conversion from current to heat will occur. Furthermore, the strength of the external magnetic field will directly affect the heating process. In summary, a conducting material can be magnetically levitated and heated to melting temperatures using electromagnetism[11,107]. This process also benefits from the fact that magnetic levitation can lift materials in solid, liquid and gaseous phase away from contact surfaces[2]. During the heating process, contact surfaces can cause contamination or changes to the material being heated. Contactless heating is thus an important application of magnetic levitation as it minimizes contamination and can allow for the study of small quantities of rare materials in their purest form[6,98,107].

The key property that has underlined the previous two examples and benefits them greatly is the ability of magnetic levitation to differentially levitate materials based on their physical properties such as density. This can be shown using equation 6 by taking some additional

considerations[1]. Primarily, for magnetic levitation we can equate the sum of the force of gravity and the opposing lifting force due to magnetism to zero ($\vec{F}_{gravity} + \vec{F}_{mag} = 0$). We can also equate the force of gravity $\vec{F}_{gravity}$ in Equation 6 to $\overrightarrow{F_{g1}} - \overrightarrow{F_{g2}}$ and subsequently (using newtons second law of motion) that to $\rho_1 V\vec{g} - \rho_2 V\vec{g}$ due to buoyancy experienced by a particle in a known volume V. Buoyancy is the resultant upward force experienced due to gravity $\vec{F}_{gravity}$ (newtons third law) acting on an object in a medium such as water or paramagnetic solution. By including these considerations, it can be shown mathematically (Appendix calculation 1) that the levitation height of a material is directly related to the density Po of a material suspended in a paramagnetic material between two like facing poles. This is presented as equation 7.

$$\overrightarrow{F_m} = \frac{\chi_s - \chi_m}{\mu_0} V\vec{B}\left(\nabla \cdot \vec{B}\right) \geq \vec{\boldsymbol{F}}_{\boldsymbol{gravity}} \quad \textbf{(Equation 6)}$$

$$\vec{F}_{gravity} = \overrightarrow{F_{g1}} - \overrightarrow{F_{g2}} \quad \text{(Buoyancy)}$$

$$\vec{F}_{g} = m * \vec{a}_{gravity} \quad \text{(Newtons second law)}$$

$$M = V * \rho \quad \text{(Archimedes' principle)}$$

$$\vec{F}_{gravity} = \rho_1 V\vec{g} - \rho_2 V\vec{g}$$

$$\overrightarrow{\boldsymbol{F_m}} = \frac{\chi_s - \chi_m}{\mu_0} \boldsymbol{V\vec{B}}\left(\boldsymbol{\nabla} \cdot \vec{\boldsymbol{B}}\right) = Vg(\rho_o - \rho_m) \text{ (Solve for 7)}$$

$$\boldsymbol{\rho_o \sim \rho_m} + \frac{(\chi_o - \chi_m)}{\mu_o * \boldsymbol{g}} * \boldsymbol{V}(\vec{\boldsymbol{B}}.\vec{\boldsymbol{\nabla}})\vec{\boldsymbol{B}} \quad \textbf{(Equation 7)}$$

Where g = 9.81ms^{-2} or is the acceleration due to gravity, ρ_m is the density (g/cm^3) of the medium the levitation is occurring in, ρ_o is the density of the object being levitated and μ_o = $4\pi\times10^{-7}$ N·A^{-2} is the magnetic permeability of a vacuum. $\boldsymbol{\chi_o}$ is the magnetic susceptibility of the lifted object and $\boldsymbol{\chi_m}$ is the magnetic susceptibility of the medium wherein the levitation is occurring such as air, water or paramagnetic solution. $\vec{\boldsymbol{B}}$ is the magnetic flux density in Tesla (T), V is the volume of the magnet (m^3) and the vector product $(\vec{B}.\vec{\nabla})\vec{B}$ represents the change in magnetic field strength along a three-dimensional axis[1]. Further considerations can be made to equate the right-hand side of this equation to the levitation height of an object. These considerations are represented in the simple schematic shown in (**Fig 9**) which displays the

capabilities of magnetic levitation to even levitate diamagnetic materials using conventional magnets to heights proportional to the materials density.

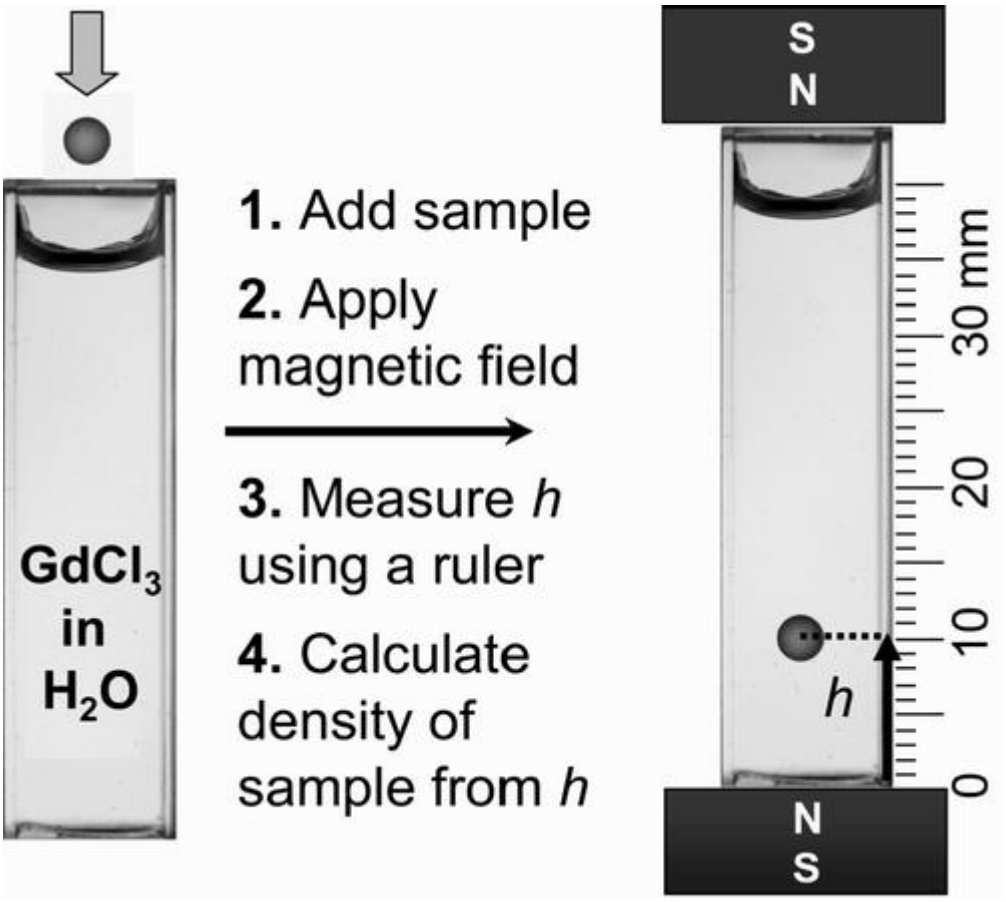

Fig 9. Schematic illustration of a density measurement by a MagLev device. (1) Diamagnetic particle is placed in the paramagnetic medium ($GdCl_3$). (2) A magnetic field is applied. (3) The levitation height h is measured. (4) The density can be calculated from visibly assessing h[12]

Thus far we have only looked at magnetic levitation in free space which is a poor conductor of magnetic fields. One easy work around to improve magnetic field strength is to utilize a paramagnetic solution[1,2,98]. A paramagnetic solution consisting of ions which are easily magnetized and can conduct magnetic fields much more consistently and powerfully than a solution that isn't magnetic or free space. This is due to paramagnetic materials experiencing attractive forces and aligning their magnetic domains with an externally applied magnetic field and sometimes even amplifying the effects of the applied magnetic field[24,96,101,102]. Thus, placing poor or non-magnetic materials into a paramagnetic solution more readily induces diamagnetism in a material as the externally applied magnetic field is more concentrated and amplified by the solution. This is shown in the schematic of (**Fig 9**).

The other major consideration made to link levitation height with density is the inclusion of a secondary and equally powerful magnet above the first one such that the like N poles face each other in an anti-Helmholtz configuration[109]. This simple inclusion removes the x and y dimensional components of the magnetic field such that they are cancelling each other out upon their interaction, leaving only one axis of symmetry and consequence[1]. Previously we described the three-dimensional vector product $(\vec{B}.\vec{\nabla})\vec{B}$ which can be shown as equal to $(\vec{B}_x\frac{\partial\vec{B}_z}{\partial x}+\vec{B}_y\frac{\partial\vec{B}_z}{\partial y}+\vec{B}_z\frac{\partial\vec{B}_z}{\partial z})$ for determining the final product of the interaction of magnetic flux in three separate dimensions. With the addition of a second magnet as shown in (**Fig 9**) the product is reduced to $(\vec{B}_z\frac{\partial\vec{B}_z}{\partial z})$, where Z is the only significant field component and axis of symmetry. Additionally, there is now a region of the system set up such that it has magnetic field = 0 present where the magnetic fields cancel each other out in the middle of the system where they meet. Given this case, we know that the magnetic field component Z can be determined using the formula $\vec{B}_z \sim B_0 - \frac{-2B_0}{d}z$ wherein B_0 is the magnetic field strength at the surface of our magnet and d is the distance between the magnets[1,12,98]. Placing this substitution in equation 7 can give the relationship between the levitation height of a diamagnetic object being levitated in a paramagnetic medium and the density of the diamagnetic object (Equation 8).

$$\boldsymbol{h} = \frac{(\boldsymbol{\rho_o - \rho_m})\,\mu_o\, \boldsymbol{g d^2}}{(\chi_o - \chi_m) * \boldsymbol{4\vec{B}_0^2}} + \frac{\boldsymbol{d}}{\boldsymbol{2}} \quad \textbf{(Equation 8)}$$

Where h is the levitation height (mm), d is the distance between the magnets (mm), g is the acceleration due to gravity, ρ_m is the density of the medium the levitation is occurring in, ρ_o is the density of the object being levitated and $\mu_o = 4\pi\times10^{-7}$ N·A^{-2} is the permeability of free space. $\boldsymbol{\chi_o}$ is the magnetic susceptibility of the lifted object, $\boldsymbol{\chi_m}$ is the magnetic susceptibility of the medium where in the levitation is occurring and $\vec{B}_0$ is the magnetic flux density at the surface of the magnets in (T)[1]. The complete derivation for all calculations are also presented in this thesis (**Appendix B**).

The density-based separation of materials is a very useful application of magnetic levitation, allowing for the fine scale separation of materials[6–8]. This property has been put to use in a number of fields because it can be done with any type of material as most materials have diamagnetic properties. In our case, we will focus on the biological applications in the coming section and elaborate on its potential.

2.9 Applications of magnetic levitation in biology

Magnetic levitation has been used in a diverse array of biological applications. These range from developing targeted antibody assays, testing the contents of plasma or food and developing novel strategies for culturing highly specific tissues[1,2,4–6,8]. The simplest example is the use of magnetically active antibodies for targeting specific substrates. The magnetically active antibodies can be levitated or simply attracted using a magnet to isolate target substrates from solutions and complex mixtures. This process is shown in (**Fig 10**). Additionally, using the density based levitation described in the previous section, it is possible to separate complex substrates such as proteins and drugs from a variety of different samples such that they can be visually observed as independent points within a MagLev system and subsequently extracted for further analysis[1,8]. This can be seen in (**Fig 11**).

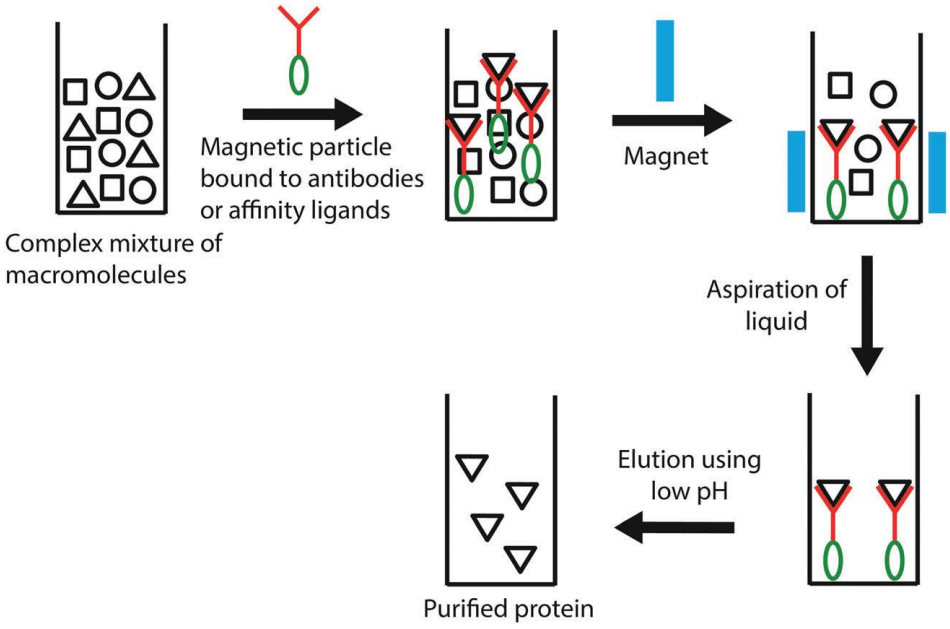

Fig 10. Magnetic separation of macromolecules from complex mixtures using magnetic antibodies. The addition of magnetic particles to affinity ligands or antibodies will allow isolation by use of a magnet and promote the separation process of protein purification[2].

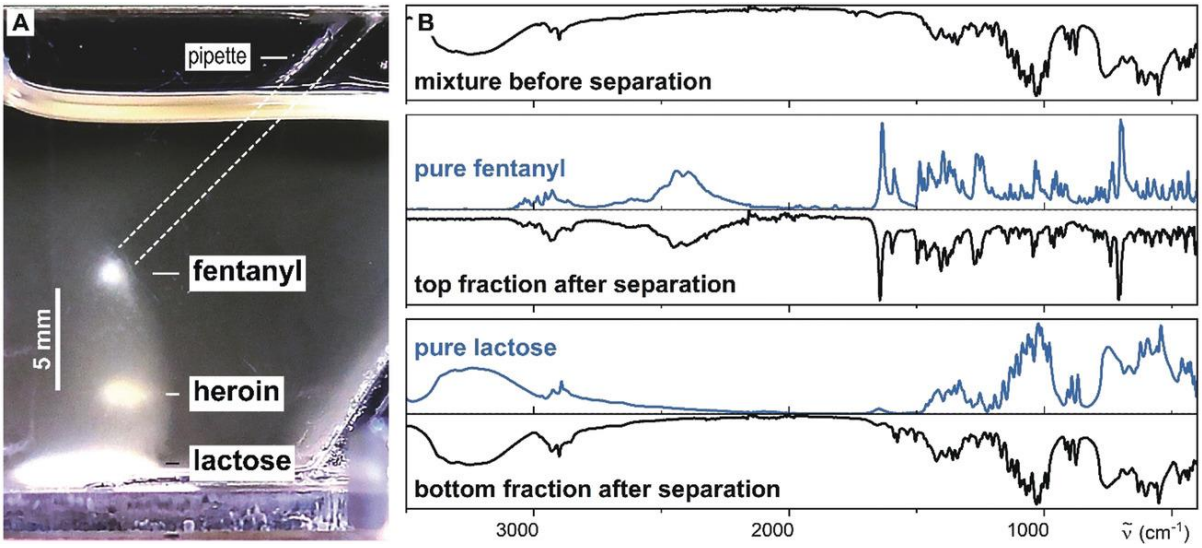

Fig 11. Successful separation and presumptive identification of fentanyl using MagLev. A) an image taken after 30 min of separation by MagLev of a powdered mixture of fentanyl-containing heroin (fentanyl·HCl (1.3 wt %), heroin·HCl (2.6 wt %), and α-lactose (96.1 wt %))[8]. B) The separated fractions were extracted, rinsed and FTIR-ATR spectra (normalized to the highest peak) were measured from the powdered mixture before separation (top spectrum) and after separation. The extracted fractions containing fentanyl and lactose (lower two black lines), and the pure compounds (blue lines) are shown below the spectra for the unseparated mixture. Following extraction, the spectra (black) match the pure drugs spectra (blue)[8].

These biological applications and many more are possible due to magnetic forces being non-invasive in nature. They do not utilize ionizing radiation, are not cytotoxic and rarely contribute to permanent changes in structure, particularly in the case of diamagnetism which is an especially weak form of electromagnetism[1,6,11]. Moreover, during magnetic resonance imaging human bodies are routinely exposed to strong magnetic fields which far exceed natural sources of magnetism without experiencing major issues[10]. These properties of MagLev lend themselves well to delicate and precise biological application. One such application is in tissue culturing which is best highlighted with the recent development of three-dimensional levitation-based tissue culturing techniques[4–6]. This is similar in principal to contactless heating, as tissue culturing is dependent on surface interactions and also prone to contamination. In many such studies of levitating living material, it is notably not the magnetic forces which effect cell death but the ionising paramagnetic solutions being used[6]. In summary, there has been a steady stream of applications for MagLev in biology since the initial demonstration that bacterial cells and proteins can be levitated using diamagnetism in real-

time[79,81]. Magnetic levitation, thus, can produce separation on a fine enough scale to differentially levitate different types of cells and allows the specific culturing of a single tissue while minimizing the effects of containers and surface interactions[4,6]. It is plausible than that viruses which have proteins and structures like cells can also be levitated, opening the door for future work relating to that application.

2.10 MagLev for the levitation of viruses

The goal of magnetic levitation of biological matter has been an ongoing process with success in various applications [1,2,4–9,31]. No experiments and methodologies however have looked at the potential of directly using magnetic forces for isolating or levitating viruses which are much smaller than other living tissues. This is in spite of the role of viruses as major sources of disease and global change[25,38,40,46]. While previous methods have relied on specific particles for binding viruses and then used magnetism for the purposes of separating viruses, this method does not use MagLev directly and require special proteins and knowledge of targets[11]. Consequently, these techniques do not benefit from the insights which can be obtained from MagLev[98] nor utilize the potential of stable contactless levitation[108]. As mentioned, one primary goal of this work is to determine the density of a virus (influenza) and develop a levitation platform which can be used with unknown samples for naïve viral identification, concentration and isolation for culture and study. Thus, addressing the identified gaps in molecular and genetic techniques routinely used in virology.

Given the non-invasive nature of magnetic forces and the reliability with which magnetic levitation can isolate all shapes and sizes of matter, we hypothesis that it would be possible to levitate viruses at a specific height within a MagLev column. Once levitated, the density of a virus can be known and if the virus is intact, it can be studied with regards to its whole structure, function and its interactions characterized in a novel way. With the growing use of magnetic levitation as a cost-effective way to culture and study biological materials[4,6], it is then a worth-while goal to develop and test such an application. To date, no prior research has merged viral identification and culturing techniques to test if viruses can be reliably levitated using diamagnetism. We aim to test the levitation properties of viruses and then show experimentally whether viruses can survive the levitation procedure.

Chapter 3. Materials and Methods

3.1 Aim 1: Investigate if viruses are levitated within the MagLev

3.1.1 Novel MagLev design and application

For our work with viruses, we sought to minimize the factors which may damage or limit our capacity to isolate viruses. Hence considerations were taken in the design of the MagLev system to increase magnetic force and resolution, utilize biologically inert and popular paramagnetic solutions available to prevent unwanted loss in viral load and create a practical system to focus on cost effectiveness and function. The final version of the system is presented in (**Fig 12**) and it utilizes permanent neodymium magnets and a disposable glass borosilicate test tube as the levitation vessel. Our downstream identification techniques required strict control of contamination hence the system was made to use cheap and disposable vessels wherein the paramagnetic solution could be placed, and the viruses injected once per trial. A new container was thus readily available for different trials and uses to prevent any viral contamination within the MagLev itself.

Fig 12. Novel MagLev system for use with viruses. The structure includes toroidal or ring-shaped neodymium magnets arranged with the N poles facing each other. The distance between the magnets is 15mm. The dimensions of the magnets are 6.35mm thickness, 25.4mm outer diameter and 12.7mm internal diameter.

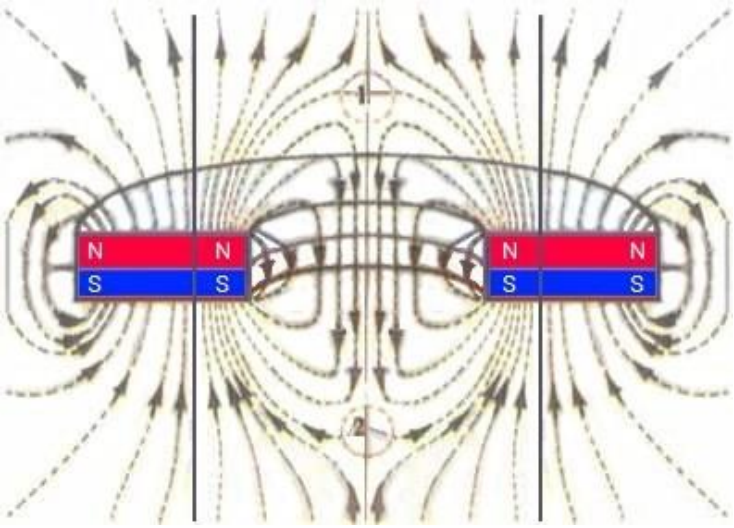

Fig 13. Magnetic field lines around a toroidal ring magnet. The field lines form a gradient unlike cubic or bar magnets due to the hole within the ring of the magnet[99,109].

As stated earlier, diamagnetic magnetic levitation is inherently stable. This is the type of magnetic levitation typically used in biological applications and as such does not require any additional sources of stabilization [1,2,4,8,101,104]. Furthermore, the magnets used in the construction of the MagLev system were permanent meaning the system is portable and does not require any external power. To further improve the resolution of the system, it was designed with toroidal or ring magnets which have unique magnetic field distribution due to their central cavity being empty (**Fig 13**).

Furthermore, the unique field properties of ring-shaped magnets improve the resolution of MagLev systems by creating a magnetic field gradient along a circular axis which runs along the length of the MagLev column[12,98]. This axis is in addition and parallel to the Z axis which has been described previously as the main focus of previous MagLev systems. Utilizing this new axis which can be considered the radial axis R or distance from the centre of the MagLev column, we can obtain three-dimensional resolution as particles are levitated along the Z axis and then separate from each other along the R axis[98]. The magnetic lifting force F_{mag} required to lift a substance against gravity thus has two components in the ring MagLev system. Force along the Z axis ($F_{mag,z}$) is experienced due to the magnetic field component B_z which is different from the magnetic force ($F_{mag,r}$) experienced due to the magnetic field component B_r along the radial axis[98]. Since, previous systems have not incorporated field gradients to differentiate between different particles of the same density, previous work lacks the resolution

between different particles of equal density as change is only observed for the vertical axis of levitation height[1]. The properties of a ring MagLev system are shown in (**Fig 14**)

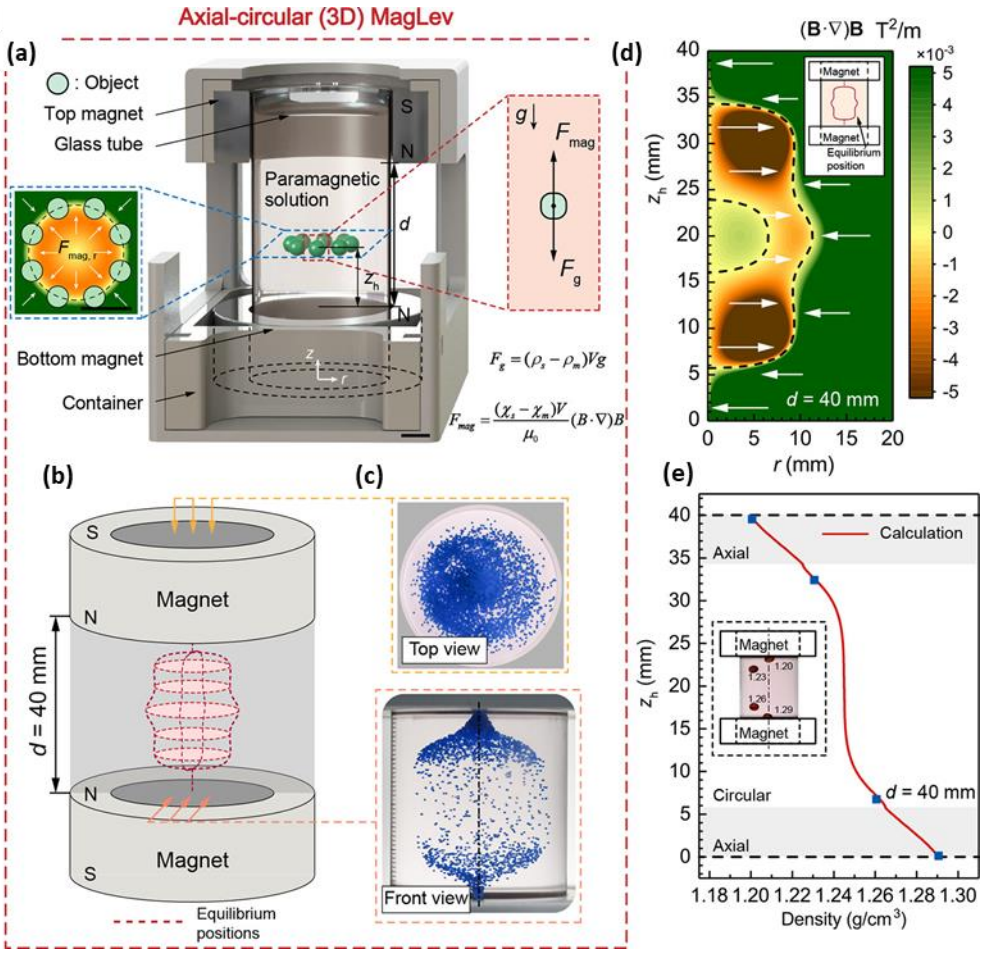

Fig 14. Axial-circular MagLev properties and function. (a) Three-dimensional (3D) diagram of an axial-circular MagLev configuration. (b) 3D schematic diagram of theoretically predicted equilibrium positions in the axial-circular MagLev device. (c) Top view and front view of the distribution of levitated positions of the blue polyethylene (PE) particles. (d) Distributions of Br(∂Br/∂r) + Bz(∂Br/∂z) in the horizontal plane. In the green zones, $\boldsymbol{F_{mag,r}}$ is pushing toward the centre line, whereas $\boldsymbol{F_{mag,r}}$ is pushing away from the centreline in the brown zones. (e) Relationship between density and levitation height in an axial-circular MagLev[98].

The ring system and its capabilities have only recently been studied in detail to show how the MagLev system distributes its magnetic field and affects diamagnetic levitation[98]. It was experimentally shown (**Fig 14**) that the magnetic field components vary dynamically across the ring MagLevs column such that field components $Br(\partial Br/\partial r) + Bz(\partial Br/\partial z)$ produce unique distribution patterns near the edges of the levitation column and in the middle of the MagLev column (**Fig 14: e, f**). In recent studies, it has been shown that the field components $Br(\partial Br/\partial r) + Bz(\partial Br/\partial z)$ are equal to zero near the middle of the MagLev allowing for more spread of the levitated materials. Alternatively, the regions of the levitation column near the magnets have a resultant $Br(\partial Br/\partial r)$ component which produces a force $F_{mag,r}$ that pushes levitated materials towards the centre of the MagLev column[98]. This central region in the levitation column is the ideal place for maximum resolution and can be calibrated using the concentration of the paramagnetic solution used. Due to the additional field components however, a new relation is mathematically established where the density of the levitated material is linearly related to the distance levitated and the distance of the levitated material from the centre of the MagLev column[98]. This is shown in equation 9 which is derived from equation 7.

$$\boldsymbol{\rho_o \sim \rho_m + \frac{(\chi_o - \chi_m)}{\mu_0 * g} * V(\vec{B}.\vec{\nabla})\vec{B}} \quad \textbf{(Equation 7)}$$

$$\boldsymbol{\rho_o = \rho_m + \frac{(\chi_o - \chi_m)}{\mu_0 * g} * V\left(\vec{B}_r \frac{\partial \vec{B}_z}{\partial r} + \vec{B}_z \frac{\partial \vec{B}_z}{\partial z}\right)} \quad \textbf{(Equation 9)}$$

Where g = 9.81ms^{-2} or is the acceleration due to gravity, ρ_m is the density of the medium the levitation is occurring in, ρ_o is the density of the object being levitated and $\mu_0 = 4\pi \times 10^{-7}$ N·A^{-2} is the magnetic permeability of a vacuum. $\boldsymbol{\chi_o}$ is the magnetic susceptibility of the lifted object and $\boldsymbol{\chi_m}$ is the magnetic susceptibility of the medium where the levitation is occurring. $\vec{\boldsymbol{B}}$ is the magnetic flux density in Tesla (T) and $\boldsymbol{V}$ is the volume of the magnet (m^3). $Br\left(\frac{\partial Bz}{\partial r}\right), Bz\left(\frac{\partial Bz}{\partial z}\right)$ are the radial and vertical components respectively of the vector product $(\vec{B}.\vec{\nabla})\vec{B}$[98].

One additional consideration was the selection of paramagnetic solution for use in the MagLev system. The concentration and magnetic susceptibility of the paramagnetic medium used in a MagLev are key factors when conducting levitation experiments[1]. The levitation range or measurable density range of a system is calibrated via the concentration of the solution placed within the MagLev. If the concentration of a paramagnetic solution is too high, it will generate too strong of an upward magnetic force F_{mag} resulting in all levitated materials being out of

the visible column and vice versa if the concentration of the magnetic solution is too low. Hence, the magnetic solution needs to be calibrated according to the material being levitated. This procedure requires trial and error in the case of viruses which have no known density values. Additionally, the concentration of magnetic solution required is greater if the magnetic permeability of the solution is low and the original field strength of the magnet is not changeable[2,8,98].

3.1.2 MagLev construction setup and usage

The MagLev structure (**Fig 12**) was 3D printed using non-magnetic plastics and screws. The N48 neodymium ring magnets (25.4mm outer diameter, 12.7mm internal diameter and 6.35mm thickness) used were purchased from (magnet4less.com). The magnets were attached to the 3D printed frame 15 mm apart with the N poles facing each other using a strong adhesive. The system was premade and designed by the Morteza Mahmoudi lab group (Michigan State University; Department of Radiology, Precision Health Program, East Lansing, Michigan, USA) for the purposes of this experiment. The system utilizes 5ml disposable glass borosilicate tubes purchased from fisher scientific (VWR:47729-570). The system requires ~2ml of paramagnetic solution in its column to function. The amount of viral stock used in the system was 10-25µl, with the substrate range which could be levitated being 5-50ul. The system was stabilized using acrylic stands for height adjustment and a level was used to set up the system before each trial to ensure levelled levitation and uniformity of magnetic fields.

For the purposes of density determination, visualizations were taken upon addition of viral stock into the MagLev system. The visualizations were taken via a cell phone (Oneplus 6T, model A6013) placed on a fixed tripod stand with lighting equipment. The dual lens camera (16-megapixel: Sony IMX 519, 20-megapixel: Sony IMX 376K) system had an autofocus feature with both lenses having an aperture of f/1.7. Images were taken for multiple trials, all paramagnetic solutions used, at fixed time points and immediately following injection of the viral stock into the system. Image files were kept at their highest resolution with minimal processing by the system OS. We used genomic and tissue culturing techniques to verify the location of viruses within the MagLev column but a visualization for viruses was also sought out to allow easy image-based identification of the virus and determination of viral density.

The MagLev system was setup within a biosafety cabinet (BSC) for use at room temperature 16-29°C. Viral stock was thawed and stored at 4°C during experiments. Each tube containing 2ml of paramagnetic solution was prepared outside of the BSC and brought into the BSC when required. Additionally, viral stock was only opened once the system was set up for injection of viral stock to the MagLev via a P20 micropipette. Steps were taken to limit the exposure of materials and solutions to the virus to maintain the accuracy and integrity of the downstream QPCR based analysis. Additional steps included regular use of a 10% Quatricide® solution and 70% ethanol to clean all materials entering the BSC and being brought into proximity of the viral stock.

Once the viral stock was injected into the MagLev via a P20 (20µl) pipette, the stock was allowed to levitate for at least 15 minutes, during which time pictures of the column were taken to capture any levitating precipitate. The 15minute time period was decided after a pilot experiment where viral stock was levitated for up to 1 hour with sample assessments taken every 15 minutes. The results of the pilot experiment showed that $_{Ct}$ values began to decline after any significant time at room temperature, but levitation results remained consistent after the initial 15minute period (**Appendix A, Fig A**). Samples were collected via p1000 pipette as 4 500µl MagLev fractions. The top of the borosilicate tube used for the MagLev column vessel was open to allow insertion of viral stock. After 15minutes of levitating the viral stock, the p1000 pipette was inserted into the system and 4 (500µl each) fractions were collected starting from the top. The total volume of the column was 2ml so the four fractions (A, B, C, D) were drawn sequentially starting from the top with a new pipette tip for each subsequent collection. The MagLev fractions were stored at -80°C until extraction or culture-based analysis. Several fractions were collected for each solution used at various time points and tested independently of each other. The general workflow is presented in (**Fig 15**).

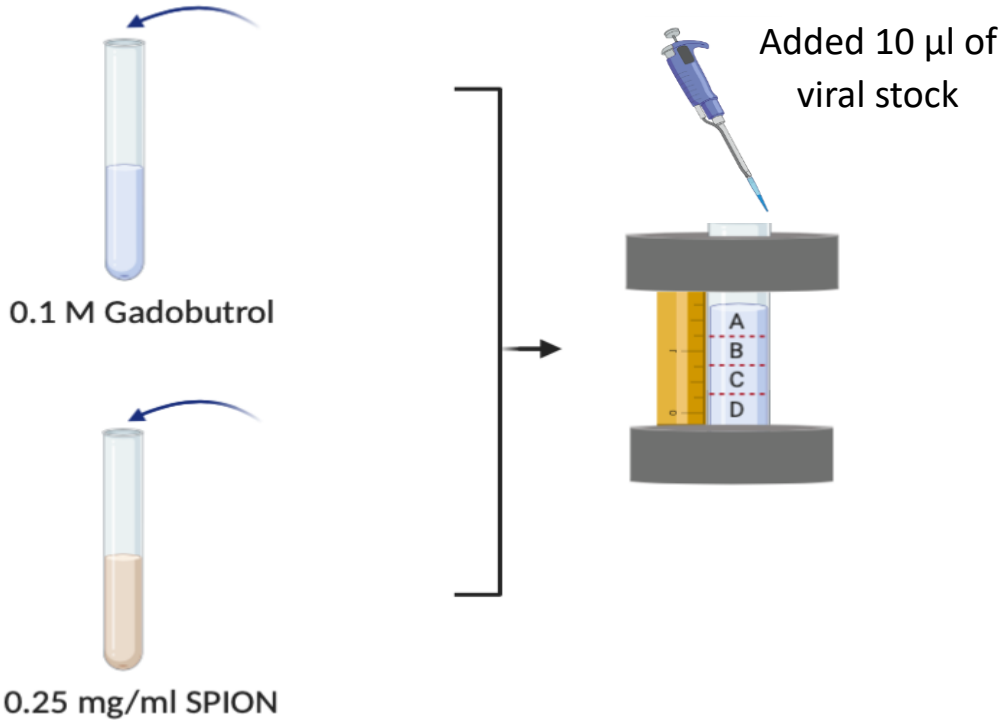

Fig 15. Overview of MagLev usage. 2ml of paramagnetic solution is placed in a tube. The tube is setup within the MagLev and 10µl of viral stock is injected into the column. After 15 minutes, the column is extracted starting from the top in 500µl fractions using a pipette.

3.1.3 Influenza viral stock preparation

For the purposes of our experiments, we prepared a highly concentrated stock of viruses to ensure that the visualizations obtained within the MagLev were only a consequence of viruses and no other material. All forms of biological matter can produce diamagnetic levitation and levitate within the MagLev column producing multiple visual bands[1]. Our goal was to find a consistent levitation band that could be linked to viruses. To obtain this fine resolution and determine the parameters at which viruses could be reliably levitated and identified, we sought to minimize exterior factors by using a pure and highly concentrated stock of viruses.

The virus chosen for our work was a lab cell culture derived strain of influenza A virus (A/Puerto Rico/8/34 (H1N1))[23,51]. Stocks were produced and maintained at the Jonathan Runstadler lab at Tufts; Cummings School of Veterinary Medicine, Centre for Infectious Disease and Global health (North Grafton, Massachusetts, USA). The virus was propagated in cell cultures of Madin-Darby Canine Kidney Cells (MDCK), grown using a growth medium. An infection medium was prepared using Advanced Dulbecco's Modified Eagle Medium (DMEM) with added Bovine Serum Albumin (BSA), antibiotics and HEPES Buffered Saline

Solution (2.5%). DMEM (Gibco life sciences: 12491023) and cell culture flasks (Greiner Bio-One:661975) were purchased through Thermo fisher. While HEPES (Lonza™ Bioscience: CC-5024), Phospho-buffer saline (Lonza™ Bioscience: BE17-515Q) and TPCK-trypsin 1mg/ml stock (Thermo Scientific™ PI20230) were purchased through fisher scientific.

Viral lab stock was stored at -80°C. For propagation, stock was first thawed and then Diluted in the infection medium so as to end up with 10*Z ml (Z = # of flasks to be inoculated). MDCK cells were incubated and grown prior to infection in a growth medium and washed with PBS before inoculation in a separate vessel. After inoculation, the cells were allowed to sit with the virus for 1 hr with regular agitation to allow spread. TPCK-trypsin was thawed on ice for about 10 min. The Added ratio of trypsin was 240µl 1mg/ml TPCK-trypsin to 16* Z ml of infection media. The column of cells was aspirated and then 14 ml of infection media supplemented with 1ug/ml trypsin was added to the cells and then left to incubate at 37°C for 72hours.

For harvesting and initial concentration, the inoculum containing virus and cell debris was aliquoted to falcon tubes and spun at 1500 RPM at 4°C for 15 minutes. The supernatant containing virus was collected and placed on ice. Following the initial centrifugation, the viral supernatant was ultra-centrifuged at 25,000 RPM for 2h at 4°C (~77,000 XG). 30ml of the viral supernatant was added to ultra-centrifuge tubes followed by 3ml of a (30%) sucrose solution in endotoxin free PBS. The sucrose solution was carefully placed at the bottom of the tube containing the viral supernatant to collect the viral pellet. Following the ultra-centrifugation, the final pellet was resuspended in PBS and aliquoted for use and stored at - 80°C. The C_t value of this ultra-centrifuged PR8 stock was found to be 13.07 (very high viral content). This stock was thawed and used with the MagLev system.

3.1.4 RNA extraction and RT-QPCR

Real time quantitative polymerase chain reaction (QPCR) is considered the gold standard for viral quantification and identification. As such we sought to quantify the amount of virus present in each of our four MagLev fractions (A, B, C, D) from the system (**Fig 15**). It was hypothesised that one fraction would produce a higher C_t value due to all or most of the virus being levitated to one height in the MagLev column. Viral fractions collected from the MagLev were stored at -80°C, extraction and QPCR was carried in one day for each set of fractions. Viral RNA was extracted using the Omega Mag-Bind® Viral DNA/RNA 96 Kit (Omega Bio-Tek: M6246-03) and a KingFisher magnetic particle processor (Thermofisher Scientific).

Following extraction, the RNA was stored at 4°C while QPCR was setup for the sample. Custom TaqMan™ TAMRA probe-based (Applied Biosystems™:450003) one-step reverse transcriptase QPCR was carried out using primers purchased from Invitrogen custom oligos listed in Table 2. The QPCR platform used was the ABI 7500 real-time Applied Biosystems StepONEPlus Real-Time PCR machine (Applied Biosystems™: 4376600). The machine was run for 45 cycles with a 20µl reaction volume. For optimal QPCR performance, qSCRIPT XLT OneStep RT-qPCR ToughMix ROX 2X (Quanta Biosciences:95133-500) was used. Influenza A/Puerto Rico/8/1934 separate from the viral stock used in the MagLev was used as a positive control for the extraction step and extracted RNA from PR8 strain IAV also served as a positive control for the PCR step. Viral transport medium (Remel) was used for negative controls in both extraction and PCR steps. An additional control for assessing the MagLev systems effectiveness in isolating viruses in one fraction was 10-25µl of viral stock added directly to 490-475µl of PBS. This control represented a comparison for all of the fractions in the MagLev, it would be the ideal result if all of the virus were to be levitated in one 500µl fraction of the MagLev. All processing was done using the platforms software.

Table 2 Primers and probes for the AI matrix protein of Influenza A[53,91]

Oligo function	Target	Primer sequence (5' -> 3')	Reference
Forward primer	AI matrix protein	ARA TGA GTC TTC TRA CCG AGG TCG	53,91
Reverse primer		TGA AAA GAC ATC YTC AAG YYT CTG	
Probe		[6-FAM]TCA GGC CCC CTC AAA GCC GA[TAMRA-6-FAM]	

Viruses have a tendency to rupture during freeze thaw cycles due to interactions with ice crystals[35]. This would result in the viral stock loosing whole viruses. Genome based techniques cannot differentiate between intact viruses and viral genomes[48]. To remove any potential confounding results due to free RNA, a pilot experiment was conducted where MagLev fractions were treated with an endonuclease to digest any free viral RNA. Omnicleave endonuclease (Lucigen: OC7850K) was purchased from fisher scientific and added (600U) to MagLev fractions left at room temperature for 1 hour. The fractions were extracted and RT-QPCR was conducted on the samples before and after treatment. These results are presented here (**Appendix A, Fig. B**)

3.2 Aim 2: Investigate the performance of different paramagnetic media

3.2.1 Selection of paramagnetic media

It is typical to use strong paramagnetic metals like gadolinium or manganese in the form of salts for making paramagnetic solutions to use with MagLev systems[1,5–8,98,108,110]. However, viruses are notoriously difficult to work with at room temperatures and biological materials in general do not remain stable in strongly ionizing solutions. In the process of designing our MagLev system we chose two main alternative solutions which have been shown previously to leave biological materials intact and viable for further study[1,6]. The first solution is an MRI agent known as Gadobutrol (Gadavist^{TM}) which is a chelate of the rare earth metal gadolinium combined with butorol($C_{18}H_{31}GdN_4O_9$) (**Fig 16**). Gadobutrol is strongly paramagnetic and routinely used in humans as an MRI agent and its chelated structure prevents the release of gadolinium ions into a solution[6,7,104,110]. Furthermore, ionic salts of gadolinium have been previously used in MagLev systems[8,12,24]. In our case, we chose it for its non-ionic nature and history of being non-invasive to biological materials[6].

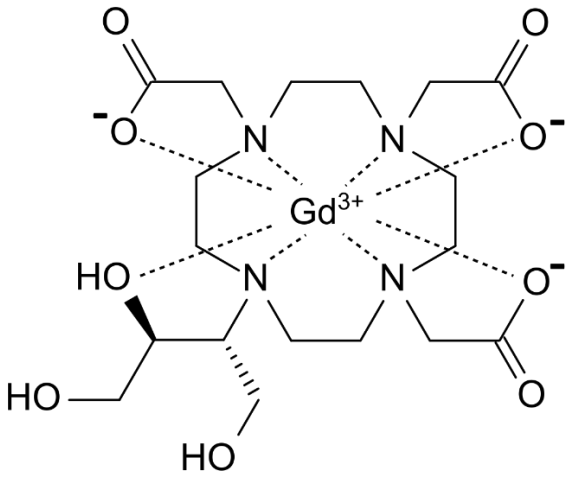

Fig 16. Chelated structure of Gadobutrol[110]. It has an effective Gd moment of 7.98μB obtained from susceptibility measurements in the paramagnetic phase[104].

The second paramagnetic solution used for the MagLev system was a suspension of superparamagnetic iron oxide nanoparticles (SPIONs) functionalized with ferumoxytol purchased from Feraheme (www.feraheme.com) and diluted with phosphate buffered saline[1]. The nanoparticles have γ-Fe2O3 cores (**Fig 17**) which are irregular in shape and have a mean diameter of approximately 3.25nm. The nanoparticles are also coated by a semi-synthetic

carbohydrate shell in an isotonic, neutral pH solution which can improve interaction with biological surfaces[111–113]. This solution has the benefit of being easily synthesized, reused by separation of SPIONs via centrifugation and offering improved resolution of the MagLev system by increasing interactions with biological materials[112]. Given our goal of creating a cost-effective MagLev system for viruses, the use of SPIONs was an important factor as other paramagnetic solutions are derived from very rare and expensive metals. The iron oxide particles show strong magnetic properties and have previously been used successfully with plasma proteins while leaving them viable for identification[1]. While similar nanoparticles have interacted invasively in the past with biological materials[113], it was a worthwhile goal to test the SPIONs performance on a MagLev system aimed towards viruses.

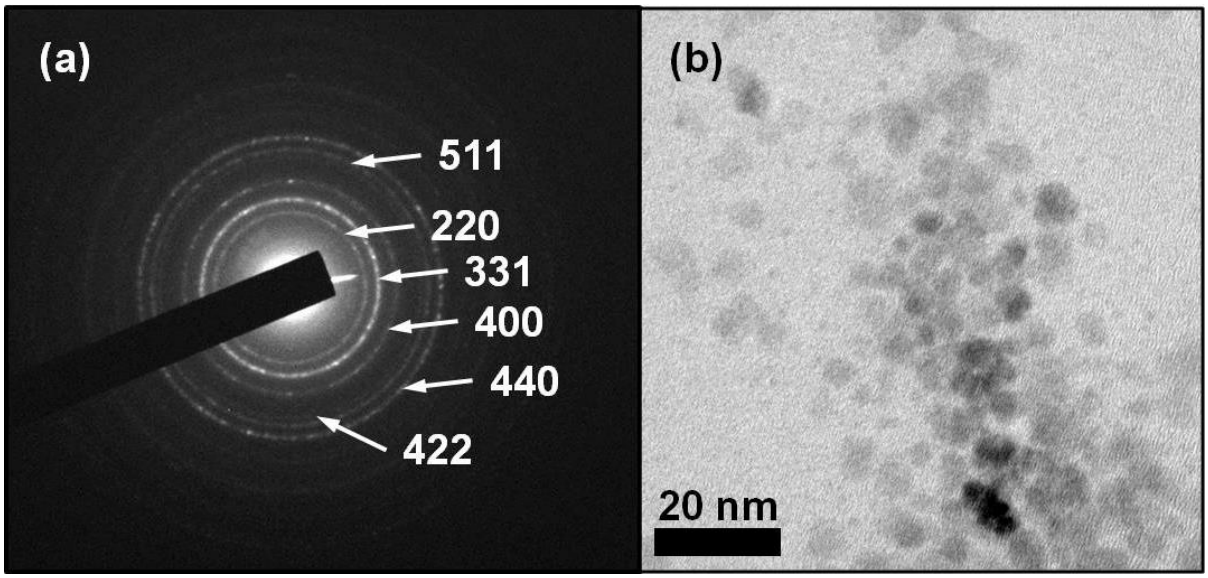

Fig 17. Superparamagnetic iron oxide nanoparticles (SPIONs) functionalized with ferumoxytol. The nanoparticles have γ-Fe2O3 cores. (a) Selected Area Diffraction image showing a cubic maghemite (γ-Fe2O3) crystal structure. (b) The transmission electron microscopy morphological analysis shows that the electron-dense feraheme cores are irregular in shape and have a mean diameter of approximately 3.25 nm[111].

3.2.2 Paramagnetic solution preparation

Paramagnetic solutions were prepared prior to use and stored at room temperature in autoclaved 20ml glass scintillation vials purchased from fisher scientific (DWK Life Sciences: 986560). Two types of solutions were used in the MagLev system, one made using Gadobutrol (Toronto Research Chemicals: G125705) and a second one made using 30mg/ml Superparamagnetic Iron Oxide Nanoparticle (SPION) solution (Fe-raheme, www.feraheme.com). The original powder and solution respectively were diluted using PBS (Lonza™ Bioscience: BE17-515Q)

to required concentrations. For Gadobutrol, a 1M stock was prepared by weighing the required amount of solution and then adding it into a closed autoclaved glass vessel. The 1M Gadobutrol solution was prepared using a magnetic heating plate and left to stir over night at a low temperature to ensure complete homogeneity. Further dilutions were prepared from the 1M Gadobutrol stock for use in the MagLev system. The SPION solution was already available as a stock of 30mg/ml and was aseptically transferred to a 20ml scintillation vial containing premeasured volume of PBS. The SPION solution was vortexed for more than ~10 minutes on preparation. Solutions were further vortexed before use and in between trials.

The final concentrations for each solution to be used in the MagLev system were determined experimentally. As stated earlier, the levitation height of a substrate within the MagLev is partly dependant on the concentration of the paramagnetic solution used. The MagLev system has a measurable range of densities within the column and that is dependent on the concentration of the paramagnetic solution because higher concentrations of paramagnetic elements in solution result in higher magnetic susceptibility and subsequently greater lift force. Alternatively, lower concentrations of paramagnetic materials result in no levitation or unstable levitation as levitated substrates fall out of levitation. Since the density of our virus was unknown, we ran trials of levitation followed by running RT-QPCR on sections of the MagLev column. This was done to determine which concentration of paramagnetic solution resulted in the virus being levitated near to the centre of the MagLev column. A series of MagLev solution calibration experiments were conducted. Through our analysis, we determined that a 0.1M concentration for Gadobutrol and a 0.25mg/ml concentration of SPION solution produced the best results. Hence, a 0.1M concentration for Gadobutrol and a 0.25mg/ml concentration of SPION solution were used in subsequent tests.

The control condition for assessing the paramagnetic solutions performance was the MagLev column filled with PBS. For this control, all usage conditions were replicated except the presence of paramagnetic solutions. This control allowed us to verify that viruses do not levitate on their own and no exterior factors besides the MagLev and paramagnetic solution are affecting the results of our downstream analysis. Viruses were injected in a MagLev setup with PBS and the workflow for each paramagnetic solution was replicated down to the RT-QPCR and tissue culturing steps.

3.3 Aim 3: Investigate if viruses are infective following levitation

3.3.1 Tissue culturing and TCID 50

To check for the viability of viruses following levitation, we sought to conduct infection assays and Tissue Culture Infectious Dose 50 (TCID 50) tests[92]. One of the potential benefits of MagLev based techniques we highlighted is the non-invasive nature of magnetic forces. There is significant potential benefit to virologic research if viruses could be levitated directly from samples, concentrated and easily extracted non-invasively for lab use and further propagation. Hence, we use tissue culturing techniques to identify whether influenza A/Puerto Rico/8/1934 virus can retain its ability to infect living cells after magnetic levitation. Additionally, we quantify each of the MagLev fractions (**Fig 15**) infectious viral load using TCID50 calculated via the Reed-Muench method[48,92] to see if one fraction contains more infectious virions than other fractions.

To conduct infection assays, Madin-Darby Canine Kidney Cells (MDCK)[82] were selected as the host and first grown to confluency in a growth medium. The growth medium consisted of Dulbecco's Modified Eagle Medium (DMEM) containing L-glutamine (Gibco life sciences: 11965084), supplemented with, DPBS (Lonza™ Bioscience: BE17-515Q), a penicillin-streptomycin stock (100 U/ml penicillin G and 100 µg/ml streptomycin) (Sigma-Aldrich) and heat-inactivated fetal bovine serum (10% FBS in the final medium) (Sigma-Aldrich: F4135). Growth medium was stored at 4°C until use. For propagation, MDCK cells were thawed and then mixed with warmed growth medium and left to incubate in cell culture flasks (Greiner Bio-One:661975) until confluency. The growth conditions were 37°C and 10% CO_2. Confluency was tested every 24hrs using a cell culture microscope and cell counts were done using a hemocytometer and trypan blue dye to count living cell. The calculation for cell counts using a hemocytometer with 10 grids and a working volume of 20ul was: number of living cells on grid*number of grids on hemocytometer (10)*dilution with dye (10ul dye to 10µl cell stock)*1000 for unit conversion from ul to ml*vials of cell stock. The calculation gives cell count/ml. Cells were split as needed to maintain their growth phase.

Cells were split based on the confluency of T-25 (~ 8million cells) and T-75 (~ 12million cells) flasks (Greiner Bio-One:661975). If visual assessment using a cell culture microscope showed an excess of cells, the tissue culture flasks were taken into a BSC and split for either use in TCID50 infection assays or split to maintain growth phase and prevent cell death. For cell splitting, all media and solutions were first warmed using a water bath to 37°C to prevent cell

death due to shock. The growth medium already in the flasks was pipetted out of the flask and aspirated into a 10% bleach solution. The cells were then washed with PBS twice and the PBS (Lonza™ Bioscience: BE17-515Q) was also pipetted into the bleach solution. EDTA trypsin (Lonza™ Bioscience: BE17-161E) was added into the tissue culture flask (1.5ml for T-25, 4mL for T-75) to release the growing cells from the wall of the flask. Flasks with EDTA trypsin were left to incubate at 37°C for ~15minutes or until most of the cells had been released. Following incubation, growth medium was added (2X the quantity of EDTA trypsin) to inactivate EDTA trypsin. The contents of the flask were then transferred to a falcon tube and centrifuged at 1500RPM for 3 minutes at 4°C to pellet the MDCK cells. Cell counts are done at this stage to determine cell count/ml for use in split or infection assay.

Once the cells were confluent in their vessel and a minimum of ~ 3 million MDCK cells were available for one Falcon® 96-Well Flat-Bottom Microplate (Stem Cell Technologies: 38022), the infection assay could be performed. Before inoculation of cells with virus, the cells must first be plated on a 96-Well Flat-Bottom Microplate and allowed to grow and form a (uniform) monolayer on the bottom. For preparing one plate, cells are treated as if for splitting and then 10 ml of cells at a concentration of $3.0*10^5$ cells/ml in growth medium are placed 100µl per well into the assay plate. The plates are then incubated overnight at 37°C and visually assessed for the formation of a monolayer in each well of the 96-well plate before infection.

An infection medium was prepared using Dulbecco's Modified Eagle Medium (DMEM) containing L-glutamine (Gibco life sciences: 11965084), supplemented with DPBS (Lonza™ Bioscience: BE17-515Q), a penicillin-streptomycin stock (100 U/ml penicillin G and 100 µg/ml streptomycin) (Sigma-Aldrich), TPCK-trypsin 1mg/ml stock (Thermo Scientific™ PI20230) (1ug/ml final concentration in each well), 1M HEPES (25 mM) (Lonza™ Bioscience: CC-5024) and 7.5% bovine serum albumin (0.2% BSA per volume of media) (Sigma-Aldrich). The incubated plates with a full monolayer are prepared by removing the growth medium and washing the cells twice with PBS. The plates are then filled with 200ul of the infection medium per well. The first well has 100ul of the infection medium removed and 146ul of viral inoculum or MagLev fraction supplemented with TPCK-trypsin (1µg/ml) added to it. 46ul is subsequently pulled from the first row and aseptically transferred to the next. The sample is thus diluted serially leaving only one row containing 200ul of the infection medium as a negative control. The plate is then incubated at 37°C for 72 hours. After incubation, the wells are visually assessed using a cell culturing microscope for the destruction of the cellular monolayer. The presence of sufficient viral infectious load results in the destruction of the

MDCK cells lining the bottom of the well which lets us quantify the amount of infectious viruses present[29,48,92].

For our experiment, three plates were done for each paramagnetic solution used in the MagLev. Each plate had one fraction of the MagLev repeated three times on it in separate wells to account for variation (**Fig 18**). QPCR was also carried out on each plated fraction the day it was inoculated to confirm the presence of virus and verify the consistency of results between QPCR and tissue culturing. A pilot experiment was conducted with just the paramagnetic solutions added to the MDCK cells without the addition of any virus. It was determined that none of our solutions resulted in the death of MDCK cells or the disruption of the monolayer. Hence, any cell death observed was a result of the virus retaining its infectious properties after magnetic levitation. The wells were analyzed, and the results of the tissue culturing were used to calculate TCID50 using the Reed-Muench method[92].

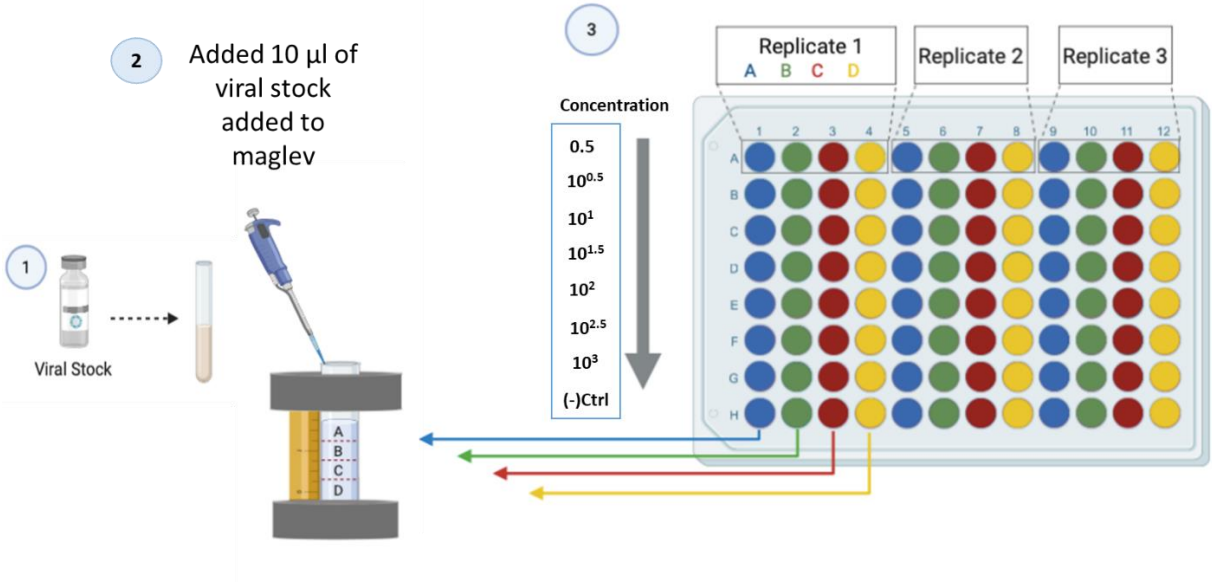

Fig 18. Overview of infection assay and TCID50 procedure. Viral stock was levitated in MagLev using either SPION solution or 0.1M Gadobutrol, 4 fractions of 500ul each were collected from the MagLev sequentially (A, B, C, D). Each fraction was plated three times on one prepared plate. The bottom row was the negative control. Each paramagnetic solution had three repeats/plates done for it.

3.4 Aim 4: Density estimate for influenza A virus

3.4.1 Density calibration of MagLev

The column of the MagLev can be calibrated using fixed density particles for any given concentration of paramagnetic solution[8,98]. Levitation heights of known density particles can

be visually assessed and linked to the physical scale of the MagLev and used for creating a linear relationship which can determine the density of an unknown substrate. For calibrating the scale of our system for the experimentally determined ideal concentration of paramagnetic solution, fixed density polyethylene microspheres were purchased from Cospheric precision spherical particles (cospheric.com). The range of particles used was between 0.9-1.1 g/cm^3. The diameters for the particles of different density ranges varied and there were slight variations in density between particles of each density. To standardize the calibration obtained, at least 3 particles of each density category were levitated independently for a minimum of 15 minutes each and standard deviation was experimentally determined. The results for the calibration of 0.1M Gadobutrol solution (**Fig 19**) and 0.25mg/ml SPION (**Fig 20**) solution are presented in the appendix as (**Appendix A**) Table A and Table B respectively.

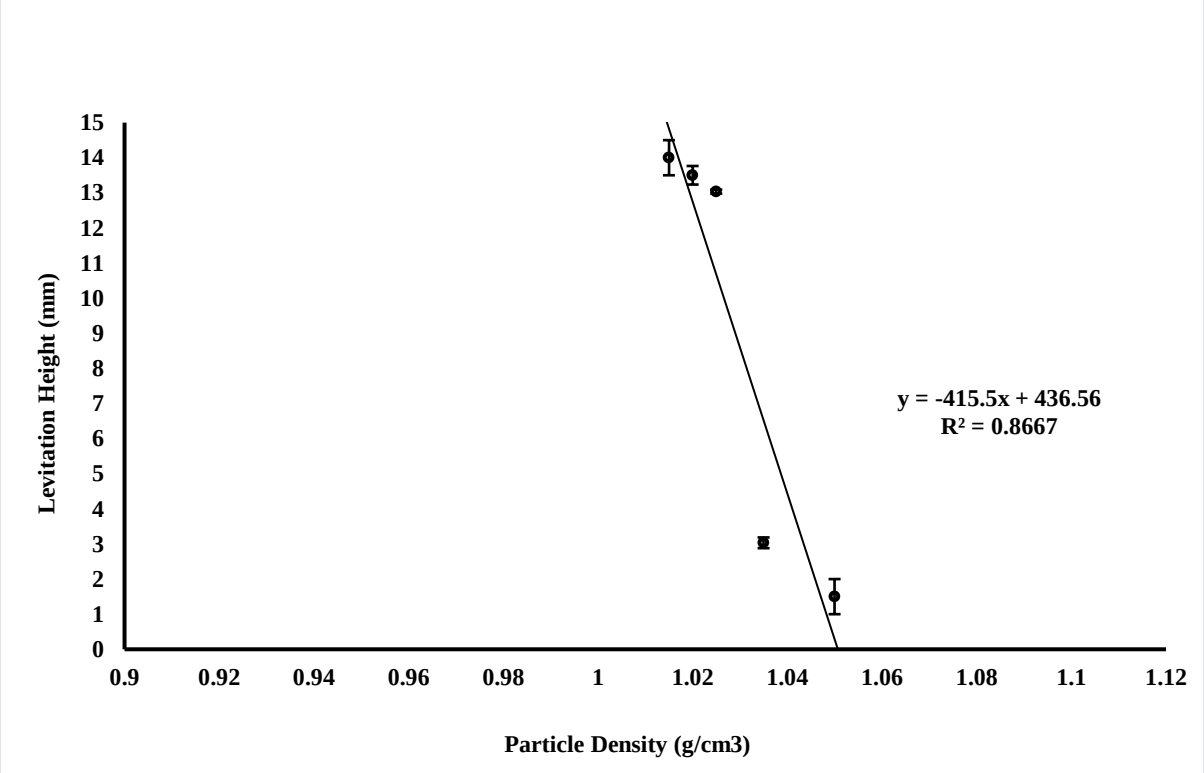

Fig 19. Calibration obtained for 0.1M Gadobutrol solution using fixed density microspheres. The measurable range for 0.1M Gadobutrol is very narrow and somewhere between 1.025 and 1.045 g/cm^3. The bars represent standard deviation. The equation for the line and R^2 is presented on the graph.

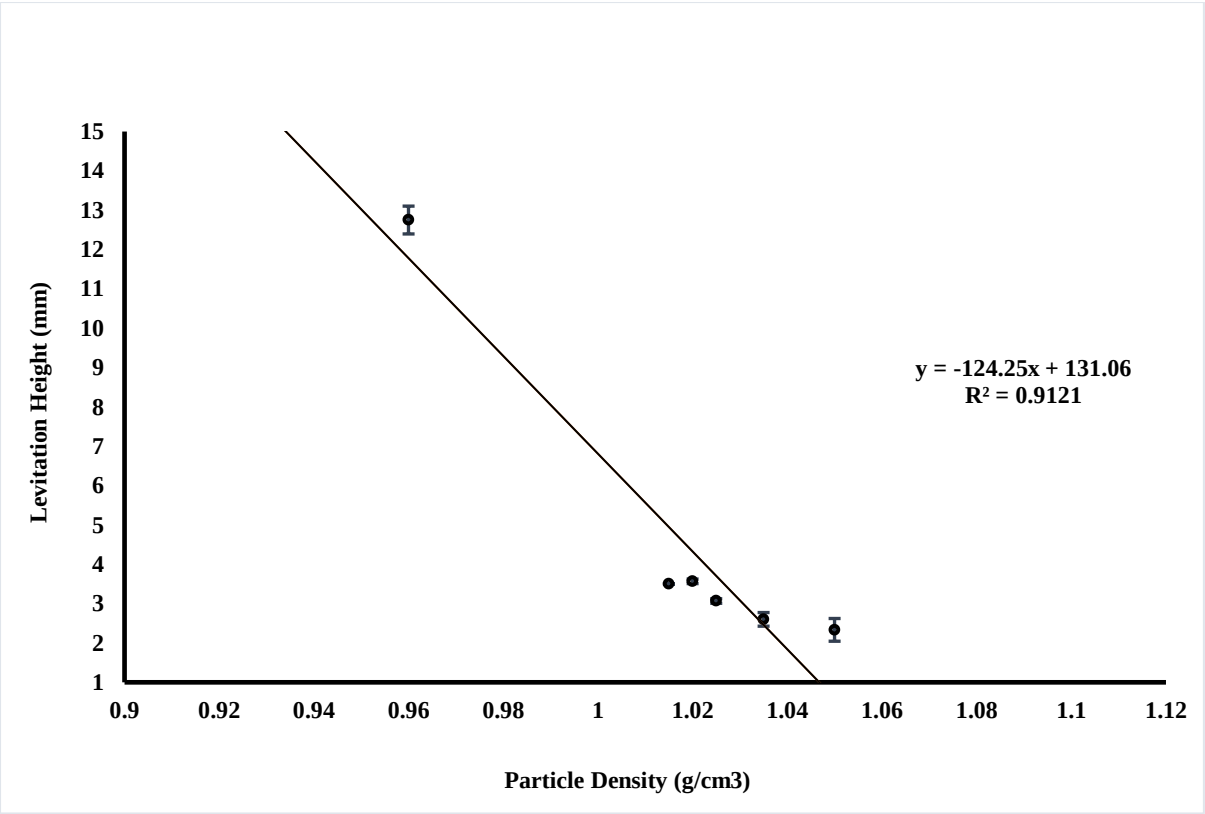

Fig 20. Calibration obtained for 0.25 mg/ml SPION solution using fixed density microspheres. The bars represent standard deviation. The measurable range is much wider than 0.1M Gadobutrol solution (0.96-1.015 g/cm^3). Some density measurements (Appendix A; Table B) were removed from the calibration to improve the R^2 value.

Chapter 4. Results and Discussion

Our results were promising and are presented in this section to match the aims stated at the beginning of this work.

4.1 Aim 1: Investigate if viruses are levitated within the MagLev

4.1.1 Visualization of influenza viral stock

The attempts to obtain a single clear visualization for viruses directly had several hurdles but visualization was obtained in two trials using 0.25mg/ml SPION solution (**Fig 21**). No visible band was observed while using 0.1M Gadobutrol solution. Throughout our experiments, visualization was not a reliable indicator of viruses within the MagLev column despite the use of highly concentrated Influenza A/Puerto Rico/8/1934 viral stock (C_t = ~13). However, the results for viral levitation were more consistent for RT-QPCR and tissue culturing which corroborated the visible band obtained using SPIONs.

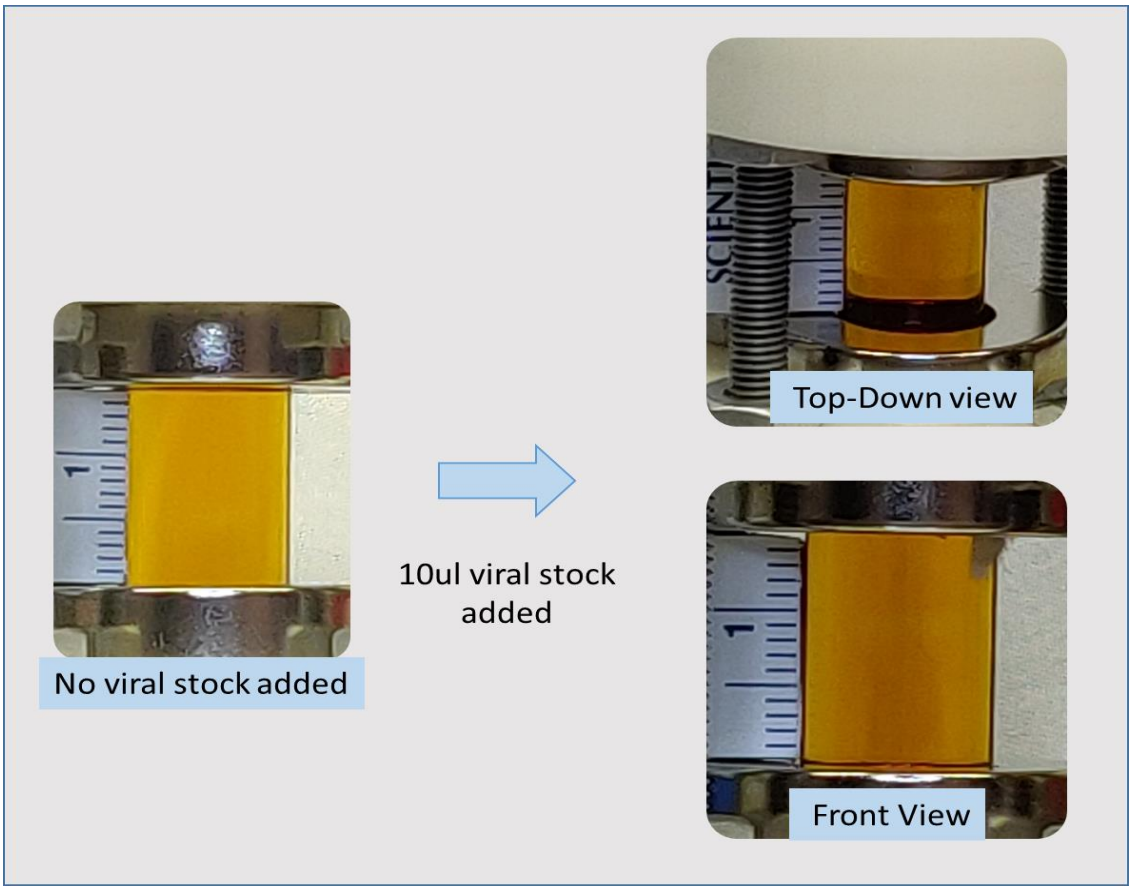

Fig 21. Visualization of viral stock at ~9.5mm in MagLev column. 10ul of viral stock was added to the MagLev containing 2ml of 0.25mg/ml SPION solution. A faint visualization was obtained in only two trials.

4.1.2 Viral quantification via QPCR

The results of the viral quantification via QPCR produced relatively consistent results. While each fraction (**Fig 15**) of the MagLev produced a C_t value indicating the presence of virus throughout the column, there were clear trends in C_t values for each paramagnetic solution (**Fig 22, 25, 26**). C_t values represent log fold change in viral quantity[86,87], hence a single increase in C_t value is a significant decrease in viral content. Here we present raw C_t values from individual QPCR plates/assays which include all MagLev fractions obtained from a levitation experiment using a given paramagnetic solution and control conditions. Internal (-) controls (VTM) also included raw paramagnetic solution and showed no contamination in the original solutions being used. Our goal was to see if the C_t values of one MagLev fraction (A, B, C, D) could match that of our positive control of 10µl concentrated viral stock added to 490µl of PBS. Each MagLev fraction was 500µl and hence if one fraction could match our positive control, it would indicate that the MagLev was levitating all or most virions to one specific height. All obtained fractions were assessed against this control and are presented here.

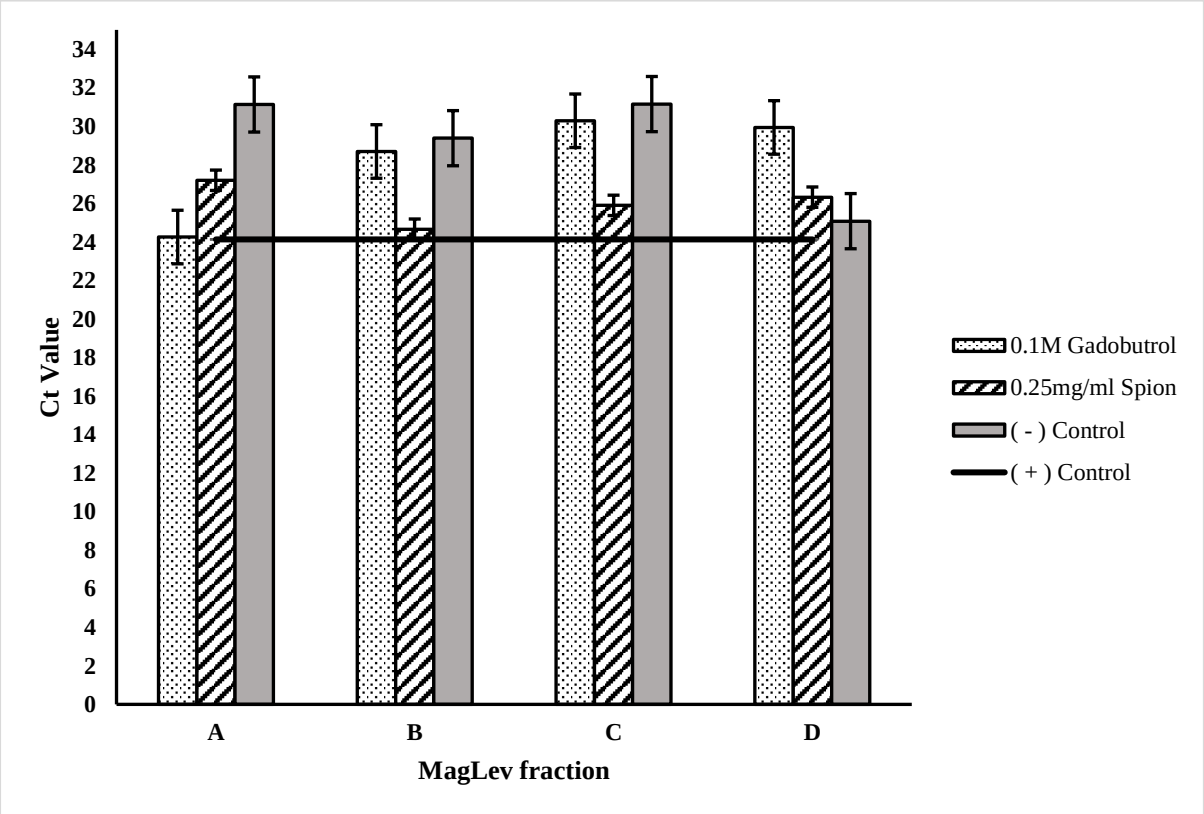

Fig 22. QPCR results of 4 MagLev fractions (A, B, C, D) obtained with PBS (-) control, 0.25mg/ml SPION and 0.1M Gadobutrol in the MagLev. Comparing the performance of each solution against our control we can observe that Gadobutrol shows a C_t value near to the (+) control in fraction A, SPIONs at fraction B and PBS at fraction D. The error bars represent standard error**.**

RT-PCR was also done on fractions of the MagLev obtained by using only PBS in the MagLev. The results show that without a paramagnetic solution present in the MagLev column, the virus most likely sinks to the bottom of the MagLev column because the lowest fraction consistently had the lower C_t value (**Fig 22, 23**). We present the results of one such test in (**Fig 23**). This shows that no levitation occurs in the absence of a paramagnetic solution. Using 0.1M Gadobutrol and 0.25mg/ml SPIONs however, the top two fractions A or B have lower C_t values. For Gadobutrol the trend shows lower C_t values at the topmost fraction (A) while the second from the top fraction (B) had the lowest C_t values for SPION solutions (**Fig 22, 23**). These results are shown here for several trials each of which is from independent plates/assays. We also confirmed via a pilot study that paramagnetic solutions do not affect C_t values on their own, except in the case of $GdCl_3$. The results are hence a direct consequence of levitation in the MagLev for 15 minutes using each respective paramagnetic solution.

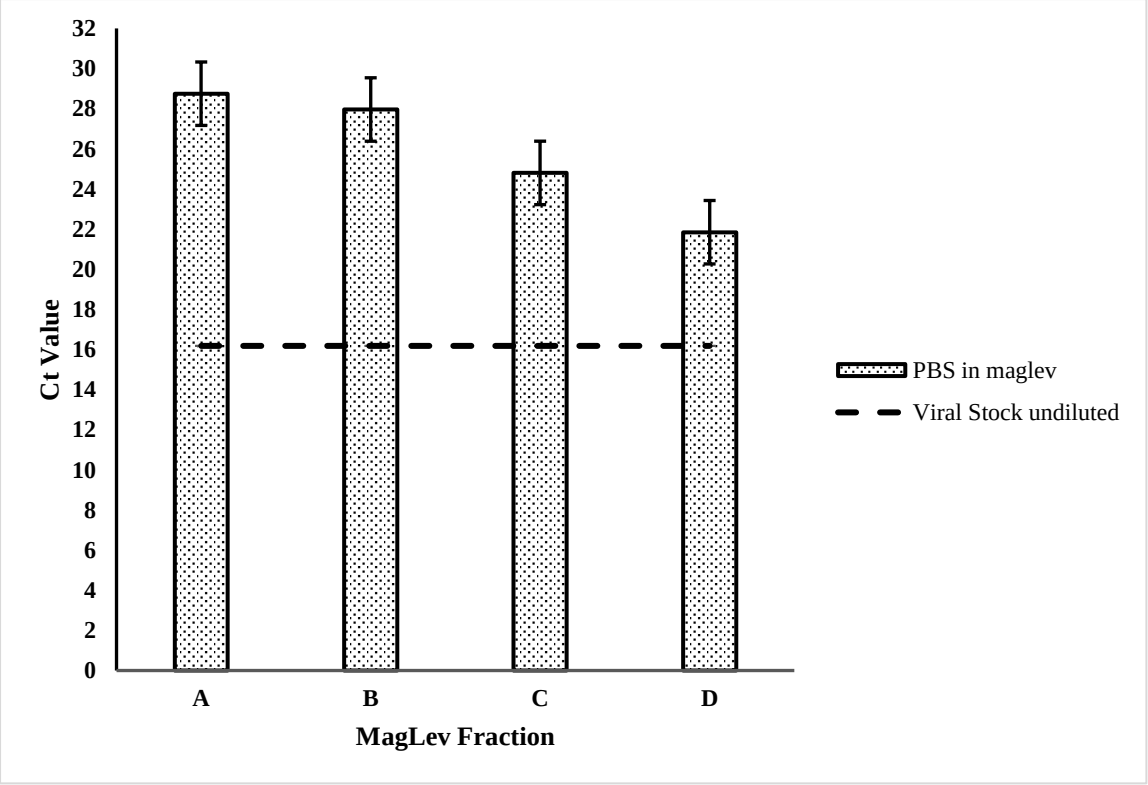

Fig 23. QPCR results of 4 MagLev fractions (A, B, C, D) obtained with only PBS added to the MagLev. C_t values represent a log fold change in viral quantity, hence a single increase in C_t value is a significant decrease in viral content. We can see that the bottom of the MagLev column (Fraction D) has the lowest C_t and thus the higher viral content. The C_t of the viral stock used is presented on the graph and the error bars represent standard error.

4.2 Aim 2: Investigate the performance of different paramagnetic media

The results show that each paramagnetic solution used besides $GdCl_3$ was not toxic to viruses or viral RNA. A direct pilot study without the use of a MagLev also showed no significant loss in viral C_t values (vRNA) with either Gadobutrol or SPIONs. However, both solutions display unique levitation properties indicating varying magnetic properties (**Fig 22, 24**). SPIONs in general however, offered a broader range of densities which could be measured (**Fig 20**). Alternatively, 0.1M Gadobutrol caused more levitation indicating its stronger magnetic properties. However, it also had a much narrower range for measurement of densities (**Fig 19**). Both solutions also proved to leave virions intact after MagLev and infectious. Notably, both solutions did not produce similar TCID50/ml values (**Fig 25**).

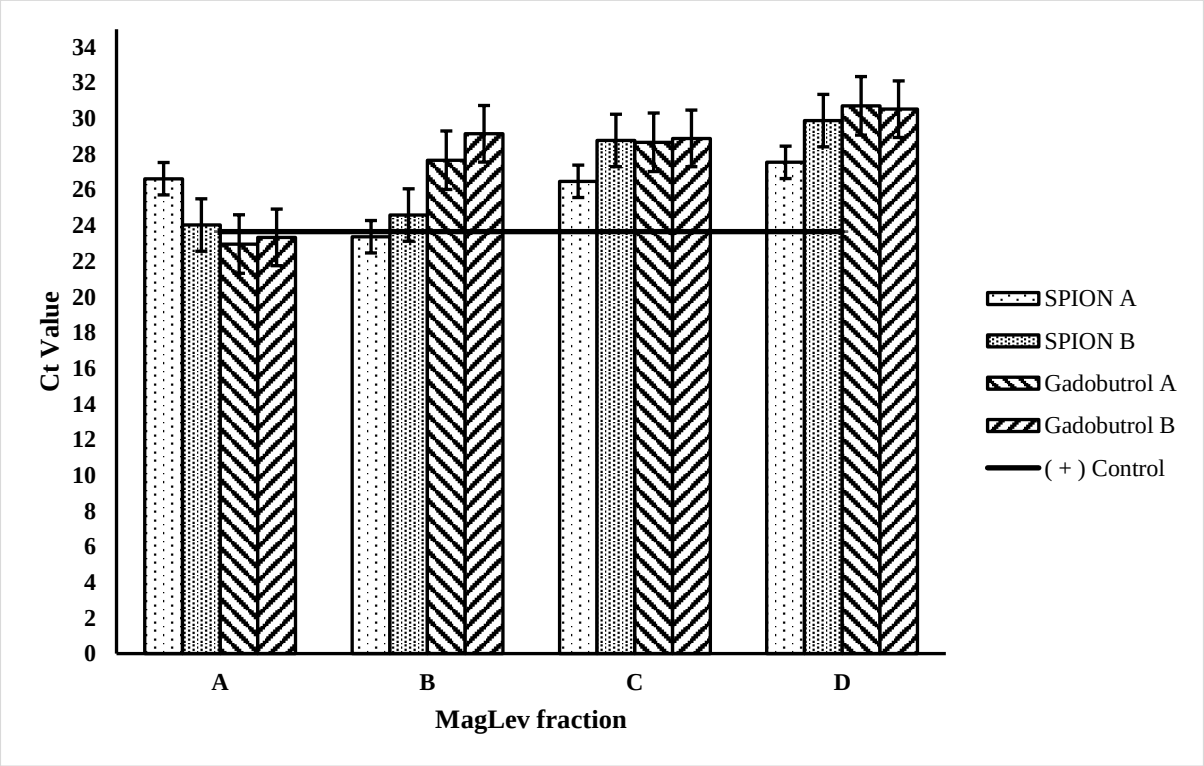

Fig 24. QPCR results of 4 MagLev fractions (A, B, C, D) obtained with 0.25mg/ml SPION and 0.1M Gadobutrol in the MagLev. Comparing the performance of each solution against our control we can observe that Gadobutrol has a C_t value near to the control in fraction A only while SPIONs do so at fraction A and B, indicating levitation. The error bars represent standard error.

4.3 Aim 3: Investigate if viruses are infective following levitation

The results of the tissue culturing showed that viruses remain infective after levitation (**Fig 25**). The results of a pilot experiment inoculating MDCK cells with only paramagnetic solutions showed that they do not contribute directly to cell death, indicating that the cell death observed

is due to viral infection. This corroborates data from other studies where cells were cultured using MagLev in paramagnetic media at higher concentrations than the ones used in our experiments[6]. Additionally, the control wells maintained their monolayer indicating no contamination or cell death from extraneous causes. Higher cell death or viral content (TCID50/ml) was found in some of the wells. This was observed for 0.1M Gadobutrol solution which showed a very high TCID50/ml for MagLev fraction A (488.8 TCID50/ml). Alternatively, 0.25mg/ml SPIONs showed high TCID50/ml for fraction B (111.94 TCID50/ml) and PBS on its own had a high TCID50/ml for fraction D (252.15 TCID50/ml) (**Fig 25**). Notably, we see that intact viruses are levitated to higher fractions in the MagLev and retain their infectivity. Furthermore, the paramagnetic solutions produce different levitation and infectivity results.

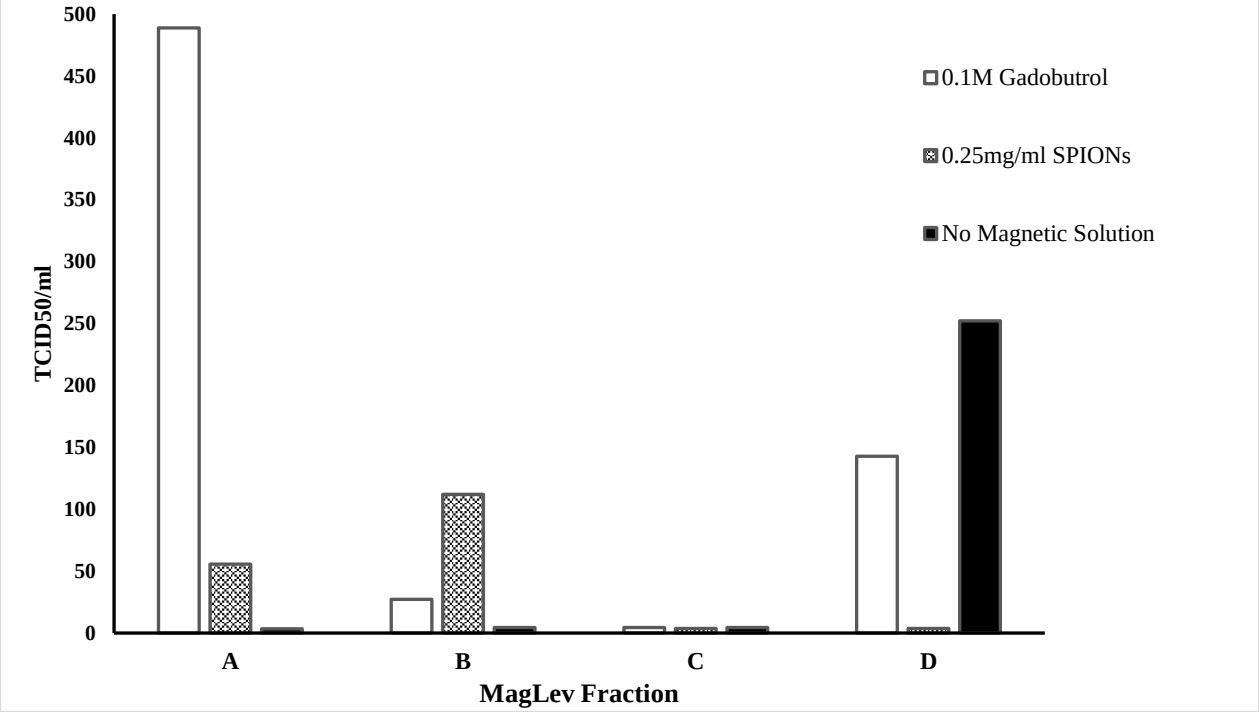

Fig 25. TCID50/ml calculated using the Reid-Muench method[48,92] for each of the 4 MagLev fractions (A, B, C, D). 3 repeats were done for 0.25mg/ml SPIONS and two each for 0.1M Gadobutrol (White), and PBS (Black) in the MagLev. The results show that whole viruses were levitated to higher fractions, and higher infectious viral load was present in higher fractions for each of the paramagnetic solutions. Gadobutrol displays notably better TCID50/ml values at fraction A.

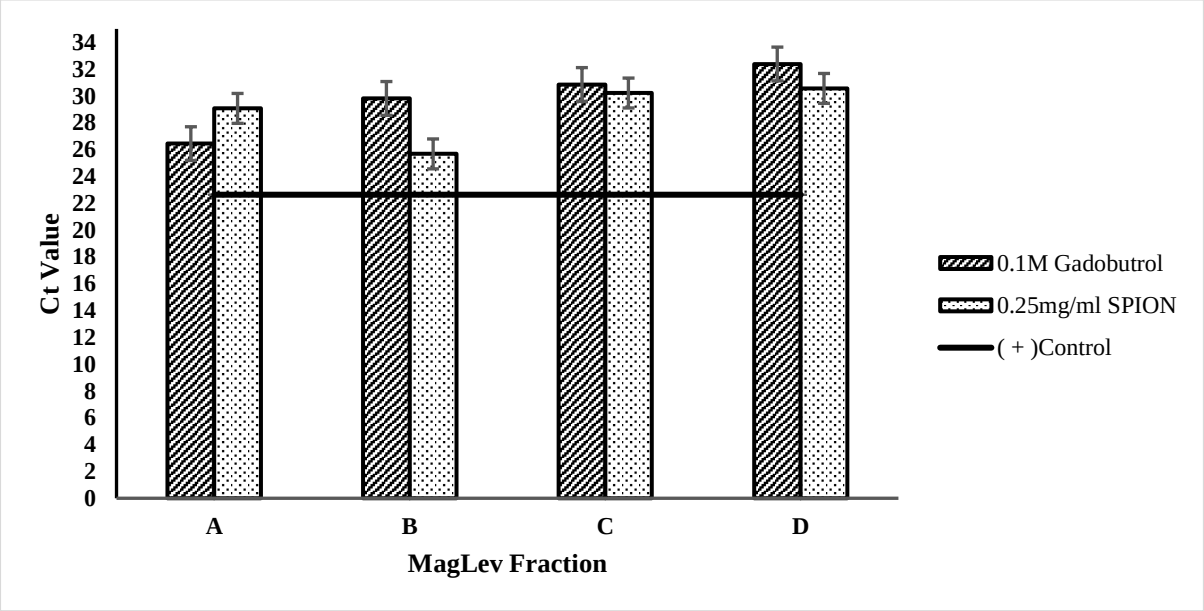

Fig 26. QPCR results of 4 MagLev fractions (A, B, C, D) used in tissue culturing obtained with 0.25mg/ml SPION and 0.1M Gadobutrol in the MagLev. Comparing the performance of each solution against our control we can observe that Gadobutrol has a C_t value near to the control only in fraction A, while SPIONs do so at fraction B, indicating levitation. Rt-PCR was done immediately after infection of tissues. The error bars represent standard error.

4.4 Aim 4: Determine a density estimate for the influenza A virus

Calibration graphs were constructed for each of the paramagnetic solutions (**Fig 19, 20**) using density readings and levitation heights from levitating fixed density microspheres (**Appendix A**). The graphs show a logistic pattern for the ring MagLev system with a linear region in the middle that flattens at the top and bottom (**Fig 14**; **(e)**). This has been validated recently[98] but in our experiment we focus on the linear region before the flattening of the density curve and consider it as the ideal measurement range for our MagLev system. The most consistent results for determining an unknown density would be obtained within this linear region. 0.1M Gadobutrol (**Fig 19**) has a much narrower range of measurement between 1.025 and 1.035g/cm^3 compared to the 0.25mg/ml SPION solution (**Fig 20**) which has a range somewhere between 0.96 and 1.015g/cm^3. While visualization was not very reproduceable, if we input the 9.5mm levitation height obtained for virus stock in two trials into the equation of the line for 0.25mg/ml SPIONs we get an estimate of density for influenza A/Puerto Rico/8/1934 ≈ 0.978 ± 0.02g/cm^3. This value is also notably within the measurable range for the MagLev system with 0.25mg/ml SPION solution and lower than previous literature estimates for influenza A density (1.014-1.265 g/cm^3)[16,19]. For the density calculation, the SPION curve was constructed

by removing some points that caused the linear relation to be skewed or lowered R^2 value. All of the measurements are available however as (**Appendix A**) table A and B.

4.5 Discussion

Here in, I show that viruses can be levitated using a MagLev based system with two very different paramagnetic solutions with varying results and degrees of success (**Fig 22, 24, 26**). Additionally, in comparison to PBS both Gadobutrol and Super Para-magnetic Iron Oxide Nanoparticles (SPIONs) did not differ significantly in their toxicity towards influenza virions or RNA. Moreover, the system shows promise in isolating most of the viruses within a sample to a specific hight, allowing levitated viruses to be isolated, collected and successfully grown in MDCK cells. While our initial goal of identifying viruses via a fixed visual band within the MagLev could not be reliably met, the results are promising with regards to improving sampling for subsequent detection. The visualization obtained (**Fig 21**) using 0.25mg/ml SPIONs, while not very reproducible, was corroborated by QPCR and TCID50 assessment. The experiment, methodology and results thus offer a new paradigm for studying influenza. Influenza A is a significant source of death[25,65] and economic concern[26,27,65] in the world and our work offers a new method for studying its dynamics and isolating it, offering faster cost-effective solutions to problems facing virologists. Viral particle dynamics and research in general have thus far been a difficult subject to broach with limited accessible-methodologies to interact with viruses directly without requiring extensive processing which introduces confounding bottlenecks[29,32,34,35,52]. The first ever MagLev based estimate of influenza A viral density (~ $0.978 \pm 0.02 g/cm^3$) alone is a major step in understanding viral particle dynamics which could not be done in the past directly or without the use of specialized equipment[16,78,93].

Influenza A is an enveloped virus[75]. While enveloped viruses like influenza and corona are major disease sources, it is important to note that there is a wealth of other non-enveloped viruses such as phages[64] which may have adverse responses to paramagnetic solutions due their protein capsids being exposed[113]. We do not provide any results for that broad category of viruses and as such it is unknown what MagLev or paramagnetic media will do to them. In principal however we can conclude that diamagnetic levitation will work for viruses other than influenza A. Another major factor identified in our work was the effect of the paramagnetic medium on TCID50 or viral infection in general. 0.1M Gadobutrol resulted in notably higher viral titter values (488.8 TCID50/ml) than 0.25mg/ml SPIONs (111.94

TCID50/ml) for their respective virus rich fractions (**Fig 25**). This can be attributed to SPIONs denaturing proteins necessary for influenza infection (HA, NA, TPCK-trypsin)[113] or Gadobutrols chelated structure (**Fig 16**)[104]. In our initial experimental design for this work we sought to utilize HA assays for determining the presence of intact virions[29,30] but the presence of Gadobutrol prevented the coagulation of blood cells even without intact influenza virions. Hence, Gadobutrol ions may help infection by preventing the clumping of virions. Alternatively, Gadobutrol may release gadolinium ions over time that may cause cell death[6], but this was not observed in pilot tests of direct cell inoculation. The clearest results were thus for $GdCl_3$ which is not mentioned in detail here because it resulted in dramatic loss of virions and vRNA due to its ionic nature resulting from free gadolinium and chloride ions. We concluded, that $GdCl_3$ should not be used for virus levitation (**Appendix A**; **Fig C**).

Another major limitation of this work is the lack of absolute or relative quantification from the QPCR results. We present the results for each PCR plate/assay individually with limited trials and repeats that are not directly comparable. A number of factors affected this decision but the consistent trend in C_t values in tandem with tissue culturing are evidence for the MagLev of viruses[48,49]. Additionally, the QPCR results show that we were unable to prevent the contamination of the whole MagLev systems column with viruses. This indicates that some viruses aren't levitating to an exact level. This result could have been due to a number of reasons including the highly concentrated influenza stock (C_t = ~13) itself which had more virions than any normal sample would, thus resulting in contamination. Another potential cause is the dependence of our workflow on hand pipetting volumes in and out of the MagLev which can disturb the levitation[1,12,98]. Stronger magnets could also have improved this outcome. This was a novel experiment and a number of issues were identified in the design of the MagLev, sample injection, handling and collection which ultimately reduce the utility of absolute viral quantification. Notably however, we confirmed that the C_t values throughout the MagLev column were not due to viral RNA (**Appendix A; Fig B**) which is much smaller than a virion and usually present in stocks as a result of damage to virions from ice crystals during Freeze/thaw[34]. This was done by treating MagLev fractions with an endonuclease to digest any free RNA which may contaminate the MagLev column before extraction and QPCR. The results presented in the appendix show no change in the overall trend of C_t values. Hence, we conclude that the MagLev while not being able to isolate all the viruses in a sample, can still function and may need further modification for use with viruses.

This is especially important with regards to design and collection methods to prevent disturbance once levitation is achieved.

The sample levitated in this experiment was very pure and concentrated viral stock. This is a highly irregular situation but was necessary for our attempts to find a visible band for influenza for use in naïve identification via visual assessment. We were not able to find any visible band using Gadobutrol and only observed a faint visual band using SPIONs in two trials. This limits the potential for our MagLev system in identifying and isolating viruses directly from clinical and environmental samples which have much lower viral titters and other complex molecules. The presence of other proteins and molecules can trap or clump viruses together to produce strong visualizations while preventing separation[1,20]. This is a hurdle to naïve identification and isolation of viruses using MagLev. It is unlikely then that without modifications to the system or the addition of specific sensors, agents like ligands or fluorescent dyes targeting viruses, that viruses can be directly identified.

Environmental factors such as temperature and pH. can play a major role in the survival of viruses[34,35] and time taken for an object to reach stable levitation[12,24,98]. Due to elevated precautions necessary when working with influenza (Bio Safety Leve 2+), the experiments were carried out within a BSC which limited the ability to regulate factors such as temperature. This has the potential to effect results but was not tested for. We additionally determined that ~15 minutes were necessary to achieve stable levitation at room temperature (no temperature control). This was done through pilot experiments which showed that without the consideration for time, the levitation varied (**Appendix A; Fig A**). This pilot experiment was not repeated for SPIONs and the effect of temperature was also not accounted for which has been shown to reduce the time taken to reach levitation[1,12]. Another drawback of the BSC was that it limited access to the MagLev such that more camera angles and lighting could not be utilized. There is potential for future MagLev systems to take these factors into account during the design stage.

The density estimate obtained for influenza A (~ 0.978 ± 0.02g/cm^3), while a potentially significant discovery also presents some further questions. It is notably lower than previous estimates (1.014-1.265 g/cm^3)[16,19] based on sucrose gradient centrifugation. While ultracentrifugation is dependant on several factors, more data is required to validate the MagLev based estimate of influenza A viral density. Additionally, PBS has a density (~ 1 g/cm^3) which is higher than that of our estimate, but in our experiments the viruses were

shown to fall to the bottom of the MagLev column after 15 minutes. While the effects of buoyancy are cancelled out when MagLev is taking place and a paramagnetic solution is in use, we would expect the influenza virions to float to the surface of PBS due their lower density. This raises questions regarding our density estimate and the interactions between the virions themselves. One possible explanation for the observation is that virions may clump together, and this results in clumps falling in solution. Pipetting can also aggravate the clumping of virions. There is currently little data available to present a conclusive answer regarding viral densities, but MagLev can potentially offer a fast and cost effective way to measure viral densities and potentially offer more precise measurements than previous ones dependent on sedimentation and sucrose gradient centrifugation[16,19]. Further research is required to validate the density estimate and ascertain the interactions between individual influenza virions and virions in general, as it can have implications in virus particle dynamics in nature and the MagLev.

Particle dynamics is a term more readily used in physics and chemistry but becomes a bigger factor in biology when working with extremely small organisms like viruses. Density and charge are both key factors in particle dynamics. In this work we acknowledge that magnetic fields are intrinsically tied with electrical fields and both exist in parallel as the electro-magnetic field spectrum[96,97]. However, the effects of charge and electric fields were not taken into consideration in this work. Only magnetic fields relating to MagLev were accounted for. Charges on influenza can play a significant role in virion-virion and virion-host interactions[114,115] and recent work has sought to study the net charge exhibited by influenza virions in more detail[116,117]. Given the importance of electro-static interactions, it is thus worthwhile to take such factors and pH. into account in future work. Viruses, like other particles hold the potential to maintain a net charge and we show in our work, that they can be considered diamagnetic. Ultimately, being able to study the physical characteristics of viruses offers novel insights into how they may behave in the air, on surfaces and in relation to other organisms or physical phenomenon. This shift towards considering biological materials in terms of their particle physics represents a paradigm shift in understanding and can help answer some of the biggest questions regarding the smallest life on this planet.

Chapter 5. Conclusion and Future Work

5.1 Conclusions; Aim 1 (Investigate if viruses are levitated within the MagLev)

The results show that viruses are levitated using a MagLev based system. While visually it was difficult to prove and study levitation, QPCR (**Fig 22, 24, 26**) and tissue culturing techniques (**Fig 25**) provide evidence for the levitation of influenza A. I also demonstrated that two paramagnetic solutions levitated viruses uniquely, linking levitation height with the magnetic properties of the MagLev system. Furthermore, it can be observed that influenza A viruses left within the MagLev without paramagnetic solution and only PBS (**Fig 23**) sink instead of floating. These results provide evidence of the diamagnetic properties of viruses.

5.2 Conclusions; Aim 2 (Investigate the performance of different paramagnetic media)

Gadobutrol and SPIONs were both found to be capable of levitating influenza A virions. Both displayed unique levitation properties, with Gadobutrol being more strongly magnetic even at low-concentrations (0.1M) and having a much narrower range for the measurement of densities (**Fig 19**). The range for 0.1M Gadobutrol was between 1.025 and 1.035g/cm^3 compared to the 0.25mg/ml SPION solution, (**Fig 20**) which had a range somewhere between 0.96 and 1.015g/cm^3, offering better resolution for smaller particles like viruses. The SPION solution however produced lower TCID50/ml values (**Fig 25**) indicating a potential effect on the infectivity of influenza A viruses following MagLev exposure. The $GdCl_3$ solution was the only paramagnetic solution tested with viruses, which displayed outright losses and indicated clearly that it should not be used in future MagLev experiments with viruses (**Appendix A; Fig C**).

5.3 Conclusions; Aim 3 (Investigate if viruses are infective following levitation)

TCID50/ml was calculated for each MagLev fraction and it was observed that some of the MagLev fractions clearly contained more infectious virions than others (**Fig 25**). This is evidence for the MagLev of infectious virions to a specific height within the MagLev system (**Fig 12**). All fractions of the MagLev however showed that they contained infectious virions. In general, we can conclude that MagLev leaves viruses infective following levitation, but the results vary based on the paramagnetic solution being used. Gadobutrol was shown to produce very high TCID50/ml values (**Fig 25**) compared to SPIONs and only PBS.

5.4 Conclusions; Aim 4 (Determine a density estimate for the influenza A virus)

Only two trials with SPIONs produced a faint visible marker for influenza A stock (**Fig 21**). This visible band however was within the region of the MagLev indicated by QPCR (**Fig 22, 24)** and tissue culturing techniques (**Fig 25**) to contain more virions. I utilized the equation (**Fig 20**) from the density calibration of the MagLev system with (0.25mg/ml) SPIONs to obtain an estimate of density for influenza A/Puerto Rico/8/1934 ≈ 0.978 ± 0.02 g/cm^3. This estimate of density was lower than literature estimates using other methods (1.014-1.265 g/cm^3)[16,19]. Without visualization, density determination was not possible using Gadobutrol.

5.5 Summary and future work

In this dissertation, I explain the theory behind MagLev for levitating biological materials[1,4,6] and then demonstrate the ability of influenza A virions to be levitated on the principals of diamagnetic levitation[96]. The experimental results indicate that viruses can be consistently levitated, and that levitation and magnetic forces do not damage virions allowing for infection of hosts. This levitation was demonstrated using QPCR and tissue culturing techniques and provided a first ever MagLev based estimate for the density of influenza A (~ 0.978 ± 0.02 g/cm^3). While a number of issues were identified in the process of this experiment pertaining to MagLev design, virion-virion interactions, virion-paramagnetic solution interaction, sample collection and visualization; the methodology and experimental evidence provide a framework for future work to build upon.

Future work is required to prove that non-enveloped viruses can also be levitated. Additionally, better MagLev systems need to be developed and tested to obtain clearer results regarding whether or not all of the virions in a sample can be isolated using MagLev. Better injection, visualization, temperature control and extraction methods need to be developed to reduce the uncertainty within MagLev systems for viruses. This is especially necessary if environmental and clinical samples are to be utilized successfully. Future work should look to expand upon the potential of MagLev systems and utilize better design philosophies and more precise measures such as absolute quantification to determine what percentage of viruses within a whole sample can be successfully obtained using MagLev. Currently, a number of issues exist within virologic research which can lead to errors in analysing viruses[33,35,55], prevent discovery of new viruses[28,30,84,85,118,119] and ultimately have real world consequences in terms of disease spread and economic losses[25,26,65]. With these issues in

mind and the results presented here in, MagLev is a very promising technology with an already established number of applications in mining and biology[4,6–8] but an as yet unutilized potential in viral research.

References

1. Ashkarran, A. A. *et al.* Evolving Magnetically Levitated Plasma Proteins Detects Opioid Use Disorder as a Model Disease. *Adv. Healthc. Mater.* **9**, 1901608 (2020).
2. Iranmanesh, M. & Hulliger, J. Magnetic separation: its application in mining, waste purification, medicine, biochemistry and chemistry. *Chem. Soc. Rev.* **46**, 5925–5934 (2017).
3. Shapiro, N. D., Soh, S., Mirica, K. A. & Whitesides, G. M. Magnetic Levitation as a Platform for Competitive Protein-Ligand Binding Assays. *Anal. Chem.* **84**, 6166–6172 (2012).
4. Anil-Inevi, M., Yilmaz, E., Sarigil, O., Tekin, H. C. & Ozcivici, E. Single Cell Densitometry and Weightlessness Culture of Mesenchymal Stem Cells Using Magnetic Levitation. in *Stem Cell Nanotechnology: Methods and Protocols* (ed. Turksen, K.) 15–25 (Springer US, 2020). doi:10.1007/7651_2019_231.
5.. Durmus, N. G. *et al.* Magnetic levitation of single cells. *Proc. Natl. Acad. Sci.* **112**, E3661–E3668 (2015).
6.. Türker, E., Demirçak, N. & Arslan-Yildiz, A. Scaffold-free three-dimensional cell culturing using magnetic levitation. *Biomater. Sci.* **6**, 1745–1753 (2018).
7. Ge, S. *et al.* Magnetic Levitation in Chemistry, Materials Science, and Biochemistry. *Angew. Chem. Int. Ed.* **59**, 17810–17855 (2020).
8. Abrahamsson, C. K. *et al.* Analysis of Powders Containing Illicit Drugs Using Magnetic Levitation. *Angew. Chem. Int. Ed.* **59**, 874–881 (2020).
9.. Lockett, M. R., Mirica, K. A., Mace, C. R., Blackledge, R. D. & Whitesides, G. M. Analyzing Forensic Evidence Based on Density with Magnetic Levitation. *J. Forensic Sci.* **58**, 40–45 (2013).
10. Hola, K., Markova, Z., Zoppellaro, G., Tucek, J. & Zboril, R. Tailored functionalization of iron oxide nanoparticles for MRI, drug delivery, magnetic separation and immobilization of biosubstances. *Biotechnol. Adv.* **33**, 1162–1176 (2015).
11. Chen, Y. *et al.* One-Step Detection of Pathogens and Viruses: Combining Magnetic Relaxation Switching and Magnetic Separation. *ACS Nano* **9**, 3184–3191 (2015).
12. Mirica, K. A., Shevkoplyas, S. S., Phillips, S. T., Gupta, M. & Whitesides, G. M. Measuring Densities of Solids and Liquids Using Magnetic Levitation: Fundamentals. *J. Am. Chem. Soc.* **131**, 10049–10058 (2009).

13. On a Contagium vivum fluidum causing the Spotdisease of the Tobacco-leaves. 8.
14. Fumian, T. M. *et al.* Detection of rotavirus A in sewage samples using multiplex qPCR and an evaluation of the ultracentrifugation and adsorption-elution methods for virus concentration. *J. Virol. Methods* **170**, 42–46 (2010).
15. Jiang, W. *et al.* An optimized method for high-titer lentivirus preparations without ultracentrifugation. *Sci. Rep.* **5**, 13875 (2015).
16. Barry, R. D. & Davies, P. The Sedimentation of Influenza Virus and its RNA in Sucrose Density Gradients. *J. Gen. Virol.* **2**, 59–69 (1968).
17. Barry, R. D. Equilibrium sedimentation of influenza virus in caesium chloride density gradients. *Aust. J. Exp. Biol. Med. Sci.* **38**, 499–507 (1960).
18. Arora, D. J. S., Pavilanis, V. & Robert, P. Two-step centrifugation method. A simplification of the density-gradient procedure for the purification of influenza virus. *Can. J. Microbiol.* (2011) doi:10.1139/m73-104.
19. Sharp, D. G., Taylor, A. R., McLean, I. W., Beard, D. & Beard, J. W. Density and Size of Influenza Virus a (PR8 Strain) in Solution. *Science* **100**, 151–153 (1944).
20. Asanzhanova, N. N. *et al.* Comparison of Different Methods of Purification and Concentration in Production of Influenza Vaccine. *Bull. Exp. Biol. Med.* **164**, 229–232 (2017).
21. James, K. T. *et al.* Novel High-throughput Approach for Purification of Infectious Virions. *Sci. Rep.* **6**, 36826 (2016).
22. Kugelman, J. R. *et al.* Error baseline rates of five sample preparation methods used to characterize RNA virus populations. *PLOS ONE* **12**, e0171333 (2017).
23. Purification of cell culture-derived influenza virus A/Puerto Rico/8/34 by membrane-based immobilized metal affinity chromatography. - Abstract - Europe PMC. https://europepmc.org/article/med/19591872.
24. Bwambok, D. K. *et al.* Paramagnetic Ionic Liquids for Measurements of Density Using Magnetic Levitation. *Anal. Chem.* **85**, 8442–8447 (2013).
25. Up to 650 000 people die of respiratory diseases linked to seasonal flu each year. *Saudi Med. J.* **39**, 109–110 (2018).
26. C, N. *et al.* Resource utilization and cost of influenza requiring hospitalization in Canadian adults: A study from the serious outcomes surveillance network of the Canadian Immunization Research Network. *Influenza Other Respir. Viruses* **12**, 232–240 (2018).

27. Hay, A. J. & McCauley, J. W. The WHO global influenza surveillance and response system (GISRS)-A future perspective. *Influenza Other Respir. Viruses* **12**, 551–557 (2018).
28. Kim, H., Webster, R. G. & Webby, R. J. Influenza Virus: Dealing with a Drifting and Shifting Pathogen. *Viral Immunol.* **31**, 174–183 (2018).
29. Takahara, Y. *et al.* Comparison of Influenza Virus Detection Methods. *Sens. Mater.* **31**, 79 (2019).
30. Trombetta, C. M., Remarque, E. J., Mortier, D. & Montomoli, E. Comparison of hemagglutination inhibition, single radial hemolysis, virus neutralization assays, and ELISA to detect antibody levels against seasonal influenza viruses. *Influenza Other Respir. Viruses* **12**, 675–686 (2018).
31. Ladd Effio, C. *et al.* Downstream processing of virus-like particles: Single-stage and multi-stage aqueous two-phase extraction. *J. Chromatogr. A* **1383**, 35–46 (2015).
32. Lee, R. T. C., Chang, H.-H., Russell, C. A., Lipsitch, M. & Maurer-Stroh, S. Influenza A Hemagglutinin Passage Bias Sites and Host Specificity Mutations. *Cells* **8**, 958 (2019).
33. Xue, K. S., Greninger, A. L., Pérez-Osorio, A. & Bloom, J. D. Cooperating H3N2 Influenza Virus Variants Are Not Detectable in Primary Clinical Samples. *mSphere* **3**, (2018).
34. Hirst, J. C. & Hutchinson, E. C. Single-particle measurements of filamentous influenza virions reveal damage induced by freezing. *J. Gen. Virol.* **100**, 1631–1640 (2019).
35. Granados, A., Petrich, A., McGeer, A. & Gubbay, J. B. Measuring influenza RNA quantity after prolonged storage or multiple freeze/thaw cycles. *J. Virol. Methods* **247**, 45–50 (2017).
36. Wang, J., Ma, J. & Wen, X. Basic Concepts of Density Gradient Ultracentrifugation. in *Nanoseparation Using Density Gradient Ultracentrifugation: Mechanism, Methods and Applications* (eds. Sun, X., Luo, L., Kuang, Y. & Li, P.) 21–36 (Springer, 2018). doi:10.1007/978-981-10-5190-6_2.
37. Organization, W. H. Coronavirus disease 2019 (COVID-19): situation report, 67. (2020).
38. Lai, C.-C., Shih, T.-P., Ko, W.-C., Tang, H.-J. & Hsueh, P.-R. Severe acute respiratory syndrome coronavirus 2 (SARS-CoV-2) and coronavirus disease-2019

(COVID-19): The epidemic and the challenges. *Int. J. Antimicrob. Agents* **55**, 105924 (2020).

39. Lu, S. EV71 vaccines: a milestone in the history of global vaccine development. *Emerg. Microbes Infect.* **3**, e27 (2014).

40. Chen, W.-H., Strych, U., Hotez, P. J. & Bottazzi, M. E. The SARS-CoV-2 Vaccine Pipeline: an Overview. *Curr. Trop. Med. Rep.* **7**, 61–64 (2020).

41. Lu, S. Timely development of vaccines against SARS-CoV-2. *Emerg. Microbes Infect.* **9**, 542–544 (2020).

42. Nakatsukasa, A. *et al.* Potency of whole virus particle and split virion vaccines using dissolving microneedle against challenges of H1N1 and H5N1 influenza viruses in mice. *Vaccine* **35**, 2855–2861 (2017).

43. Park, Y. C. & Song, J. M. Preparation and immunogenicity of influenza virus-like particles using nitrocellulose membrane filtration. *Clin. Exp. Vaccine Res.* **6**, 61 (2017).

44. Hawksworth, A., Jayachander, M., Hester, S., Mohammed, S. & Hutchinson, E. Proteomics as a tool for live attenuated influenza vaccine characterisation. *Vaccine* **38**, 868–877 (2020).

45. Hutchinson, E. C. Influenza Virus. *Trends Microbiol.* **26**, 809–810 (2018).

46. Shi, M. *et al.* The evolutionary history of vertebrate RNA viruses. *Nature* **556**, 197–202 (2018).

47. Abachin, E. *et al.* Comparison of reverse-transcriptase qPCR and droplet digital PCR for the quantification of dengue virus nucleic acid. *Biologicals* **52**, 49–54 (2018).

48. LaBarre, D. D. & Lowy, R. J. Improvements in methods for calculating virus titer estimates from TCID50 and plaque assays. *J. Virol. Methods* **96**, 107–126 (2001).

49. Petrie, S. M. *et al.* Reducing Uncertainty in Within-Host Parameter Estimates of Influenza Infection by Measuring Both Infectious and Total Viral Load. *PLOS ONE* **8**, e64098 (2013).

50. Fang, Y. *et al.* Sensitivity of Chest CT for COVID-19: Comparison to RT-PCR. *Radiology* **296**, E115–E117 (2020).

51. Differential activation of host cell signalling pathways through infection with two variants of influenza A/Puerto Rico/8/34 (H1N1) in MDCK cells- ClinicalKey. https://www-clinicalkey-com.ezproxy.library.ubc.ca/#!/content/playContent/1-s2.0-S0264410X1001087X?returnurl=null&referrer=null.

52. Dadonaite, B., Vijayakrishnan, S., Fodor, E., Bhella, D. & Hutchinson, E. C. Filamentous Influenza Viruses. *J. Gen. Virol.* **97**, 1755–1764 (2016).

53. Cummings, C. O. *et al.* Evidence of Influenza A in Wild Norway Rats (Rattus norvegicus) in Boston, Massachusetts. *Frontiers in Ecology and Evolution* vol. 7 https://doaj.org (2019).
54. Minodier, L. *et al.* Risk factors for seasonal influenza virus detection in stools of patients consulting in general practice for acute respiratory infections in France, 2014-2016. *Influenza Other Respir. Viruses* **13**, 398–406 (2019).
55. Nagy, A., Jiřinec, T., Jiřincová, H., Černíková, L. & Havlíčková, M. In silico re-assessment of a diagnostic RT-qPCR assay for universal detection of Influenza A viruses. *Sci. Rep.* **9**, 1630 (2019).
56. Duesberg, P. H. Distinct subunits of the ribonucleoprotein of influenza virus. *J. Mol. Biol.* **42**, 485–499 (1969).
57. Lechevalier, H. Dmitri Iosifovich Ivanovski (1864-1920). *Bacteriol. Rev.* **36**, 135–145 (1972).
58. Flint, S. J., Racaniello, V. R., Rall, G. F. & Skalka, A. M. *Principles of Virology: Bundle*. (ASM Press, 2015).
59. Hutchinson, E. C. *et al.* Conserved and host-specific features of influenza virion architecture. *Nat. Commun.* **5**, 4816 (2014).
60. Lefkowitz, E. J. *et al.* Virus taxonomy: the database of the International Committee on Taxonomy of Viruses (ICTV). *Nucleic Acids Res.* **46**, D708–D717 (2018).
61. Handel, A. Cell Biology by the Numbers by Ron Milo and Rob Phillips. *Q. Rev. Biol.* **92**, 477–477 (2017).
62. Forth, J. H. African Swine Fever Virus – Exploring Virus Evolution and Vector Dynamics. (2019).
63. Baltimore, D. Expression of animal virus genomes. *Bacteriol. Rev.* **35**, 235–241 (1971).
64. Comeau, A. M., Bertrand, C., Letarov, A., Tétart, F. & Krisch, H. M. Modular architecture of the T4 phage superfamily: A conserved core genome and a plastic periphery. *Virology* **362**, 384–396 (2007).
65. Ren, R. Q., Zhou, L. & Ni, D. X. [An overview on the history of global influenza pandemics]. *Zhonghua Liu Xing Bing Xue Za Zhi Zhonghua Liuxingbingxue Zazhi* **39**, 1021–1027 (2018).
66. First Global Estimates of 2009 H1N1 Pandemic Mortality Released by CDC-Led Collaboration | CDC. https://www.cdc.gov/flu/spotlights/pandemic-global-estimates.htm (2019).

67. Goodson, J. L., Alexander, J. P., Linkins, R. W. & Orenstein, W. A. Measles and rubella elimination: learning from polio eradication and moving forward with a diagonal approach. *Expert Rev. Vaccines* **16**, 1203–1216 (2017).
68. Lee, N. *et al.* Genome-wide analysis of influenza viral RNA and nucleoprotein association. *Nucleic Acids Res.* **45**, 8968–8977 (2017).
69. Langat, P. *et al.* Genome-wide evolutionary dynamics of influenza B viruses on a global scale. *PLOS Pathog.* **13**, e1006749 (2017).
70. Influenza (Seasonal). https://www.who.int/news-room/fact-sheets/detail/influenza-(seasonal).
71. Gao, Q., Brydon, E. W. A. & Palese, P. A Seven-Segmented Influenza A Virus Expressing the Influenza C Virus Glycoprotein HEF. *J. Virol.* **82**, 6419–6426 (2008).
72. Su, S., Fu, X., Li, G., Kerlin, F. & Veit, M. Novel Influenza D virus: Epidemiology, pathology, evolution and biological characteristics. *Virulence* **8**, 1580–1591 (2017).
73. Selective packaging of the influenza A genome and consequences for genetic reassortment. - Abstract - Europe PMC. https://europepmc.org/article/med/24798745.
74. Chaimayo, C., Hayashi, T., Underwood, A., Hodges, E. & Takimoto, T. Selective incorporation of vRNP into influenza A virions determined by its specific interaction with M1 protein. *Virology* **505**, 23–32 (2017).
75. CDC. Types of Influenza Viruses. *Centers for Disease Control and Prevention* https://www.cdc.gov/flu/about/viruses/types.htm (2019).
76. Koutsakos, M., Nguyen, T. H., Barclay, W. S. & Kedzierska, K. Knowns and unknowns of influenza B viruses. *Future Microbiol.* **11**, 119–135 (2015).
77. Pflug, A., Lukarska, M., Resa-Infante, P., Reich, S. & Cusack, S. Structural insights into RNA synthesis by the influenza virus transcription-replication machine. *Virus Res.* **234**, 103–117 (2017).
78. Calder, L. J. & Rosenthal, P. B. Cryomicroscopy provides structural snapshots of influenza virus membrane fusion. *Nat. Struct. Mol. Biol.* **23**, 853–858 (2016).
79. J, L. *et al.* MOV10 sequesters the RNP of influenza A virus in the cytoplasm and is antagonized by viral NS1 protein. *Biochem. J.* **476**, 467–481 (2019).
80. Krug, R. M. Functions of the Influenza A Virus NS1 Protein In Antiviral Defense. *Curr. Opin. Virol.* **12**, 1–6 (2015).
81. Scholtissek, C. & Müller, K. Effect of dimethylsulfoxide (DMSO) on virus replication and maturation. *Arch. Virol.* **100**, 27–35 (1988).

82. Genzel, Y., Behrendt, I., König, S., Sann, H. & Reichl, U. Metabolism of MDCK cells during cell growth and influenza virus production in large-scale microcarrier culture. *Vaccine* **22**, 2202–2208 (2004).
83. Smith, C. J. & Osborn, A. M. Advantages and limitations of quantitative PCR (Q-PCR)-based approaches in microbial ecology. *FEMS Microbiol. Ecol.* **67**, 6–20 (2009).
84. Gaby, J. C. & Buckley, D. H. The Use of Degenerate Primers in qPCR Analysis of Functional Genes Can Cause Dramatic Quantification Bias as Revealed by Investigation of nifH Primer Performance. *Microb. Ecol.* **74**, 701–708 (2017).
85. Parras-Moltó, M., Rodríguez-Galet, A., Suárez-Rodríguez, P. & López-Bueno, A. Evaluation of bias induced by viral enrichment and random amplification protocols in metagenomic surveys of saliva DNA viruses. *Microbiome* **6**, 119 (2018).
86. real-time-pcr-handbook.pdf.
87. Heid, C. A., Stevens, J., Livak, K. J. & Williams, P. M. Real time quantitative PCR. *Genome Res.* **6**, 986–994 (1996).
88. Hirose, R. *et al.* Long-term detection of seasonal influenza RNA in faeces and intestine. *Clin. Microbiol. Infect.* **22**, 813.e1-813.e7 (2016).
89. Lindsley, W. G. *et al.* Measurements of Airborne Influenza Virus in Aerosol Particles from Human Coughs. *PLOS ONE* **5**, e15100 (2010).
90. Typing (A/B) and subtyping (H1/H3/H5) of influenza A viruses by multiplex real-time RT-PCR assays. - Abstract - Europe PMC. https://europepmc.org/article/med/18598722.
91. Spackman, E. *et al.* Development of a Real-Time Reverse Transcriptase PCR Assay for Type A Influenza Virus and the Avian H5 and H7 Hemagglutinin Subtypes. *J. Clin. Microbiol.* **40**, 3256–3260 (2002).
92. REED, L. J. & MUENCH, H. A SIMPLE METHOD OF ESTIMATING FIFTY PER CENT ENDPOINTS12. *Am. J. Epidemiol.* **27**, 493–497 (1938).
93. Reimer, C. B. *et al.* Purification of Large Quantities of Influenza Virus by Density Gradient Centrifugation. *J. Virol.* **1**, 1207–1216 (1967).
94. Howell, C. L. & Miller, M. J. Effect of sucrose phosphate and sorbitol on infectivity of enveloped viruses during storage. *J. Clin. Microbiol.* **18**, 658–662 (1983).
95. Kordyuk, A. A. Magnetic levitation for hard superconductors. *J. Appl. Phys.* **83**, 610–612 (1998).
96. *Physics of Ferromagnetism*. (Oxford University Press, 2009).

97. Mattis, D. C. History of Magnetism. in *The Theory of Magnetism I: Statics and Dynamics* (ed. Mattis, D. C.) 1–38 (Springer, 1981). doi:10.1007/978-3-642-83238-3_1.

98. Zhang, C. *et al.* Axial-Circular Magnetic Levitation: A Three-Dimensional Density Measurement and Manipulation Approach. *Anal. Chem.* **92**, 6925–6931 (2020).

99. Sears and Zemansky's University Physics. /content/one-dot-com/one-dot-com/us/en/higher-education/product.html.

100. Mattis, D. C. Quantum Theory of Angular Momentum. in *The Theory of Magnetism I: Statics and Dynamics* (ed. Mattis, D. C.) 67–94 (Springer, 1981). doi:10.1007/978-3-642-83238-3_3.

101. Wáng, Y. X. J. & Idée, J.-M. A comprehensive literatures update of clinical researches of superparamagnetic resonance iron oxide nanoparticles for magnetic resonance imaging. *Quant. Imaging Med. Surg.* **7**, 8822–8122 (2017).

102. Myers, H. P. *Introductory Solid State Physics*. (CRC Press, 1997). doi:10.1201/9780429320286.

103. Mattis, D. C. Magnetism in Metals. in *The Theory of Magnetism I: Statics and Dynamics* (ed. Mattis, D. C.) 207–283 (Springer, 1981). doi:10.1007/978-3-642-83238-3_6.

104. Fraga, G. L. F., Pureur, P. & Cardoso, L. P. Impedance and initial magnetic permeability of gadolinium. *J. Appl. Phys.* **107**, 053909 (2010).

105. Mattis, D. C. From Magnons to Solitons: Spin Dynamics. in *The Theory of Magnetism I: Statics and Dynamics* (ed. Mattis, D. C.) 138–206 (Springer, 1981). doi:10.1007/978-3-642-83238-3_5.

106. Jones, W. Earnshaw\textquotesingles theorem and the stability of matter. *Eur. J. Phys.* **1**, 85–88 (1980).

107. Hennet, L., Holland Moritz, D., Weber, R. & Meyer, A. Chapter 10 - High-Temperature Levitated Materials. in *Experimental Methods in the Physical Sciences* (eds. Fernandez-Alonso, F. & Price, D. L.) vol. 49 583–636 (Academic Press, 2017).

108. Sassonker, I. & Kuperman, A. Electro-mechanical modeling of electromagnetic levitation melting system driven by a series resonant inverter with experimental validation. *Energy Convers. Manag.* **208**, 112578 (2020).

109. Keppens, R., Toth, G., Westermann, R. H. J. & Goedbloed, J. P. Growth and saturation of the Kelvin-Helmholtz instability with parallel and anti-parallel magnetic fields. *J. Plasma Phys.* **61**, 1–19 (1999).

110. Pre-clinical evaluation of gadobutrol: a new, neutral, extracellular contrast agent for magnetic resonance imaging. *Eur. J. Radiol.* **21**, 1–10 (1995).
111. Bullivant, J. P. *et al.* Materials Characterization of Feraheme/Ferumoxytol and Preliminary Evaluation of Its Potential for Magnetic Fluid Hyperthermia. *Int. J. Mol. Sci.* **14**, 17501–17510 (2013).
112. Mahmoudi, M., Stroeve, P., Milani, A. S. & Arbab, A. S. *Superparamagnetic iron oxide nanoparticles: Synthesis, surface engineering, cytotoxicity and biomedical applications*. (Nova Science Publishers, Inc., 2011).
113. Mahmoudi, M. *et al.* Irreversible changes in protein conformation due to interaction with superparamagnetic iron oxide nanoparticles. *Nanoscale* **3**, 1127–1138 (2011).
114. Kobayashi, Y. & Suzuki, Y. Compensatory Evolution of Net-Charge in Influenza A Virus Hemagglutinin. *PLOS ONE* **7**, e40422 (2012).
115. Saad-Roy, C. M. *et al.* Implications of localized charge for human influenza A H1N1 hemagglutinin evolution: Insights from deep mutational scans. *PLOS Comput. Biol.* **16**, e1007892 (2020).
116. Heidari, A., Righetto, I. & Filippini, F. Electrostatic Variation of Haemagglutinin as a Hallmark of the Evolution of Avian Influenza Viruses. *Sci. Rep.* **8**, 1929 (2018).
117. Virus Isoelectric Point Determination Using Single-Particle Chemical Force Microscopy | Langmuir. https://pubs.acs.org/doi/abs/10.1021/acs.langmuir.9b03070?casa_token=egfBq2G8__wAAAAA:yzVc4AtlDdObdFwumj2MHYNd_wuYd6juL5yYiKRbRkyPIP6i_0UQXsXqWF72ZDDGUV5dAuSBqkpC4-Y.
118. Goya, S. *et al.* An optimized methodology for whole genome sequencing of RNA respiratory viruses from nasopharyngeal aspirates. *PLOS ONE* **13**, e0199714 (2018).
119. Boussier, J. *et al.* RNA-seq accuracy and reproducibility for the mapping and quantification of influenza defective viral genomes. *RNA* **26**, 1905–1918 (2020).

Appendices

Appendix A; Supplemental information

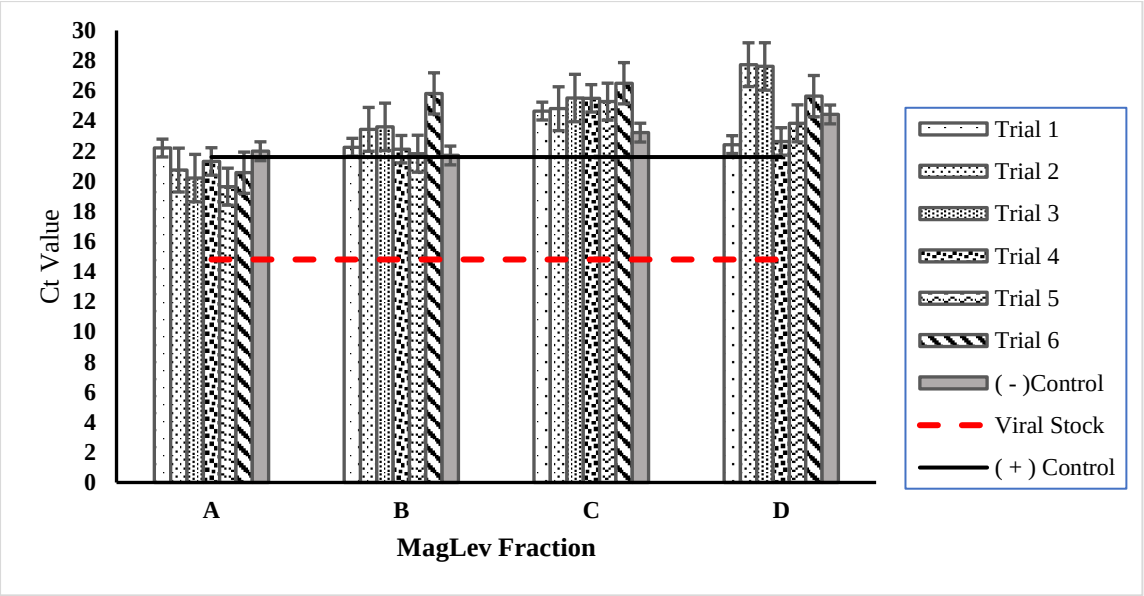

Fig A. QPCR results of 4 MagLev fractions (A, B, C, D). The MagLev was used with 0.1M Gadobutrol and PBS (-) Control. 6 trials were conducted for 0.1M Gadobutrol. The results were inconsistent with each other due to time not being a controlled variable. This experiment showed that levitation does not complete until at least 15 minutes for the Gadobutrol solution. Additionally, viruses remain in the column with PBS in the MagLev until 15 minutes, after which they may fall to the bottom of the column. Comparing the performance of each solution against our control, Gadobutrol has a C_t value near to the (+) control in fraction A but this is not consistent. The error bars represent standard error.

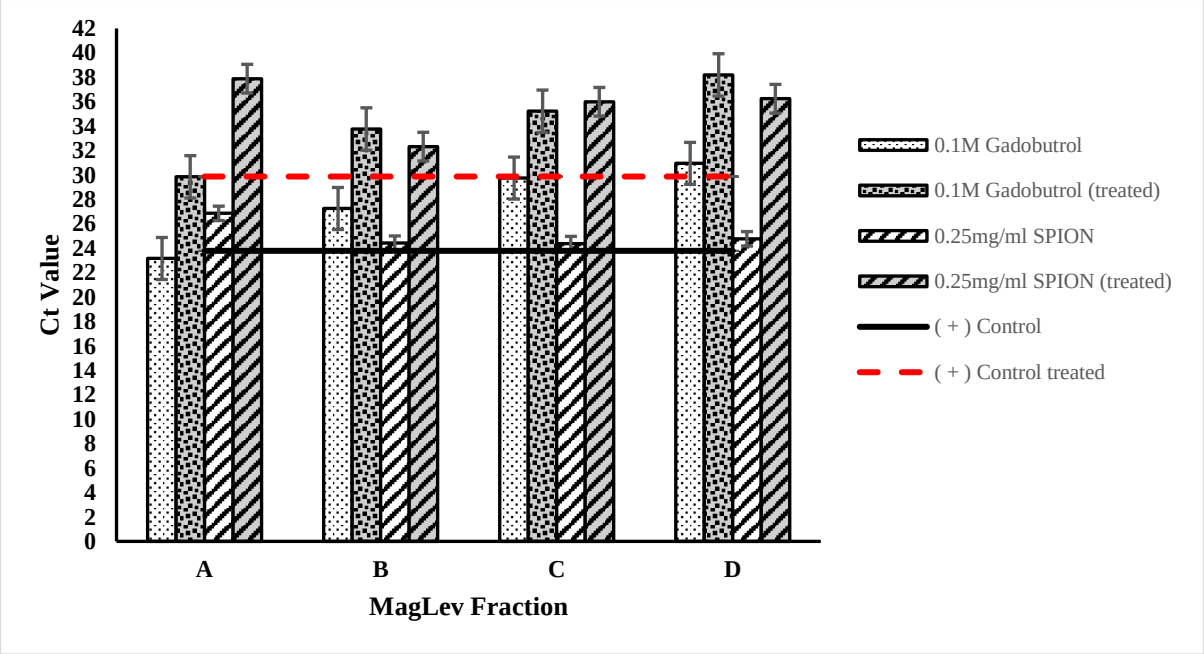

Fig B. QPCR results of 4 MagLev fractions (A, B, C, D) before (White) and after (Grey) treatment with an endonuclease to digest RNA, leaving only intact viruses. The MagLev was used with 0.25mg/ml SPION and 0.1M Gadobutrol. Comparing the performance of each solution against our control and treated control we can observe that Gadobutrol has a C_t value near to the control in fraction A while SPIONs do so at fraction B. The trend is maintained even though C_t values are lost/increase after treatment. We can also conclude that there is no specific trend attributable to vRNA. The error bars represent standard error.

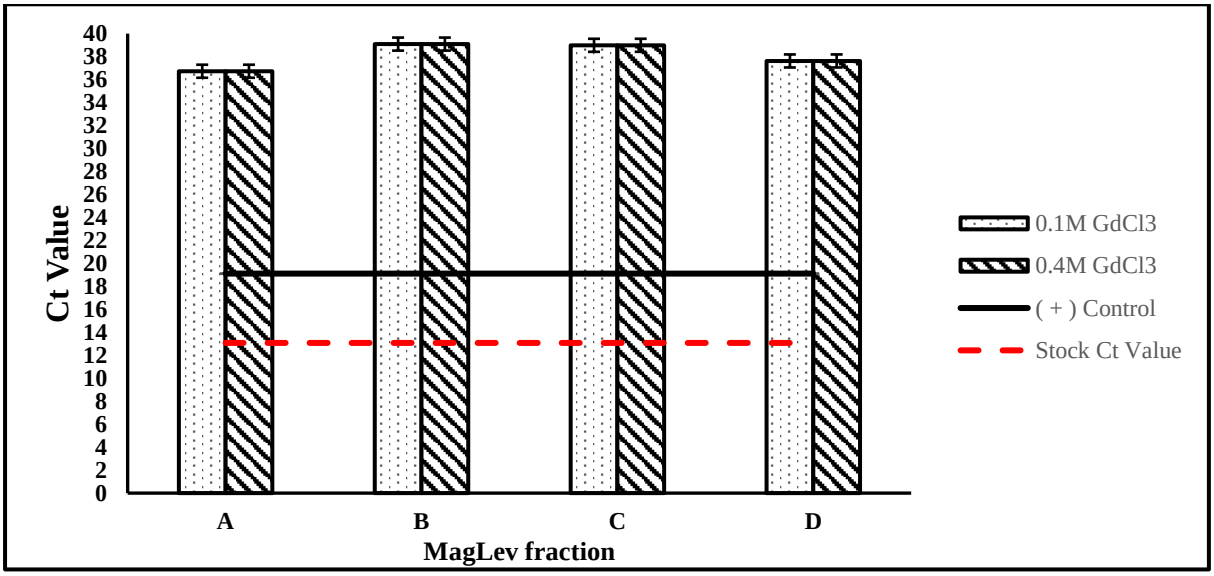

Fig C. QPCR results of 4 MagLev fractions (A, B, C, D) obtained with $GdCl_3$ paramagnetic medium. The MagLev was used with 0.1 and 0.4M molar $GdCl_3$. The results of three repeats were averaged and show a significant loss in viral load compared to the (+) Control indicating the invasive and destructive nature of $GdCl_3$ towards viral particles and RNA. The error bars represent standard error

Table A. Calibration for 0.1M Gadobutrol solution using fixed density microspheres. A minimum of three different particles from each density category were levitated within the MagLev and their corresponding levitation height (mm) noted for constructing a calibration curve. * represents densities which were outside the column.

	Levitation height (mm)			
Particle density (g/cm^3)	**Trial 1**	**Trial 2**	**Trial 3**	**Average**
0.92	*	*	*	*
0.96	*	*	*	*
0.995	*	*	*	*
1.015	14	14.5	13.5	14.00
1.02	13.6	13.7	13.2	13.50
1.025	13	13	13.1	13.03
1.035	2.9	3.2	3	3.03
1.05	2	1.5	1	1.50
1.08	*	*	*	*
1.1	*	*	*	*

Table B. Calibration for 0.25 mg/ml SPION solution using fixed density microspheres. A minimum of three different particles from each density category were levitated within the MagLev and their corresponding levitation height (mm) noted for constructing a calibration curve. * represents densities outside the column.

	Levitation height (mm)			
Particle density (g/cm^3)	**Trial 1**	**Trial 2**	**Trial 3**	**Average**
0.92	15	*	15	15.00
0.96	*	13	12.5	12.75
0.995	11	11	10.9	10.96
1.015	3.5	3.5	3.5	3.50
1.02	3.6	3.5	3.6	3.56
1.025	3	3.1	3.1	3.06
1.035	2.4	2.7	2.7	2.60
1.05	2.5	2.5	2	2.33
1.08	1.5	1.5	1.5	1.50
1.1	0.2	0.5	0.8	0.50

Appendix B; Calculations

Appendix B.1: Equation for stable levitation within a MagLev system

$$\overrightarrow{F_g} + \overrightarrow{F_m} = (\rho_s - \rho_m)V\vec{g} + \frac{(\chi_s - \chi_m)}{\mu_0}V(\vec{B} \bullet \nabla)\vec{B} = 0$$

(Equation 7)

Where the force due to gravity $\vec{F}_g$ cancels out the lift force from the magnet $\vec{F}_m$

$$\overrightarrow{F_g} = \overrightarrow{F_m}$$

From newtons second law and using the relation between density, mass and volume we get:

$$\vec{F} = m\vec{g} = \rho V\vec{g}$$

From buoyance which results from newtons third law of motion we know total $\overrightarrow{F_g}$ acting on an object in a medium:

$$\overrightarrow{F_g} = \overrightarrow{F_{g1}} - \overrightarrow{F_{g2}}$$

$$\overrightarrow{F_g} = \overrightarrow{F_{g1}} - \overrightarrow{F_{g2}} = \rho_1 V\vec{g} - \rho_2 V\vec{g}$$

$$\overrightarrow{F_g} = (\rho_1 - \rho_2)V\vec{g}$$

The calculation for $\overrightarrow{F_m}$ is as follows where $\vec{B}$ is the magnetic field and ∇ the vector component and χ is the magnetic susceptibility for either substrate being levitated (χ_s) or medium in which levitation is occurring(χ_m). μ_0 is the permeability of free space/vacuum.

$$\overrightarrow{F_m} = \vec{\mu}(\nabla \cdot \vec{B})$$

$\vec{\mu} = \frac{\chi}{\mu_0}V\vec{B}$ (magnetic moment)

$$\Rightarrow \overrightarrow{F_m} = \frac{\chi}{\mu_0}V\vec{B}(\nabla \cdot \vec{B})$$

$$\overrightarrow{F_m} = \frac{\chi_s - \chi_m}{\mu_0}V\vec{B}(\nabla \cdot \vec{B})$$

Equating the two sides $\overrightarrow{F_g} = \overrightarrow{F_m}$ gives us:

$$\overrightarrow{F_g} + \overrightarrow{F_m} = (\rho_s - \rho_m)V\vec{g} + \frac{(\chi_s - \chi_m)}{\mu_0}V(\vec{B} \bullet \nabla)\vec{B} = 0 \quad \textbf{(Equation 7)}$$

Appendix B.2: Linking levitation height to the density of a levitating object

Solving for the field components of $\vec{B}(\nabla \cdot \vec{B})$ in an anti-Helmholtz configuration and derivation gives us:

$$\overrightarrow{F_g} + \overrightarrow{F_m} = (\rho_s - \rho_m)V\vec{g} + \frac{\chi_s - \chi_m}{\mu_0}V\left(\frac{4{B_0}^2}{d^2}z - \frac{2{B_0}^2}{d}\right) = 0 \quad \textbf{(Equation 7)}$$

$$\frac{\chi_s - \chi_m}{\mu_0}V\left(\frac{4{B_0}^2}{d^2}z - \frac{2{B_0}^2}{d}\right) = (\rho_s - \rho_m)Vg$$

$$\left(\frac{4{B_0}^2}{d^2}z - \frac{2{B_0}^2}{d}\right) = (\rho_s - \rho_m)Vg\frac{\mu_0}{\chi_s - \chi_m}\frac{1}{V}$$

$$\frac{4{B_0}^2}{d^2}z = (\rho_s - \rho_m)Vg\frac{\mu_0}{\chi_s - \chi_m}\frac{1}{V} + \frac{2{B_0}^2}{d}$$

$$z = (\rho_s - \rho_m)Vg\frac{\mu_0}{\chi_s - \chi_m}\frac{1}{V}\left(\frac{d^2}{4{B_0}^2}\right) + \frac{2{B_0}^2}{d}\left(\frac{d^2}{4{B_0}^2}\right)$$

$$z = (\rho_s - \rho_m)\cancel{V}g\frac{\mu_0}{\chi_s - \chi_m}\frac{\cancel{1}}{\cancel{V}}\left(\frac{d^2}{4{B_0}^2}\right) + \frac{\cancel{2}^1\cancel{B_0}^{\cancel{2}}}{\cancel{d}}\left(\frac{d^{\cancel{2}}}{\cancel{4}^2\cancel{B_0}^{\cancel{2}}}\right)$$

$$=> \boldsymbol{h} = (\boldsymbol{\rho_s} - \boldsymbol{\rho_m})\boldsymbol{g}\frac{\boldsymbol{\mu_0}}{\boldsymbol{\chi_s - \chi_m}}\frac{\boldsymbol{d^2}}{\boldsymbol{4{B_0}^2}} + \frac{\boldsymbol{d}}{\boldsymbol{2}} \quad \textbf{(Equation 9)}$$

$$=> \boldsymbol{\rho_s} = \frac{\boldsymbol{(\chi_s - \chi_m)4{B_0}^2}}{\boldsymbol{g\mu_0 d^2}}\boldsymbol{h} + \boldsymbol{\rho_m} - \frac{\boldsymbol{(\chi_s - \chi_m)2{B_0}^2}}{\boldsymbol{g\mu_0 d^2}} \quad \textbf{(Equation 10)}$$

Where ρ_s is density of substrate levitating, χ_s is its magnetic susceptibility, B_0 is field at surface of magnet, d the distance between magnets, h the height of levitation, g the acceleration due to gravity and μ_0 the permeability of free space/vacuum.